Fall 2021

Shape-Selective Silver Catalysts for Ethylene Epoxidation

Kaveh Shariati

SHAPE-SELECTIVE SILVER CATALYSTS FOR ETHYLENE EPOXIDATION

by

Kaveh Shariati

Bachelor of Science
Shiraz University, Shiraz, Iran, 2016

Master of Science
University of Tehran, Tehran, Iran, 2019

Submitted in Partial Fulfillment of the Requirements

For the Degree of Master of Science in

Chemical Engineering

College of Engineering and Computing

University of South Carolina

2021

Accepted by:

Jochen Lauterbach, Director of Thesis

Andreas Heyden, Reader

Christopher Williams, Reader

Melissa Moss, Reader

Tracey L. Weldon, Interim Vice Provost and Dean of the Graduate School

ACKNOWLEDGEMENTS

First and foremost, I would like to give my greatest acknowledgement to my advisor Professor Jochen Lauterbach for his great support and help in the past two years I have been working in his group. I could not stand here without his valuable advice, especially while tackling the challenges and research problems. I learned how to be independent, productive, and think outside of the box in his research group. I greatly appreciate his trust and the excellent opportunity he gave me during these years.

I would also acknowledge my committee members Professor Andreas Heyden, Professor Christopher Williams, and Professor Mellisa Moss, for their precious time dedicated to helping me. Thanks to Prof. Heyden for everything I learned in his classes and for his trust in giving me a teaching assistantship opportunity that gave me an excellent experience.

A special thanks should also go to all the SAGE members for being great friends, supporters, kind and friendly. Many thanks to Michael, who trained me very patiently and kindly, to Blake, who helped me to organize research plans and stay in a right way to be productive, and to Andrew, who helped me a lot in improving this thesis. I really appreciate Jennifer, and Rasika's supports.

ABSTRACT

Epoxidation of ethylene with oxygen over promoted silver catalyst is one of the most important examples of heterogeneous catalysis to date with a multi-billion dollar annual market. Ethylene oxide (EO) can be used directly as a sterilizer, disinfectant, and fungicide, or as an intermediate chemical for producing ethylene glycol, detergents, antifreeze, polyesters, as well as a variety of other commercial chemicals. Thus, ethylene oxide is known as one of the highest volume chemicals produced in the chemical industry, accounting for approximately 40-50% of the total value of organic chemicals produced by heterogeneous oxidation. Considering the application of EO in detergents and sterilizers, the importance of EO production has been increased more than before due to the COVID-19 pandemic. Preventing the total oxidation and improving the yield of selective products can be counted as one of the major challenges in selective oxidation reactions.

It has been shown in the literature that the selectivity of ethylene oxide, among many other factors, depends on silver faceting of the catalyst nanoparticles. However, it is not exploited in industry, where the silver is mainly being used in nanoparticles with (111) facets due to the preparation and stability issues of the other structures. Thermodynamically, the Ag(111) facet is the most stable but the least active facet among the others ,while Ag(100) has been shown theoretically to exhibit the highest selective facet for EO formation. In this thesis, silver nanowires catalysts were synthesized via hydrothermal method and were deposited on α-aluminum oxide supports using wet

impregnation method. Obtaining a pure nanowires sample in not possible, however, some synthesis parameters such as time, temperature, and chemicals' concentrations that are parameters possibly affecting the morphology, yield, length, and diameter of nanowires were varied to increase the nanowires yield. Low yield, thin nanowires resulted from a shorter synthesis time while a mixture of nanorods and nanospheres were fabricated for longer synthesis times. An optimum time (24hours) was selected for synthesis time as one of the most effective synthesis parameters.

Unpromoted supported silver nanowires catalyst with an average diameter of less than 100nm and unpromoted semi-spherical silver catalyst with (111) facets that was synthesized using wet impregnation method, were tested in a single channel reactor at atmospheric pressure and for different temperatures. Structure of silver nanowires thinner than 100 nm were changed at the reaction condition while thicker nanowires remined intact.

TABLE OF CONTENTS

LIST OF TABLES

LIST OF FIGURES

LIST OF ABBREVIATIONS

AA.....Acetaldehyde

DFT..... Density Functional Theory

EO.....Ethylene Oxide

ER..... Elley-Ridal

ETO.....Ethylene Epoxidation Reaction

HREELS.....High-resolution Electron Energy Loss Spectroscopy

LH..... Langmuir Hinshelwood

OMC.....Oxametallacycle

TPD.....Temperature programmed Desorption

TPR.....Temperature programmed reduction

TOF.....Turnover Frequency

CHAPTER 1

INTRODUCTION

Ethylene epoxidation reaction is one of the oxidation reactions that has been investigated for a long time since the original work by Lefort in 1931[1]. While the industrial process has been established for quite some time, ethylene epoxidation still is one of the reactions that researchers are working on due to the high value of ethylene oxide. Ethylene oxide (EO) accounts for 40-50% of the total value of organic chemicals produced in heterogeneous catalysis, with 86% of the global capacity utilization[2,3]. The worldwide EO production in 2018 was more than 25 million metric tons and is expected to exceed 35 million metric tons by 2023[4]. It has been reported the EO market value in 2018 was more than 40 billion US dollars and is estimated to reach a global market cap of more than 55 billion US dollars by 2023 from EO production[5]. EO can be used either directly as a sterilizer, disinfector, and fungicide[6] or indirectly as an intermediate agent for ethylene glycol, antifreeze, polyester, detergents, etc[6,7]. Based on some of the EO applications, and due to the COVID-19 pandemic, the importance of EO production has been increased in recent years. The EO industry production shifted towards sanitizers and cleaning agent products more during the pandemic in 2020. The role of EO as a sterilizer was also increased because more than 50% of medical devices are sterilized with EO. However, the overall EO market decreased due to COVID-19, which could be related to an 80% decrease in EO usage in the textile industry in China, since it is one of the biggest countries in EO production[8].

Ethylene epoxidation over catalyzed silver is a good example of green chemistry. Previously, ethylene oxide was produced with a non-catalytic route called epichlorohydrin process discovered by Von A. Wurtz in 1859 and was industrialized by BASF in 1914. In this process, chloride reacts with a hydroxide salt (such as sodium hydroxide) and produces hypochlorous acid. Hypochlorous acid then reacts with ethylene to form epichlorohydrine. Ethylene oxide and calcium chloride are the products of a reaction between epichlorohydrine with calcium hydroxide[9,10]. Salts containing chlorine once dumped into rivers as a means of disposal, a method that is not acceptable these days[11]. Nowadays, however, silver is used as a unique catalyst for ethylene epoxidation with some dopants such as cesium, chlorine, or noble metals to increase the ethylene oxide selectivity from less than 50% to about 90%[3,12,13]. However, considering what was mentioned previously, increasing even 1% of EO selectivity could bring about more profit.

As previously mentioned, silver is a unique catalyst for ethylene epoxidation. Some other oxidation catalysts such as Pd, Pt, or Ni result in complete combustion[14]. Although the main reason for the uniqueness of silver is not fully understood yet, the silver and oxygen interaction is the key to its high selectivity[15]. Au and Cu are two other transition metals that have been suggested as potential catalysts for this reaction. It is shown that Cu-Ag bimetallic catalysts can increase the ethylene oxide selectivity compared to pure silver itself[3,7]. However, in comparing silver, gold, and copper, silver can be selected as the best catalysts for this reaction because of the higher EO selectivity[15].

Molecular oxygen dissociation on the silver surface is one of the critical parts of this reaction which has considerable activation energy, even though it is not a rate-determining step (except on Ag(111) at a pressure above ~2 bar)[6,16,17]. Thus, the interaction

between metal and oxygen molecules should be strong enough in order to dissociate molecular oxygen to atomic oxygen. Moreover, strong metal-oxygen interaction prevent ethylene oxide from desorbing from the surface, which can result in undesirable products by activating the C-H bond[15]. Furthermore, the metal should have an optimum interaction with the oxygen molecule. The metal-oxygen interaction in the case of copper is a strong result of better oxygen dissociation but leads to an increase in the activation barriers and desorption energy for an intermediate compound called Oxametallacycle (OMC), which is to be explained in detail later, that make the copper an inappropriate choice in comparison to silver.

Since the 1930s, much progress has been made in ethylene epoxidation, both theoretically and practically. A lot of research was initially geared toward the role of oxygen in the ethylene epoxidation (ETO) reaction. Once, it was believed that the atomic oxygen is responsible for undesirable products following the reaction below:

$$O(ads) + C_2H_4 \rightarrow OC_2H_4(ads) \xrightarrow{5O(ads)} 2CO_2 + 2H_2O$$

Where the "ads" is indicating adsorbed, and the intermediate is acetaldehyde that is decomposed quickly to form carbon dioxide and water. While the claimed that the molecular oxygen is responsible for the selective product, ethylene oxide:

$$O_2(ads) + C_2H_4 \rightarrow C_2H_4O + O(ads)$$

Since these two reactions have the same reaction orders and similar activation energies, they combined them as one general reaction as seen below:

$$7C_2H_4 + 6O_2(ads) \rightarrow 6C_2H_4 + 2CO_2 + 2H_2O$$

Based on this equation, and is generally claimed in the literature, the highest EO selectivity that can be reached considering the fact that EO does not oxidize to acetaldehyde and then undesirable products is 6/7 or 85.7%[18]. However, EO selectivity higher than 85.7% was obtained soon after that research. Those results proved that atomic oxygen might also result in EO rather than carbon dioxide and water[15,18]. Moreover, investigation on the mechanism of the reaction using temperature-programmed reduction (TPR) spectroscopy proved that the atomic oxygen is responsible for EO production[19]. Through further investigation, it was found that atomic oxygen is responsible for both desirable and non-desirable products, depending on the valance charge of adsorbed oxygen. Electrophilic atomic oxygen results in EO formation while the nucleophilic oxygen can move the reaction to carbon dioxide production by breaking H from adsorbed ethylene in order to form acetaldehyde[20].

Ethylene epoxidation can occur in two different reaction mechanisms, either with the Langmuir-Hinshelwood (LH) mechanism or via the Elley-Ridal (ER) mechanism. EO formation through the ER mechanism is known as direct epoxidation reaction, while an intermediate called Oxametallacycle (OMC or OME) is produced with LH mechanism, then EO and acetaldehyde are formed through OMC decomposition. The difference between these mechanisms is related to oxygen coverage. In both mechanisms, molecular oxygen adsorbed on the silver surface, which dissociates two atomic oxygen. However, in ER mechanism, gaseous ethylene reacted with atomic adsorbed oxygen on the silver surface since the coverage of oxygen is high. On the other hand, in the LH mechanism, ethylene also adsorbs on the silver surface and then reacts with atomic oxygen to produce OMC. In the following section, the direct epoxidation mechanism and the discovery of OMC will be discussed in detail[6,15]. It is computationally suggested that the direct route of

ethylene epoxidation can happen on the oxide surface of silver $Ag_2O(001)$ in the presence of electrophilic oxygen. In this route, the electrophilic oxygen interacts with the double carbon bond of gaseous ethylene and directly produces an inactive form of ethylene oxide while releasing 174 kJ/mol and desorbing EO with 73 kJ/mol. The overall energy of this step is the same as the OMC route of ethylene epoxidation but with fewer reaction steps. It has been claimed that in the LH mechanism, because of ethylene adsorption, atomic oxygen can interact with the C-H bonds and produce acetaldehyde. In contrast, in the direct route, this atomic oxygen mainly interacts with the C=C bond. However, with this route, when the atomic oxygen is consumed, ethylene can get adsorbed, and the mechanism will shift toward the LH mechanism. Thus, to have the ER mechanism, the surface of silver should always be kept in an oxide state, and all the oxygen vacancies should be blocked[15].

As it was mentioned before, one of the essential discoveries for ETO reaction was the OMC discovery as an intermediate that can be converted to either EO or acetaldehyde by Barteau et al. using both experimental and computational techniques such as temperature-programmed desorption (TPD), high-resolution electron energy loss spectroscopy (HREELS), and density functional theory (DFT)[3,16,21]. The stable OMC was discovered by back adsorbing EO on the silver surface (111) at 250K where the EO ring was opened to form stable surface intermediate and then reacted again to form EO, ethylene and water at 310K. The spectrum obtained by the HREELS from back adsorbing the EO on the silver surface were different to the products and reactants spectra of the reaction. By the comparison of HREELS and DFT results the structure of the OMC on Ag(111) was obtained[22]. The structure of OMC om different silver surfaces is shown in Figure 1-1:

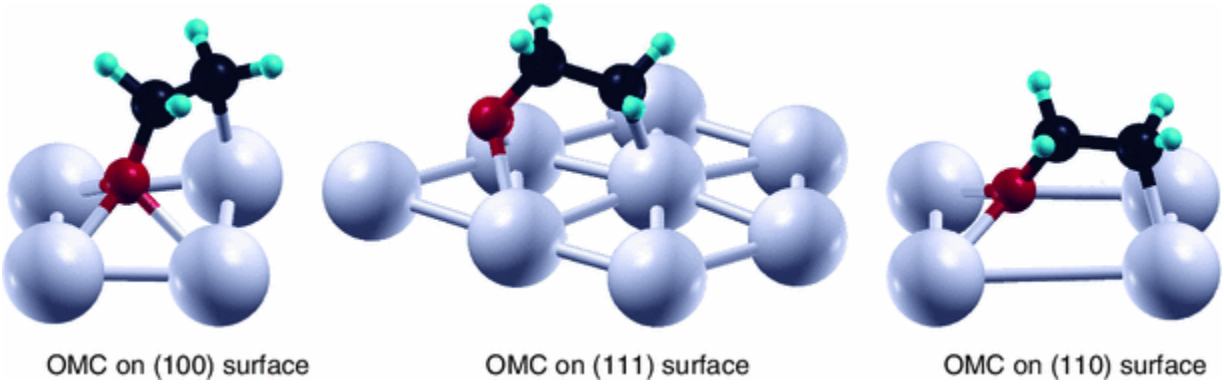

Figure 1-1. OMC structure on different silver surfaces [15].

The mechanism of the reaction then was explained as below:

$$O_2 + * \leftrightarrow 2O_*$$

$$C_2H_4 + 2 * \leftrightarrow C_2H_{4^*}$$

$$C_2H_{4^*} + O_* \leftrightarrow CH_2CH_2O *$$

$$CH_2CH_2O * \leftrightarrow CH_2CH_2O +*$$

where OMC intermediate is denoted as $CH_2CH_2O *$. Thus, the oxygen would dissociate on the surface to produce atomic oxygen. The formation of OMC from adsorbed ethylene and oxygen on the surface happens after the ethylene adsorption. Ethylene oxide can be produced in the next step, which is dependent on the stability of the OMC. These couple of studies helped to further understanding the microkinetic modeling of the ETO reaction mechanism. The formation of this intermediate has been proven in industrial conditions too[17]. Although there were differences in the conclusions reached, as it was concluded that the oxygen dissociation and EO formation are the rate-limiting steps. This fact was investigated on different surfaces of silver by Hus et al. [6] It was computationally investigated that the rate-determining step for the Ag(100) and Ag(111) is the EO

formation; oxygen dissociation is the next rate-limiting step, and it is more limiting step in Ag(111) in higher pressure than the atmospheric.

In this part, we are explaining the mechanism of the ethylene epoxidation reaction on different surfaces. One of the important assumptions that has been used in the literature is that the total oxidation and bulk oxidation (Ag_2O) do not happen on the surface or bulk. This means that the coverage of oxygen will not reach full coverage. This assumption was calculated by ab initio calculation is an important consideration since it can change the reaction mechanism on the surface. The most common mechanism that happened on the silver surface for ethylene epoxidation is the Langmuir-Hinshelwood mechanism. However, it was reported that the Elley-Ridal mechanism could happen. To clarify more, the dissociated oxygen atoms can either react with adsorbed ethylene or gaseous ethylene and produce the OMC intermediate. Reaction energies for elementary steps ethylene epoxidation reaction on the different surfaces are shown in Figure 1-2. Oxygen dissociation, OMC formation, and conversion of OMC to the EO or acetaldehyde are the most significant rate-limiting steps compared to the other steps that happen on the surface. It should be noted that the carbon dioxide and water formation from acetaldehyde were not considered in the calculations, because the acetaldehyde decomposition step is too fast. Comparing the activation energy differences between EO and acetaldehyde on different surfaces illuminate the fact that the acetaldehyde energy barrier is considerably lower than EO on both (110) unreconstructed and reconstructed surfaces, which results in being the inappropriate choice for epoxidation reaction. This difference in energy barrier on the (111) facet is close and competitive. The story is slightly different on the (100) facet, where the OMC intermediate would prefer to go through the EO formation path rather than

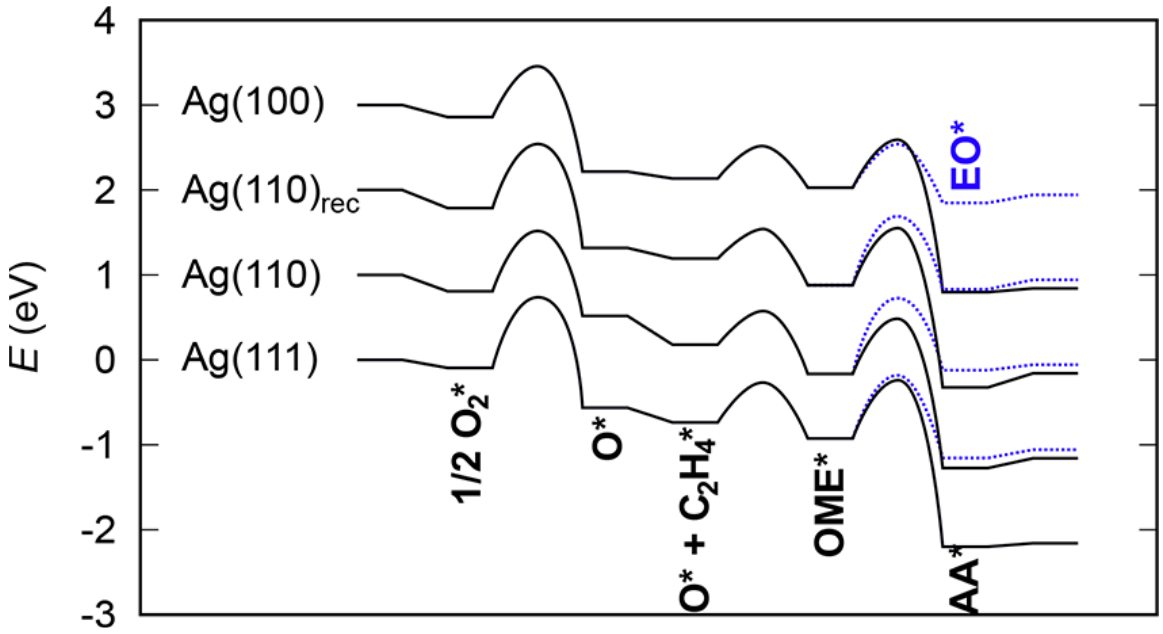

Figure 1-2. Reaction energy landscapes for ethylene epoxidation on different silver catalyst's facets. [6]

acetaldehyde formation. The apparent activation energy on (111) and (100) facets for both EO and AA formation were calculated at 1.34 bar and 10% ethylene and oxygen. The results showed that the energy barrier for AA formation on (111) is less than EO by 0.06 eV. However, this energy barrier for (100) faceting was 0.07 eV more favorable toward EO formation. Among all the surfaces, the (100) was the only structure with higher EO selectivity than the undesirable product. The EO selectivity, at the conditions previously mentioned above for activation energy, was plotted versus different temperatures (left) and different pressure (right) on various facets. The EO selectivity showed the highest amount on Ag(100) with around 80% while the amount on Ag(111) was predicted to be between 20% to 40% for different temperatures. These predictions were consistent with experimental amounts. As it is cleared in the Figure 1-3, EO selectivity showed a weak dependency on the pressure change. However, pressure can affect the reactant coverage and reaction rates.

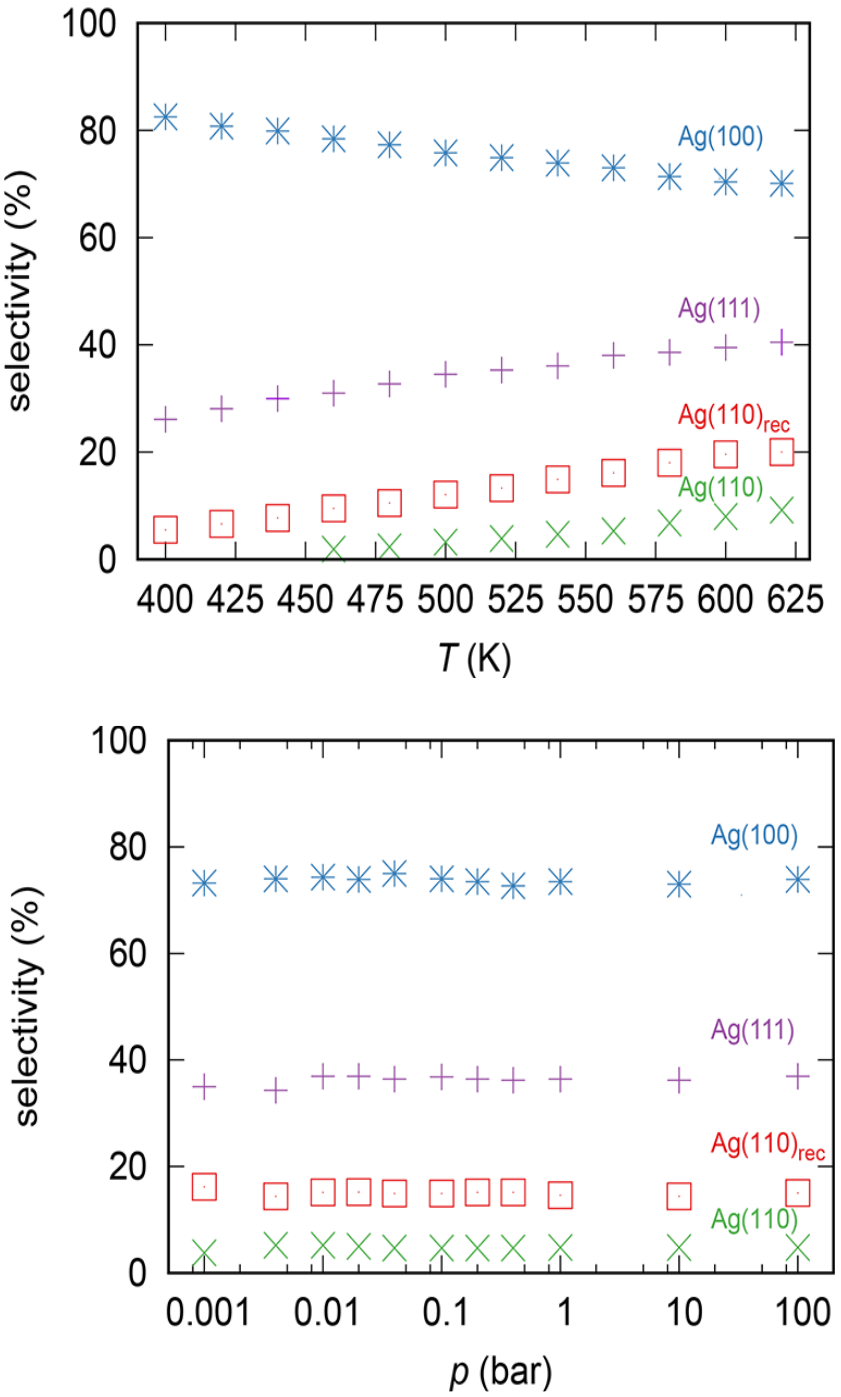

Figure 1-3. EO selectivity as a function of temperature and pressure for different silver catalyst's facets[6]

There are a few experimental works that have investigated the different silver structures for ethylene epoxidation reactions. In one of these investigations, the comparison between both (100) and (111) facets were studied where the silver nanowires and nanocubes were synthesized as silver catalysts with dominant (100) facets while silver nanospheres with (111) faceting were used. As shown in Figure 1-4, both silver nanowires and silver nanocubes showed higher selectivity rather than nanospheres. It should be mentioned that the catalysts did not promote with any promoters such as cesium. Moreover, chlorine salt was noy used as an additive to the feed. Thus, it was shown that an increase in EO selectivity from almost 30% to more than 70% using silver nanocubes rather than nanospheres catalysts was possible. The most exciting question that should be addressed here is the reason(s) that the silver nanocubes demonstrated higher selectivity rather than both nanowires and nanospheres. In addition to the reasons mentioned previously regarding the reason that silver (100) is more effective than silver (111), the higher turnover frequency (TOF) of nanocubes compared to nanowires and nanospheres accounted for a higher EO selectivity. Although the TOF of nanowires and nanospheres were the same, the number of active sites per volume in nanowires was higher than nanospheres. Unfortunately, the reasons that the nanocubes had higher EO selectivity rather than nanowires still remains a mystery, even when both of them have mostly (100) facets. However, based on the images in their supplementary files, it can be observed that the nanowires had a lower yield compared to nanocubes meaning that the (111) to (100) facets ratio was higher for nanocubes than nanowires. Additionally, it was claimed that more defect sites existed on nanowires relative to nanocubes. The common area of the edges in nanowires is not sharp, and it has a small thickness, which results in a different type of

defect site. Although the nanocubes could have these defect sites, these sites were more in nanowires, which caused a better performance for nanocubes in comparison. Another outcome of the Figure 1-4 is that a larger particle size would result in higher EO selectivity. The particle size is related to the ratio of undercoordinated size over coordinated size as it is shown in the Figure 1-5. The larger a particle is, the lower undercoordinated sites over total sites it has. Since the rate of non-selective products formation is related to the concentration of undercoordinated size, as mentioned in the Figure 1-5, the larger particles had higher EO selectivity. It should be noted that the size here means the characteristic length, which is the side length for nanocubes and the diameter for nanowires and nanospheres.

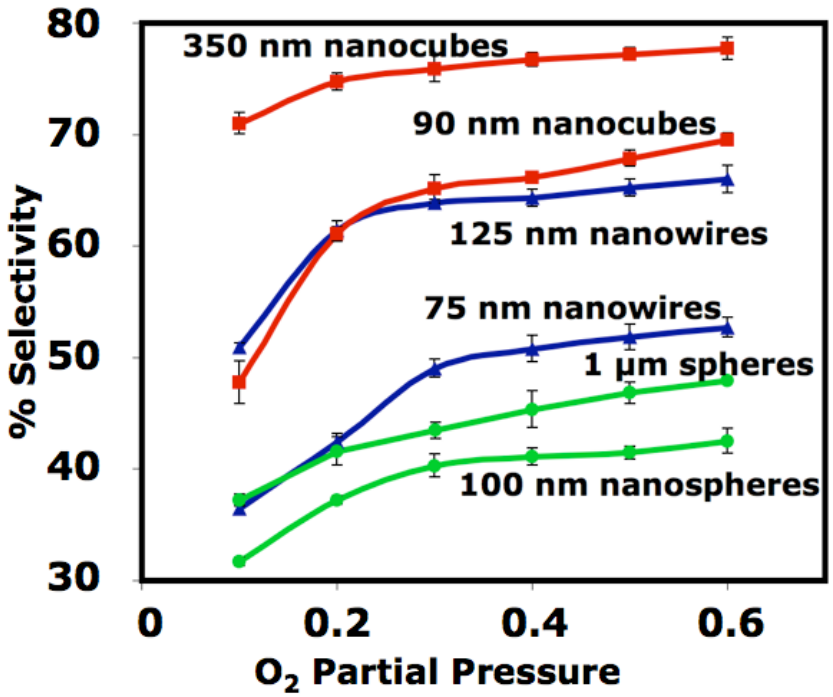

Figure 1-4. EO selectivity for different silver structures and sizes as a function of oxygen partial pressure.[24]

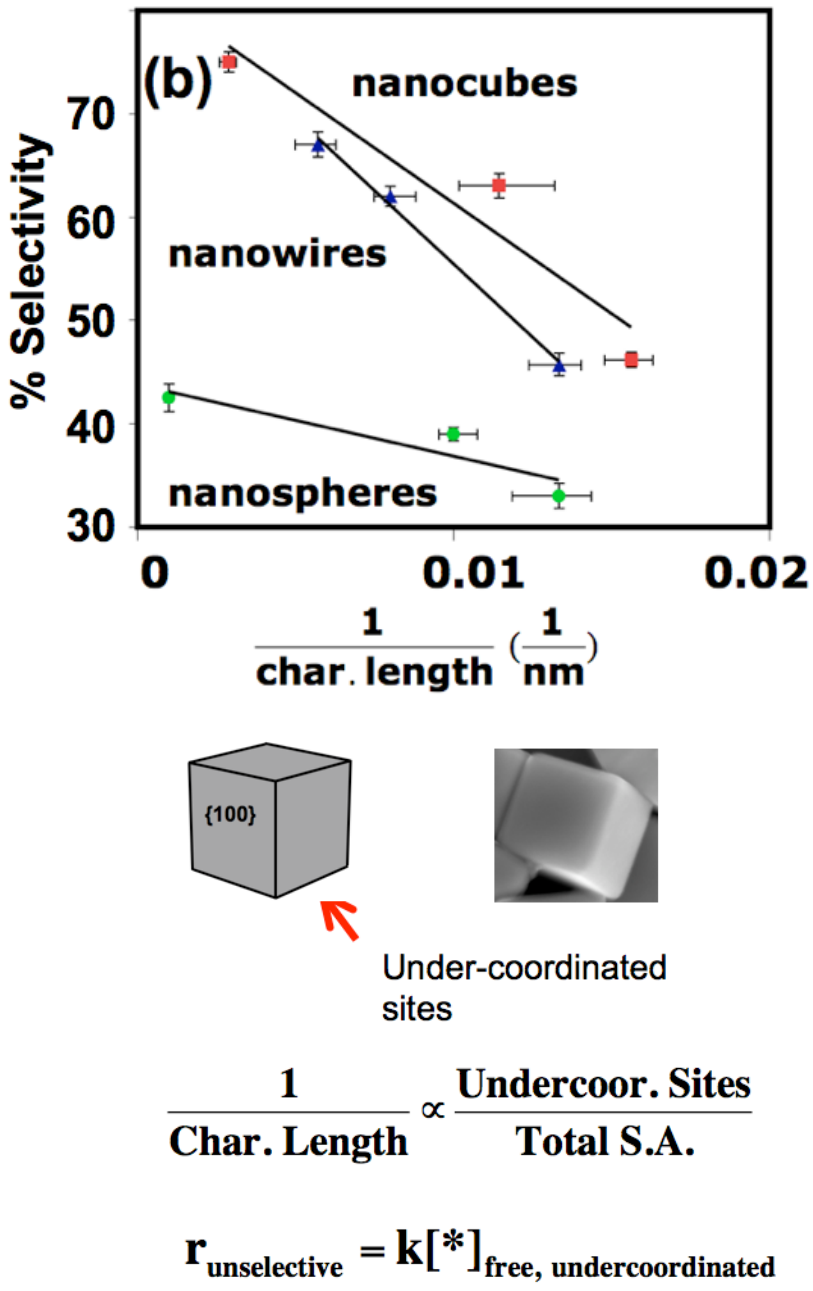

Figure 1-5. EO selectivity for different silver structure as a function of inverse characteristic length. [24]

Another result the authors referred to, was the increase in EO selectivity with an increase in oxygen partial pressure. In an experiment demonstrated within the literature, the ethylene partial pressure was held at a constant 0.1 while an increase in the oxygen partial pressure followed by a decrease in the nitrogen partial pressure. Nitrogen is mainly

used as the inert gas in this reaction rather than gases such as argon due to its higher heat capacity in order to keep the reactor temperature constant, since ethylene epoxidation is highly exothermic. The first reason for the increase in EO selectivity was explained, as the reaction order related to oxygen, which is a positive number[23,24]. Although many papers reported the reaction orders with different numbers, either experimentally or computationally, the common results were that the reaction orders related to both ethylene and oxygen are positive numbers, and oxygen has a much larger reaction order than ethylene[6,15]. It is also mentioned that increasing the oxygen partial pressure may results in more active sites by involving the undercoordinated sites that were chemically active. It could also play a role similar to that of chlorine in this reaction by blocking the defect sites[24].

Although the ethylene epoxidation process has industrialized since 1931, there are still a lot of researchers working on this process in order to develop the process or find out more about the chemistry and mechanism of the reactions. However, the majority of works include a focus on the silver with the (111) faceting rather than other silver catalysts structures. Some of the most recent and prestigious papers were mentioned in the previous sections, both computational and experimental studies[23,24,25,26,27,28,29]. Differences between computational and experimental studies are inevitable. Some of these differences might be explained by more studies. For example, in the computational study for silver catalysts with (100) facets, the differences between nanocubes and nanowires in the reaction atmosphere were not considered[6] while it was shown that the silver nanocubes have higher EO selectivity rather than silver nanowires[24]. Moreover, reaching to pure silver nanostructured that have less thermodynamic stability is not feasible. Thus, in the studies

that investigated silver nanocubes or nanowires catalysts, these structures were accompanied by a considerable amount of silver semispherical particles with (111) planes, a fact that computational papers did not consider. Experimentally, previous studies showed about 12% or 15% silver on alumina support showed the best EO selectivity[7],[30],[31]. It was claimed in the study shown in an earlier paragraph, that the composition of silver nanowires and nanocubes on the alumina support were about 10%, and they were also distributed uniformly. However, the maximum silver catalysts loading on 1 g of alumina support were 0.014 g and 0.063 g for nanowires and nanocubes, respectively. It means that the total catalysts weight loading were about 1.4% for nanowires and 6% for nanocubes[24]. Additionally, some studies showed that the ethylene conversion and EO selectivity varied since the reaction started before reaching steady-state, which could be between 24 to 48 hours[31]. However, in the study did by Sangaru[27] neither ethylene conversion nor EO selectivity were changed as a function of time even after 24 hours for silver nanocubes. All the studies that were mentioned here, especially those with a focus on different silver structures, helped the researchers to discover more about the ethylene epoxidation reaction, silver catalysts, etc. These studies, in addition to a lot of unanswered questions and vague points, as well as consideration of the importance of EO, intrigued us to start this study. Here, we tried to address various simple methodologies that were not mentioned in previous published papers but are crucial to reach a reasonable output.

CHAPTER 2

SYNTHESIS

Synthesizing metal nanoparticles in different shapes has been investigated extensively[32]. Silver is one of the metals with unique features that make it attractive for researchers. Among the metals, silver has high thermal conductivity and the highest electrical conductivity. Adding a specific shape to the silver, with the mentioned features, can enhance its advantages for a specific application. For example, silver nanowires are used extensively in electronic devices such as LEDS and solar panels due to their high aspect ratio as well as their electrical and heat conductivities[33,34,35]. Figure 2-1. shows the different silver structures that have been investigated[32]. However, many of these different shapes of silver were not tested under reaction conditions. Although there are some papers that used silver nanowires and nanocubes for epoxidation reactions[24,23,26], silver semi-nanospheres particles with dominant (111) plane are mostly being used either in academia or industry.

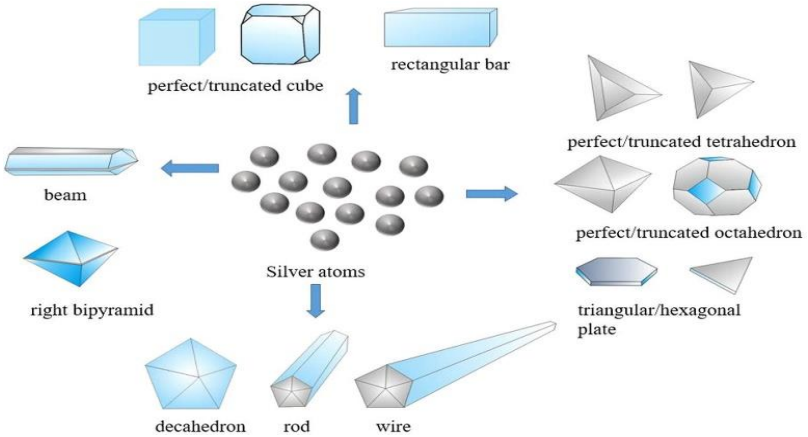

Figure 2-1. Most important synthesized silver nanoparticles [32].

In this thesis, silver nanoparticles such as nanospheres, nanowires were investigated; some preliminary work with silver nanocubes was also conducted, which is going to be our focus in future studies. Synthesizing silver nanostructures with (100) facets is not simple as (111) facets due to the lower thermodynamic and thermal stability of this facet. During our research, we found out that there are simple but crucial tricks in the synthesis that a lot of papers did not mention. Here, we tried to cover these important experimental tricks as much as possible. Two methods were used for silver nanowires synthesis: the Hydrothermal method and the Polyol process method. Additionally, incipient wetness/wet impregnation method was used to synthesize silver nanosphere particles.

2.1 Hydrothermal Method

Hydrothermal method for synthesizing different structures of nanoparticles is one of the well-known synthesis procedures due to the simplicity, low cost, environmentally friendliness (although some trace of cl^- observed in EDS each time), and its ease of scale-up[36]. The simplicity of the hydrothermal method can be attributed to its one-step synthesis method. However, this can sometimes be a disadvantage due to issues with controlling the dimensions of the shapes, such as diameter and length, when compared to other methods. For example, in polyol method, the morphology, yield, and dimensions of nanowires can be varied by changing the injection rate, the stirring rate during the reaction, and the order of adding the chemicals[37]. In both the hydrothermal method and the polyol process method, a polymer is used as capping agent. However, there are some papers which did not use any polymer with hydrothermal method and still successfully synthesized nanowires[38,39]. In our case, polyvinylpyrrolidone (PVP) was used as capping agent. Glucose was also added as a soft reducer (the role that ethylene glycol plays in the polyol method). By adding the silver

nitrate aqueous solution and glucose, silver seeds are formed in addition to nitic acids based on the equation below:

$$2AgNO_3 + C_6H_{12}O_6 + H_2O \rightarrow C_6H_{12}O_7 + 2HNO_3 + 2Ag$$

This unprotected silver can be converted to silver nitrate again in the presence of nitic acids. However, with the addition of sodium chloride addition, silver chloride particles are produced. Silver chloride solubility in water is low and it can precipitate into the bottom of the solution. Thus, the Cl^- ion concentration is crucial in the silver nanowire formation. Glucose reduces the silver chloride to silver cations and then silver seeds; overall, this process relatively slow, which helps in to prevent the creation of big nanoparticles[36]. At this point, the capping agent plays a pivotal role by adsorbing on the (111) facet of silver seeds. In our case, PVP adsorbs on the (111) facets and helps in one dimensional growth of silver seeds to the silver nanowires in (110) direction.

The experimental procedure for silver nanowires synthesis with hydrothermal method was followed from the Bari. et al paper[36]. Four solutions of 15 ml of 0.02 M silver nitrate (Sigma-Aldrich, 209139), 15 mL of 0.04 M sodium chloride (Sigma-Aldrich, S7653), 5 mL of 0.12 g glucose (Alfa Aesar, A11090), and 5 mL of 1 g PVP (Sigma-Aldrich, 856568) were provided separately all in DI water. For better dissolution of PVP into water, the solutions were sonicated in a sonication bath at 65 ℃ for about 1 hour, resulting in a clear solution at the end. All the other solutions were stirred on the stir plate at room temperature at about 200-250 rpm for the stirring condition. Glucose aqueous solution was added to the silver nitrate solution at first. After 10 minutes of stirring, we added the PVP solution to the prepared solution. The solution was then stirred for 20 minutes. The sodium chloride solution was added dropwise using a syringe pump with a rate of about 0.2 mL/min. Although the injection rate plays a crucial role for the polyol

method, changing the injection rate from 0.2 mL/min to 0.6 mL/min did not result in any significant differences. With the beginning of sodium chloride aqueous solution injection, the color of the preparing solution changed from colorless to a milky solution with alight purple tint. Figure 2-2 shows the color differences of the solutions before and after injecting the sodium chloride. The prepared solution was then transferred into a 50 mL Teflon-lined stainless-steel autoclave and heated for 24 hours at 160 ℃ in a furnace in atmospheric air. The autoclave then was cooled at room temperature for a couple of hours and the solution was transferred into a centrifuge tube. The Teflon bottle was rinsed with DI water to be sure that we did not have any wasted silver nanowires. The solution was centrifuged at 2500 rpm for 20 or 30 minutes usually two times with DI water and two times with ethanol. Centrifugation or any other similar methods, are being used for two purposes: 1. Separation of silver nanowires/nanocubes from silver nanoparticles, and 2. Removing unreacted chemicals (such as PVP, and nitrate precursor) used for synthesis from the silver nanoparticles. Here DI water and ethanol were used in order to remove the organic and inorganic, unreacted chemicals from the silver nanowires. High nonconductivity was observed in the SEM images of supernatant, which was likely due to the removal of the nonconductive chemicals from sample during the centrifugation. Moreover, small nanoparticles were observed in the supernatant SEM image. Figure 2-3 shows the silver sample settled at the bottom of the centrifuge tube and the supernatant at the top after the first cycle of centrifugation. The centrifuge cycles should be continued until the supernatant becomes colorless, which typical happens after 3,4 centrifuge cycles. Using paper filter as another method for separation of nanoparticles with different sizes was also tried with the washing cycles, much like in the centrifugation method. The yield of nanowires in the

centrifuge case was better, probably because of the fact that nanoparticles can be trapped between the net of nanowires, which can cause issues with their removal from the filter paper, even if the pores of the paper are higher than the diameter of nanoparticles.

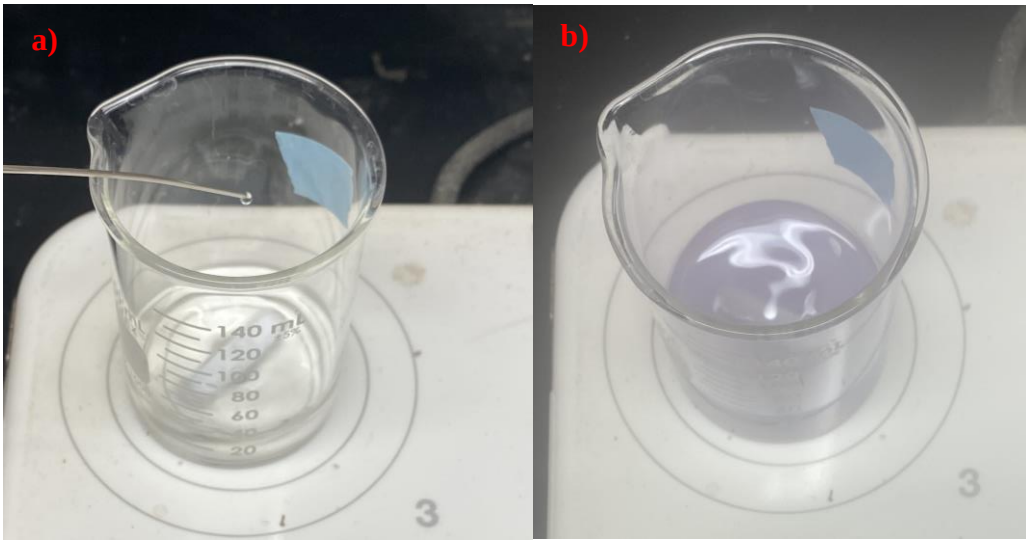

Figure 2-2. Solution preparation for silver nanowires synthesis (a)before and (b) after sodium chloride aqueous solution injection

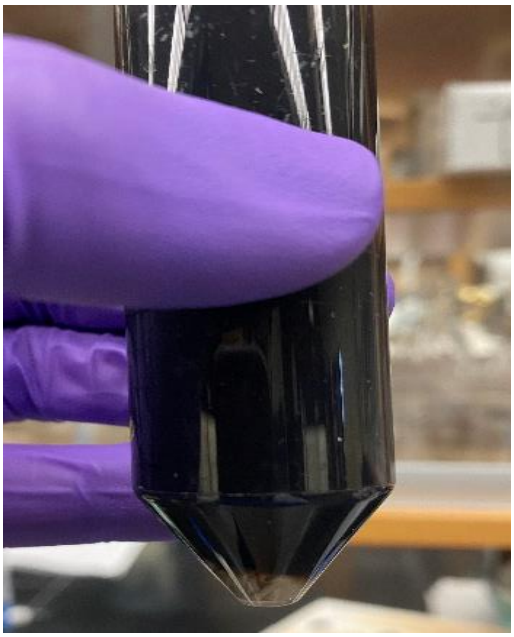

Figure 2-3. Settled down silver nanoparticles after first cycle centrifuge.

Characterization of nanowires:

After finishing the centrifuge cycles, the sample containing silver particles formed a pellet at the bottom of the tube. The pellet was removed from the centrifuge tube and was put either on the glass slide or SEM stub pins to be dried for a couples of hours. Putting the sample directly on the SEM stub pins was preferred, since in the case of glass slide, the sample must be spread by a spatula and transferred on the SEM stub pins; this resulted in the need for an additional push onto the stub pins to ensure the sample was actually sticking to the carbon tape. The Zeiss Gemini500 Thermal Field Emission Scanning Electron Microscope (FESEM) was used for collecting SEM images. The incident electron beam energy was set to 15 kV for all the images. The composition of the supported silver catalyst was determined with Energy Dispersive X-ray Spectroscopy (EDS) connected to the FESEM instrument. X-Ray Diffraction (XRD) patterns of the silver samples were collected using a Rigaku Miniflex II equipped with a Cu-Kα X-ray source and a high-speed silicon strip detector. Scans were collected between 10° to 90° with a 2θ angle at a rate of 2°/min with a step size of 0.02°.

Figure 2-4 shows the silver nanowires synthesized with the hydrothermal method as described before. To distribute the pellet containing silver particles at the bottom of the centrifuge tube, 3 to 5 mL of ethanol was added after centrifugation and the solution was sonicated for 10-15 minutes, resulting in a suspension of silver particles. Then a droplet of the suspension was dropped onto the carbon tape of SEM stub pins and let it dry for couples of hours at room temperature. As it is obvious in the Figure 2-4, in addition to the silver nanowires with different thicknesses, there are also silver semi-spherical particles among them. Based on our experience, after making a lot of supported and unsupported silver

nanowires, removing these nanoparticles and increasing the yield of nanowires to almost a pure nanowires sample, is not feasible.

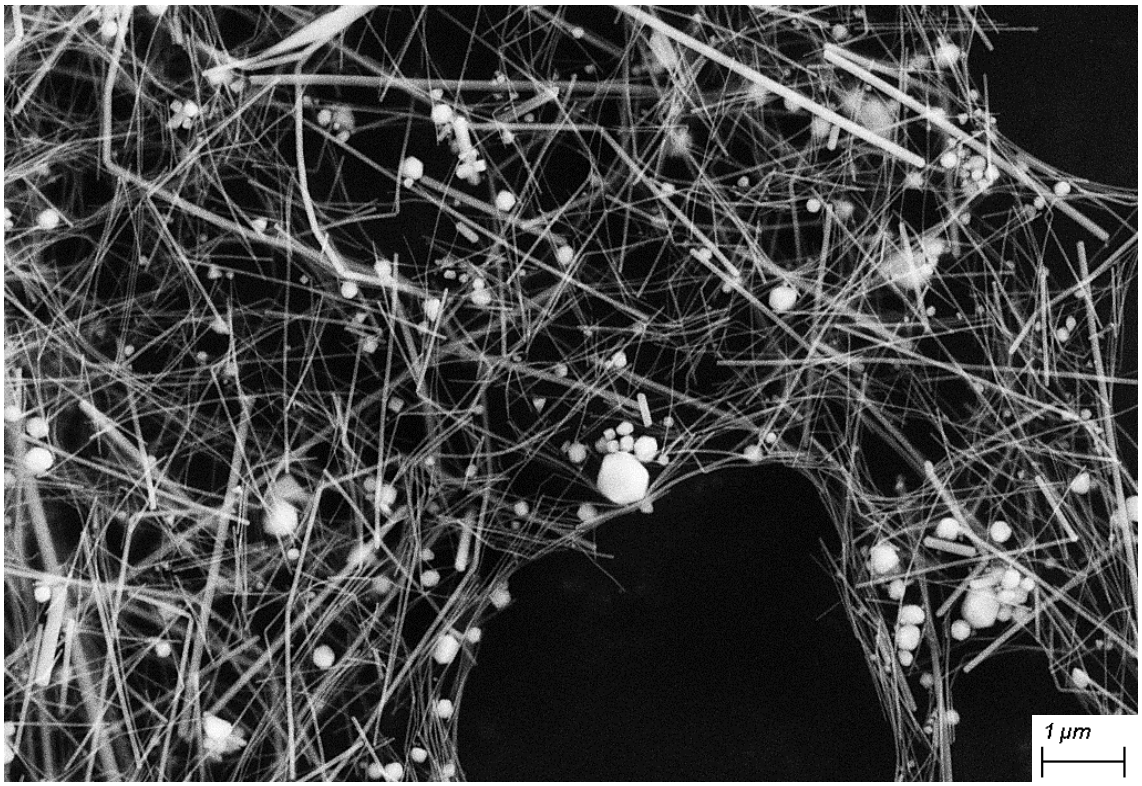

Figure 2-4. SEM image of silver nanowires synthesized with the hydrothermal method.

Sonicating the sample of silver nanowires settled at the bottom of centrifuge tubes, after finishing the centrifuge cycles, was found out a step that helps in a better silver particles distribution on the support. Sonication has been reported in the literature for putting the sample on the grids that are being used for conducting the TEM images. If the sonication step is skipped, the SEM stub pin is prepared by applying the pellet of silver particles settled at the bottom of the centrifuge tube directly to the SEM stub pin or a glass slide. The resulting SEM image can be seen in Figure 2-5.

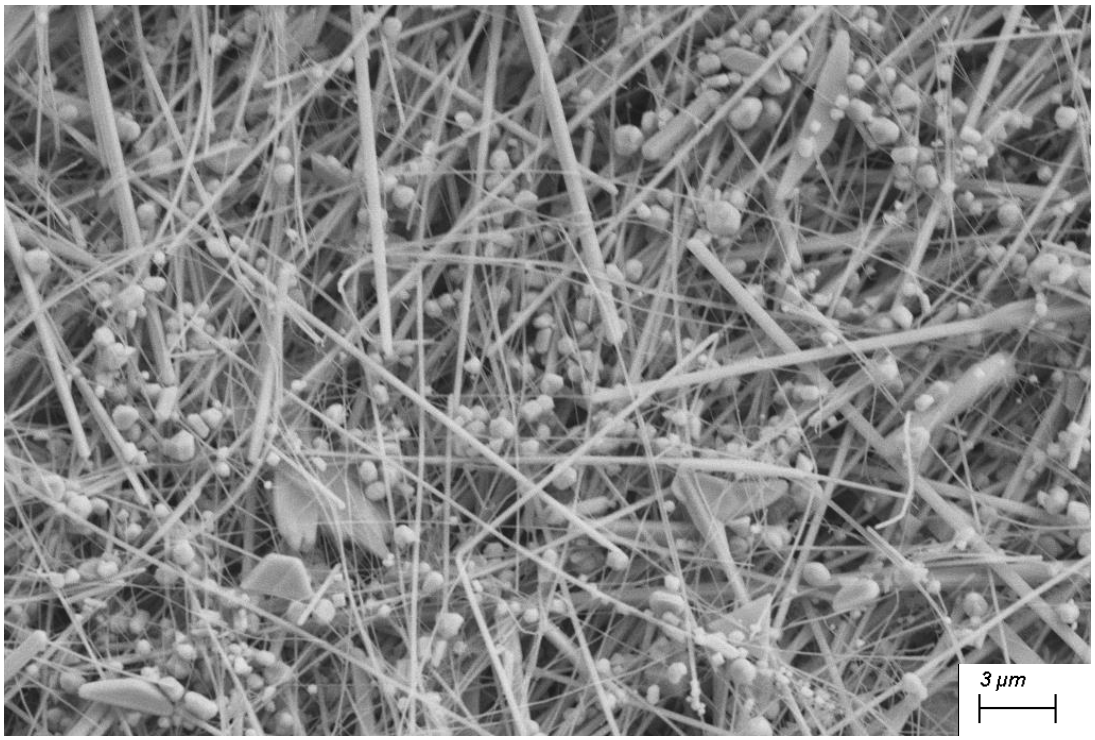

Figure 2-5. SEM image of silver nanowires without sonication step.

Generally, most studies used the centrifuge method for separating the nanowires or nanocubes from the nanoparticles or microparticles. As previously mentioned, a filter paper was also used to find out which separation method would be most effective. A 12.5 cm diameter, P8 fisher brand filter paper was put on the ceramic Buchner funnel before it was inserted into a clean 2 L filter flask. The filter flask was connected to a water stream to provide the vacuum in order to accelerate the supernatant passage through the filter paper. The centrifuged sample was poured over the filter paper and just like in the centrifuge process, the silver sample was washed 2 times with DI water and then 2 times with ethanol. The filter paper, which contained separated silver particles, was dried at room temperature and then the silver particles were removed and seated on the SEM stub pins in preparation for imaging. Figure 2-6 shows the SEM image of the silver particles. Obviously, the silver

particles were present in this sample varied greatly from those observed in the Figure 2-5 using the centrifuge as the separation method. The yield of nanowires obtained from the centrifugation method was higher compared to the filtration method. The most probable reason is that in the case of filter paper, the silver particles (semi-spherical particles) might stick between the net of silver nanowires and are unable to be removed as effectively as in centrifugation method. Moreover, trace amounts of filter paper were observed during SEM imaging which could be because of scratching the dried silver particles from the filter paper. It will be discussed more later in this thesis that for impregnating the silver particles onto the support, the synthesized silver particles need to be sonicated with a specific amount of a solvent after separation. However, sonication is not recommended in the case of filter paper method since there might be trace of filter paper residuals in the silver sample, and the waste during the separation would be higher in this case compared to centrifuge method.

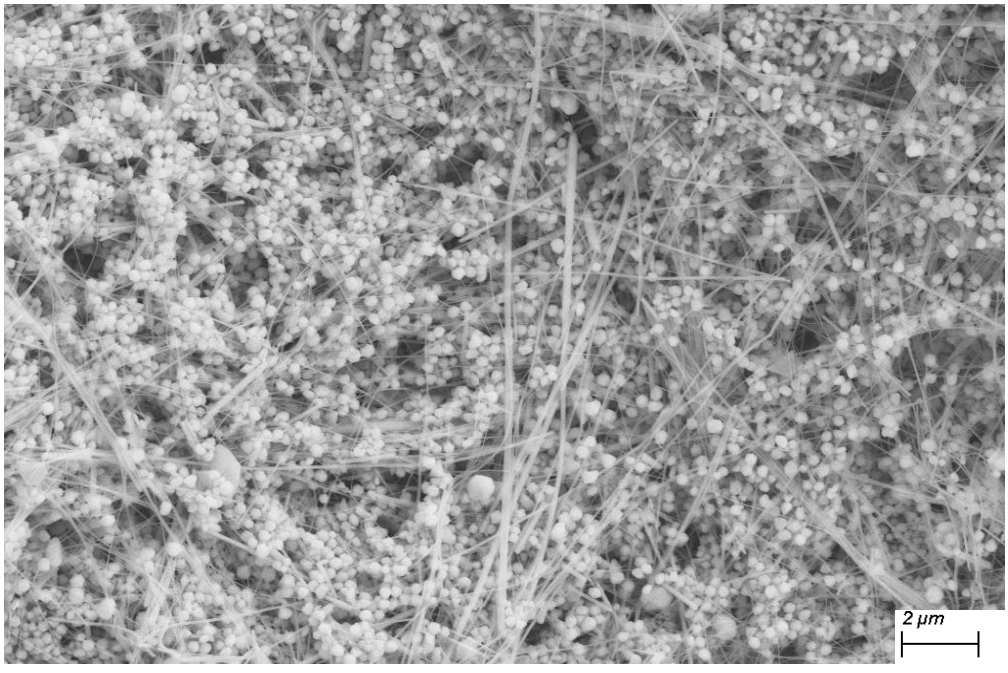

Figure 2-6. SEM image of silver particles using the filter paper as the separation method.

Obtaining a pure nanowires sample is challenging. As previously mentioned, and showed in the SEM images, there were semi-spherical silver particles in the samples as well as nanowires. Moreover, some other silver particles with different shapes were observed during SEM imaging. As shown in Figure 2-7, silver particles in the form of triangular and hexagonal microplates existed in the sample as well as silver nanowires. There are some studies that have investigated the triangular and hexagonal silver nanoplates synthesis; however, these studies used different synthesis methods than had previously been discussed[40,41,42]. It has been shown that the triangular silver nanoplates are formed through seed-mediated growth of silver nanoparticles. Thermodynamically, these particles are less stable than the hexagonal nanoplates. Thus, with higher synthesis time and with a crucial effect of heat, those particles change to the hexagonal nanoplates, as seen in Figure 2-7 as well[41]. Thus, existence of both triangular and hexagonal nanoplates at the same time makes sense; however, formation of these particles via hydrothermal method, even with low yields, could be interesting for further mechanism studies of silver nanoparticles.

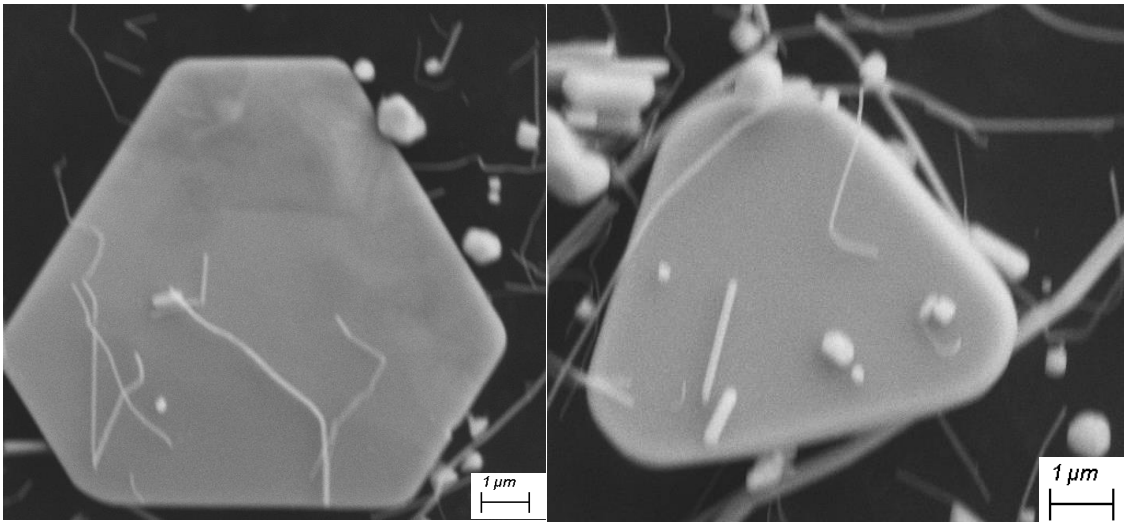

Figure 2-7. SEM images of silver triangular and hexagonal plate particles.

Literatures in the synthesis of metal nanoparticles usually include the parametric studies in order to discover the reaction mechanisms during the synthesis and investigate the effects of the synthesis parameters on the aspect ratio and yield of particles. However, the goal here was not to conduct a parametric study of silver nanowires formation, but to find and vary the effective parameters in order to reach higher yields and a specific diameter and length for said nanowires. There are many parameters that can affect the yield, length, and diameter of nanowires, such as synthesis time, temperature, and chemical concentrations. Among all these parameters, time of synthesis had the most considerable effect on the nanowires' yield and diameters in the ranges that were studied in this thesis. The synthesis time that was mentioned in the reference paper[36] reported a synthesis time of 22 hours. Synthesis times of 12, 15, 18, 21, and 24 hours were investigated to discern the effect of synthesis time on the silver nanowires yield and diameter. For the 12 hour synthesis time, which was the shortest time selected, there were two separate phenomenon that were observed during imaging. The first phenomenon, as it is shown in Figure 2-8, includes the thin silver nanowires with small silver particles in semi-spherical shape, which is similar to what was shown before. Figure 2-9 shows the SEM images of the other observed phenomenon. The particles in this image are silver chloride particles that existed in the structure are different than the silver particles, which is consistent with literature[38],[39]. As it was explained earlier in this chapter, silver nitrate and sodium chloride react together and form silver chloride particles. Silver chloride particles are reduced and converted to the silver seed with the help of glucose, which and grow anisotropically in the existence of PVP to produce silver nanowires. As it was observed, a synthesis time of 12 hours was not enough for silver chloride particles to be reduced and converted to silver seeds.

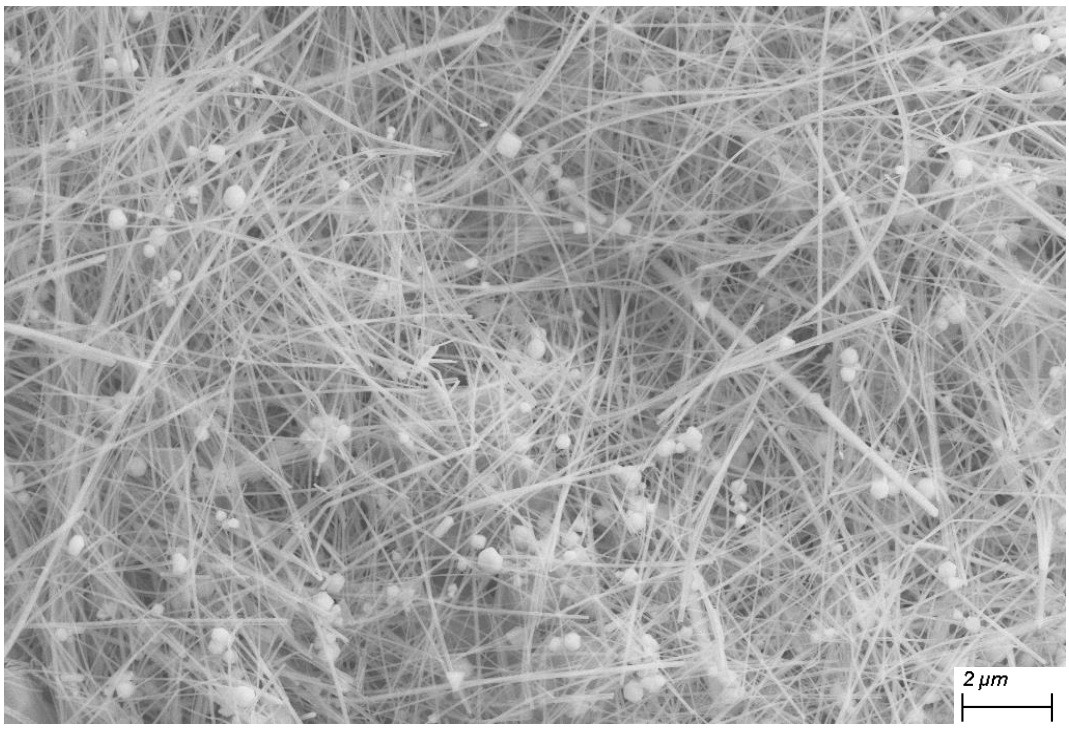

Figure 2-8. SEM image of silver nanowires with a 12 hour synthesis time.

With increasing synthesis time, the silver chloride particles continue to be reduced, resulting in the formation of more silver seeds. Thus, more silver nanowires would be produced. Figure 2-10 shows the silver chloride particles, in addition to the silver nanowires and semi-spherical particle. The concentration of silver chloride particles with a 15 hour synthesis time was still considerable but less than 12 hours. By increasing the synthesis time to 18 hours, the concentration of these particles was significantly decreased. Figure 2-11 shows the silver chloride particles existence in a few parts of the silver particles sample. The silver chloride particles were observed in different batches with the 18 hour synthesis time, but in low concentration. These particles were hardly observed for the synthesis times after 18 hours, such as 21 and 22 hours. Thus, this is likely the time that

almost all the silver chloride particles had been reduced to produce the silver seeds needed for nanowires formation.

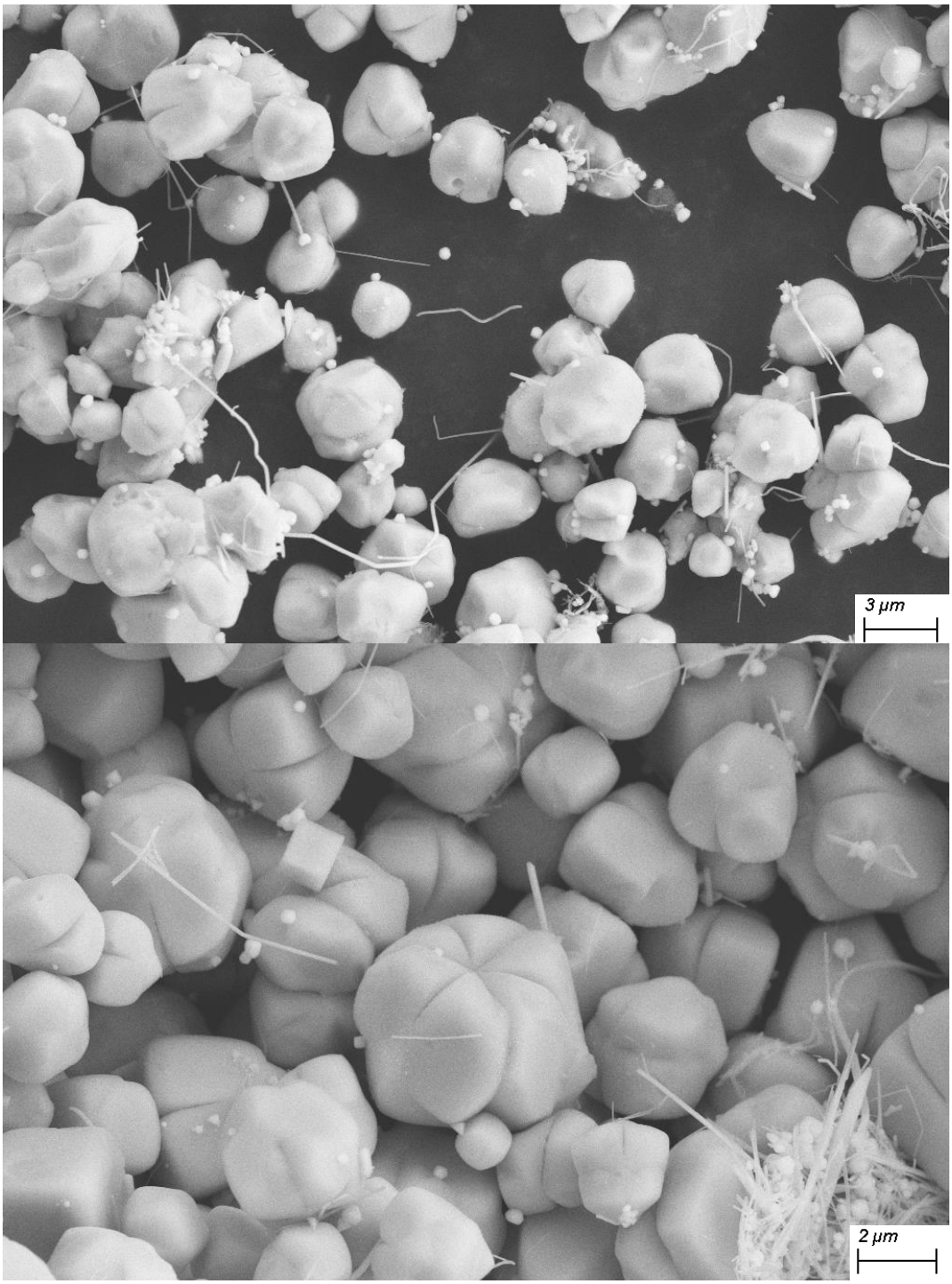

Figure 2-9. SEM image of silver chloride particles with a 12 hour synthesis time.

Figure 2-10. SEM image of silver chloride particles with a 15 hour synthesis time.

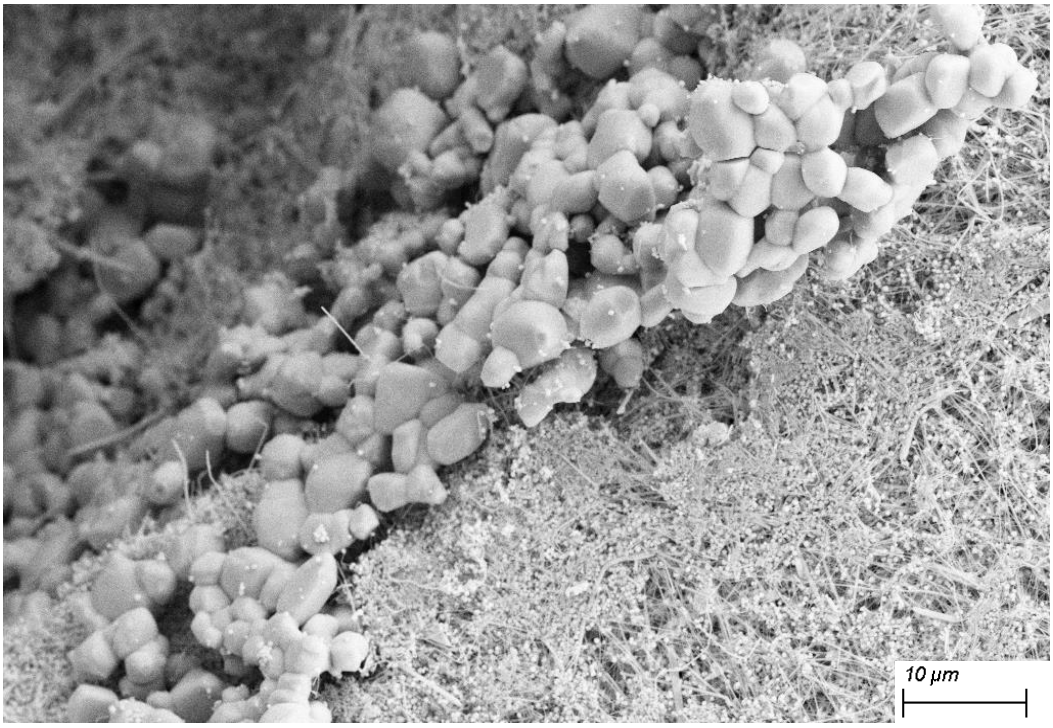

Figure 2-11. SEM image of silver particles with a 18 hour synthesis time.

Although the silver chloride particles were rarely observed with 22 hours synthesis time, we did not find any single silver chloride particles within the 24 hour samples. Figure 2-12 is the SEM image using 21 hour synthesis time. The reason that we chose 21 was to have similar step for the synthesis times. In addition to the two silver chloride particles, that can be seen in this image, the silver semi-spherical particles concentration was considerable. One reason to explain this is that the silver seeds needed more time for adsorbing the PVP and anisotropically growth. However, it also could be related to lack of PVP concentration as well. Thus, we chose the 24 hours as our time for synthesis to be sure that all the silver chloride particles had enough time to be reduced, which resulted in the production of the silver seeds. The silver seeds would then absorb PVP and grow in the [110] direction to produce silver nanowires.

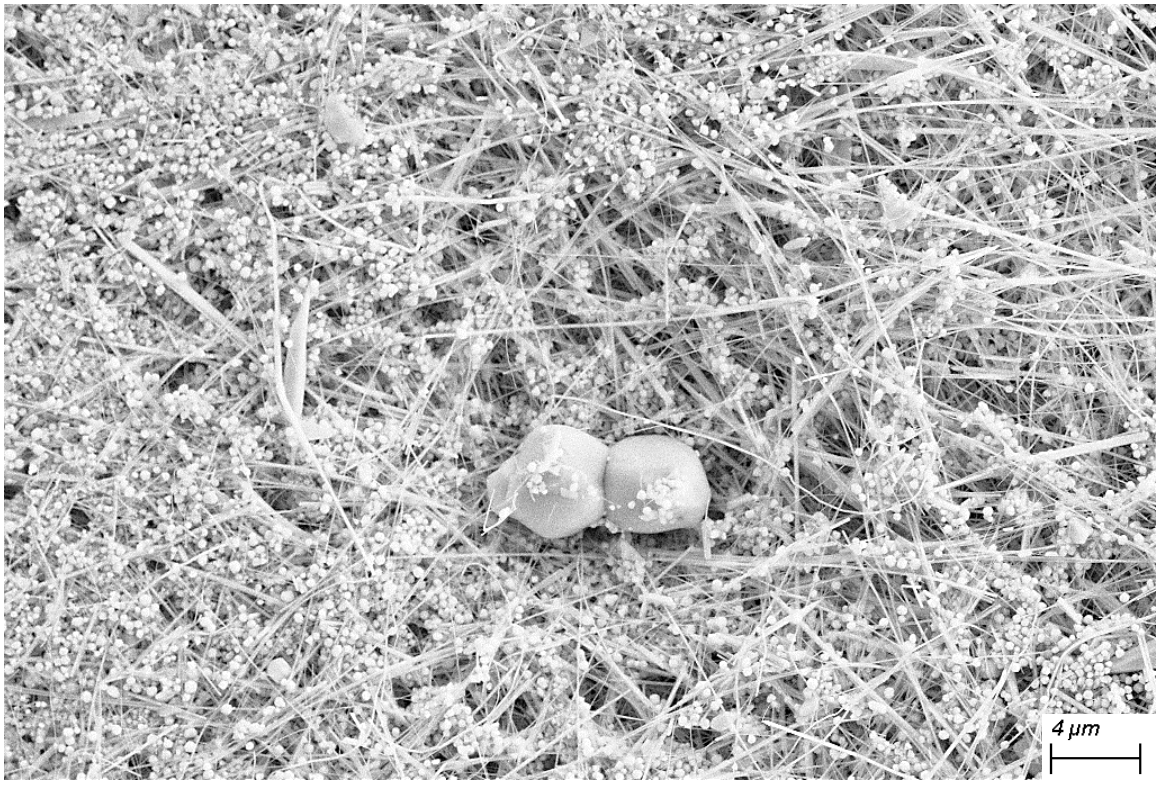

Figure 2-12. SEM image of silver particles with a 21 hour synthesis time.

Figure 2-13. SEM image of silver particles with a 24 hour synthesis time.

XRD patterns of the samples with 12, 15, 18, 21, and 24 hour synthesis times are shown in Figure 2-14. The peaks related to silver are specified with a "*" while the peaks for silver chloride particles are specified with "o". Silver chloride peaks are considerable in the samples with 12 and 15 hour synthesis times. A result that is consistent with the SEM images shown previously, where the large silver chloride particles were the dominant particles rather than the silver particles. Increasing the synthesis time from 12 hours to 15 hours, where the concentration of silver chloride particles decreased, can also be verified with the decrease in intensity of silver chloride particles. As it was mentioned previously, low silver chloride particles were observed in the 18 and 21 hour synthesis time samples. The concentration of these particles was low enough not to see any related peaks in their

XRD patterns. Silver related peaks are for (111), (200), (220), and (311) facets, respectively. For longer synthesis times, the intensity ratio of (111) to (200) facets of silver particles with the FCC structure increased, indicating a reduction in high-index Miller planes being reduced and the enhancement of the (111) abundance in the silver nanowires[25,43]. The calculated lattice constant related to (111) planes is 4.081 $\dot{A}$, which is consistent with standard value (4.086 $\dot{A}$).

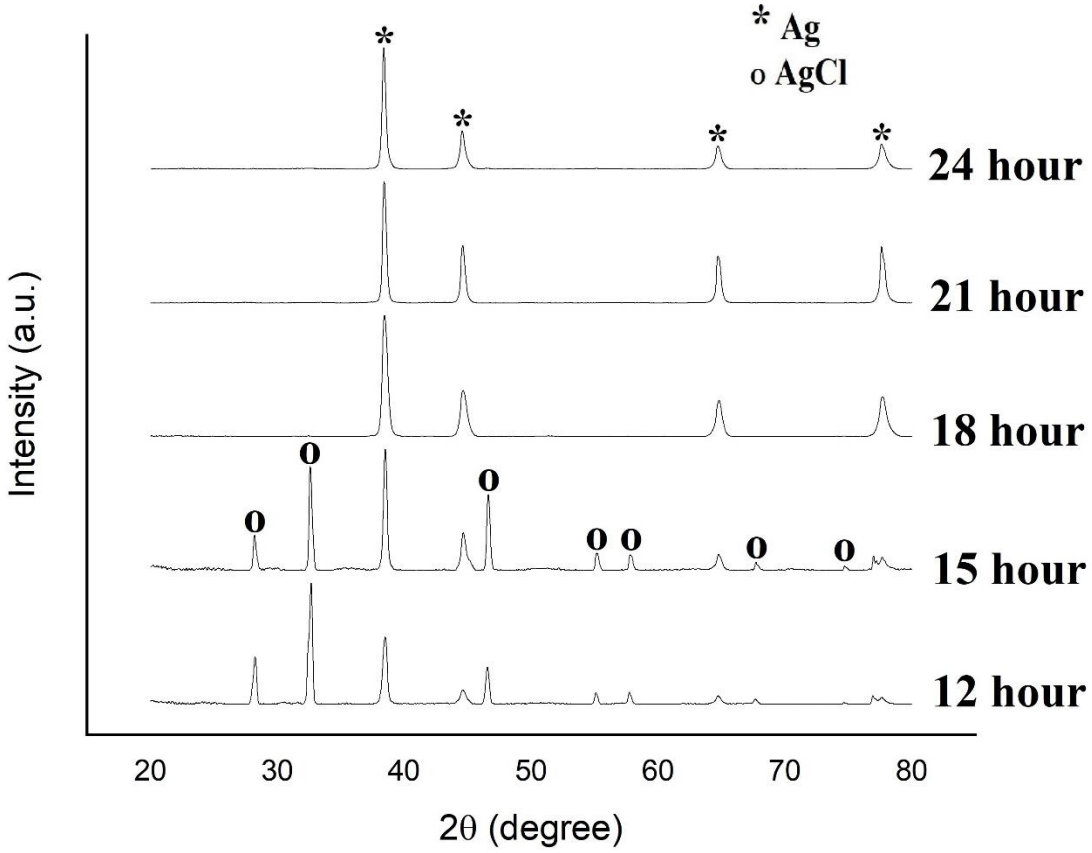

Figure 2-14. XRD patterns for silver samples with 12, 15, 18, 21, and 24 hour synthesis time.

Increasing the synthesis time does not necessarily result in an increase in the yield of nanowires. Two other synthesis times, longer than 24 hours, were tested; however, with a much larger step. The goal was not to find the optimum synthesis time, but to find out how does longer synthesis time affect the yield of silver nanowires. Figure 2-15 and 2-16 show the silver particles for 40 and 60 hour synthesis times. Obviously, the yield of nanowires in these samples were lower than previous ones, indicating that the reactions that happen to form silver nanowires could be reversible, and the nanowires could disappear in this condition to form silver particles that are more thermodynamically stable.

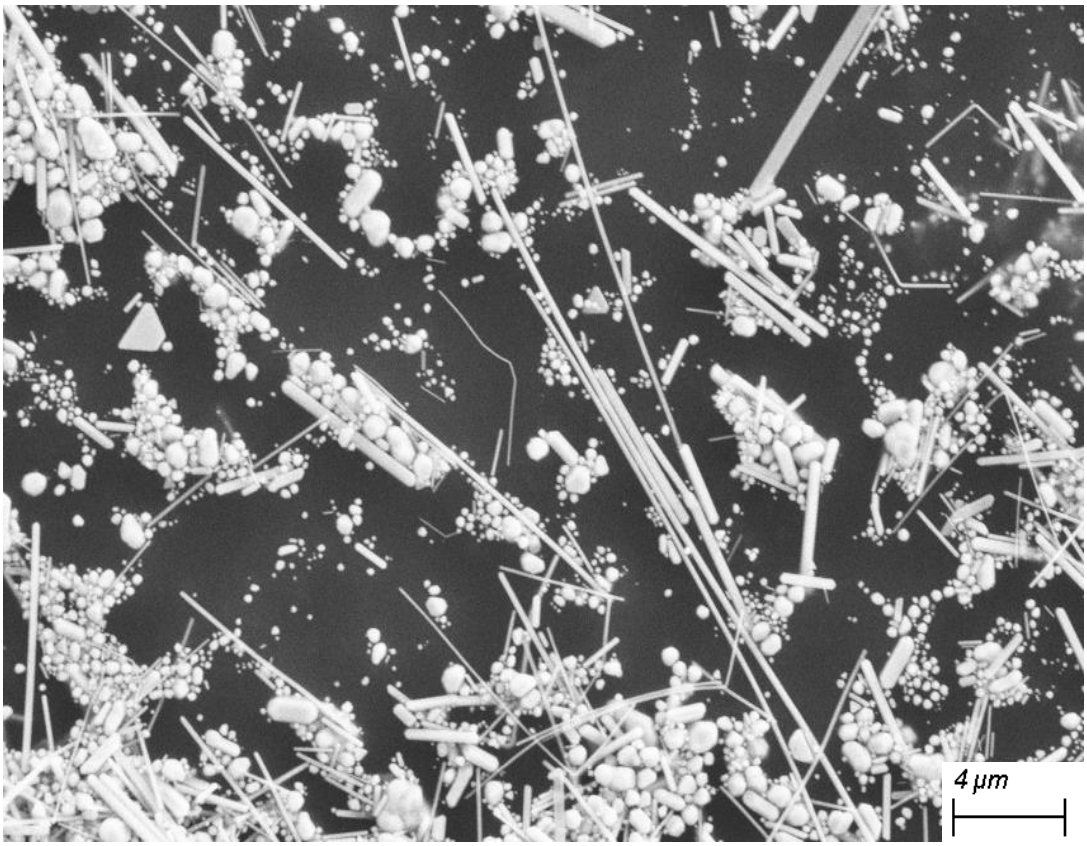

Figure 2-15. SEM image of silver particles with a 40 hour synthesis time.

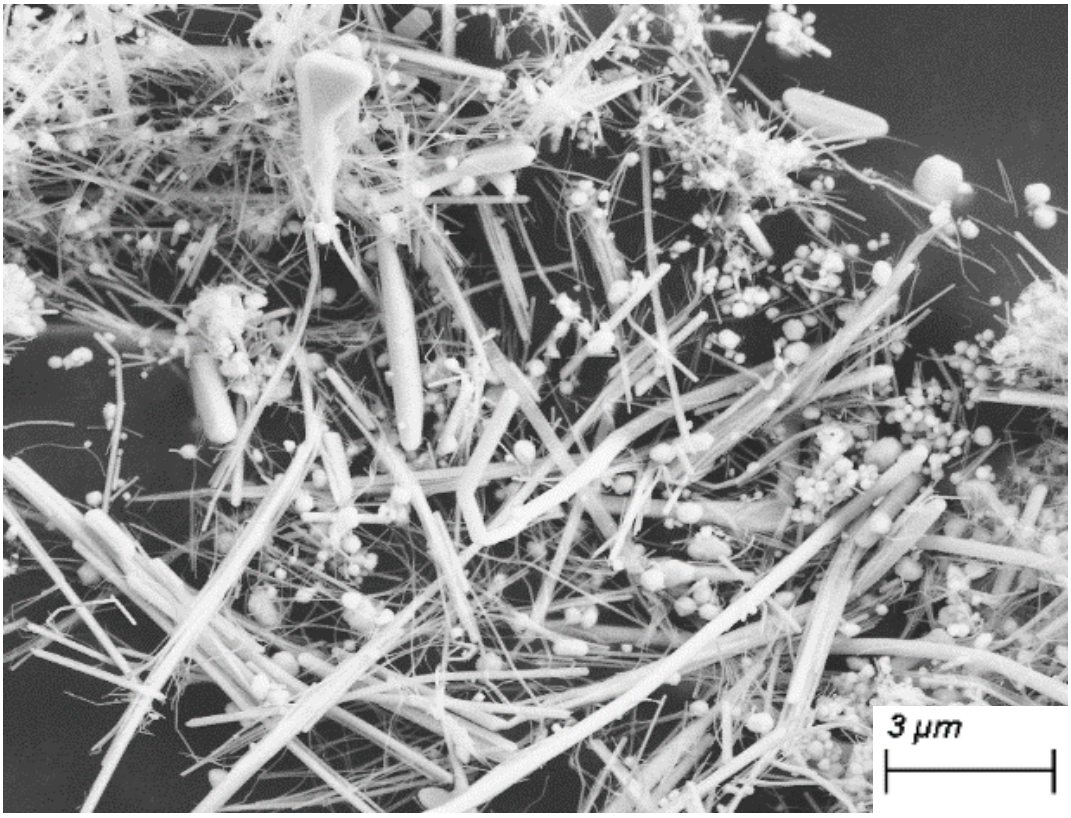

Figure 2-16. SEM image of silver particles with a 60 hours synthesis time.

The next step was to vary the chemical concentrations to see how the yield, length, and diameter of the nanowires would change. Our purpose was to change the synthesis conditions in small ranges, close to the reference literature, to increase the yield of nanowires. As it was explained in chapter one, the silver semi-spherical particles could affect the EO selectivity. The silver nitrate concentration, which is a precursor of silver seeds in the reaction, was selected as the first chemical concentration to vary. In order to choose a new silver nitrate concentration, the growth mechanism of nanowires should be taken into consideration. The existence of silver semi-spherical particles could be due to the abundance of silver seeds during the nanowires growth. Thus, those silver seeds aggregate to each other to form a bigger particle with mostly (111) facets, which is more

thermodynamically stable. Then, to have less excess silver seeds, which would inhibit their aggregation, two lower concentrations were chosen while 0.02 M acted as reference for the silver nitrate concentration. 0.015 M and 0.01 M silver nitrate concentration with other similar synthesis conditions were tested. For the lowest silver nitrate concentration, 0.01 M, as it is shown in Figure 2-17, the silver nanowires existed in the sample; however, the yield of nanowires is very low, and the silver particles, such as semi-spherical particles, were dominant. The reason could be related to the high ratio of PVP to silver nitrate. Generally, the PVP molecules adsorb on the (100) planes and prevent silver seed adsorption on those facets and the silver particles growth in [110] direction, which leads to the production in silver nanowires. By decreasing the silver nitrate concentrations, the silver cations and the silver nuclei decreased while the concentration of PVP was unchanged. Thus, the PVP molecules could adsorb on the (111) as well, which would prevent the anisotropic growth of the silver seeds. Thus, the parametric studies were mostly conducted via the polyol method in the literature[37,44] while the ratio of silver nitrate over PVP was changed.

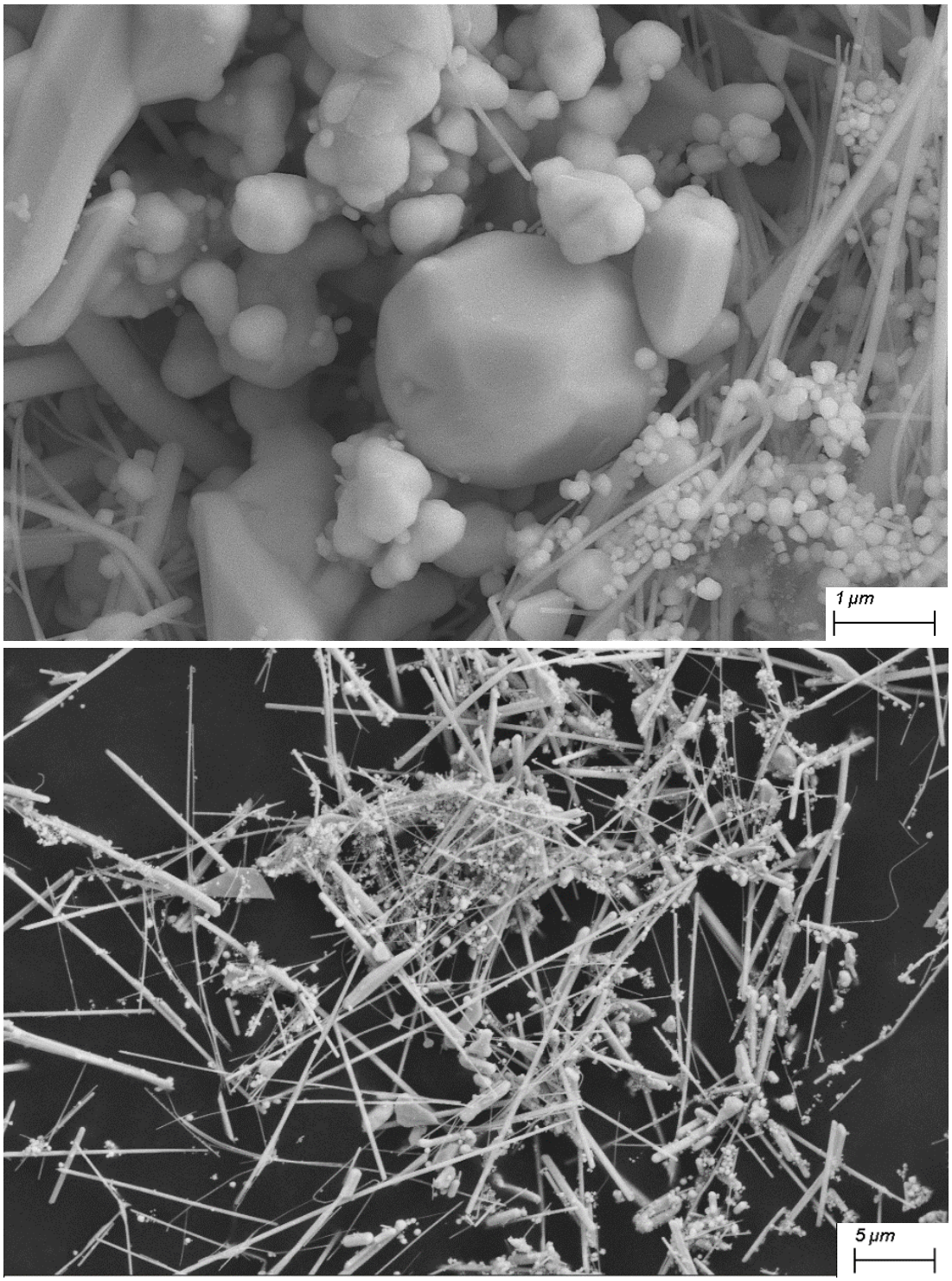

Figure 2-17. SEM images of silver particles with 0.01 M silver nitrate concentration.

Figures 2-18 and 2-19 are the SEM images for silver particles with the 0.015 M and 0.02 M silver nitrate concentrations, respectively. In both samples, a higher yield of silver nanowires was observed when compared to the least concentrated silver nitrate solution that was tested (0.01 M silver nitrate concentration). However, in the sample with 0.015 M silver nitrate concentration, thinner silver nanowires were obtained compared to the 0.02 M sample. This has been reported also in the literature[25] that variation in silver nitrate or any other silver precursor concentration can affect the diameter of nanowires. As a result, a 0.02 M silver nitrate concentration was selected, and the following experiments were conducted in this thesis, based on what was observed with the three different silver nitrate concentrations.

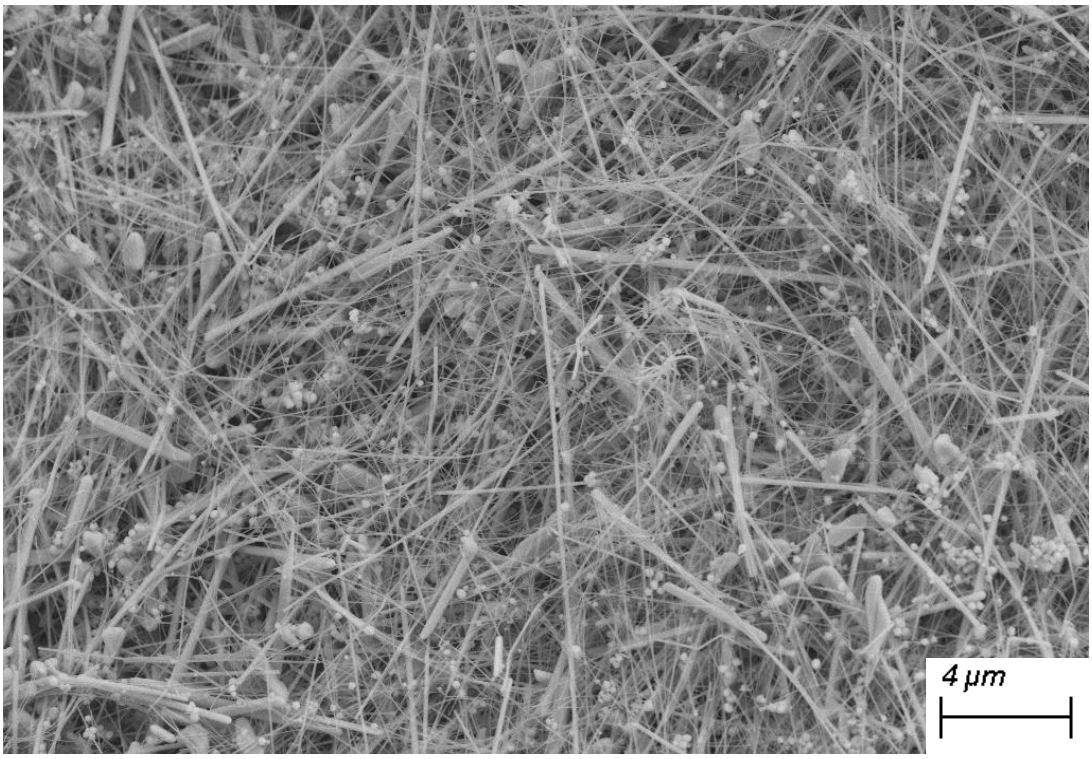

Figure 2-18. SEM image of silver particles with 0.015 M silver nitrate concentration.

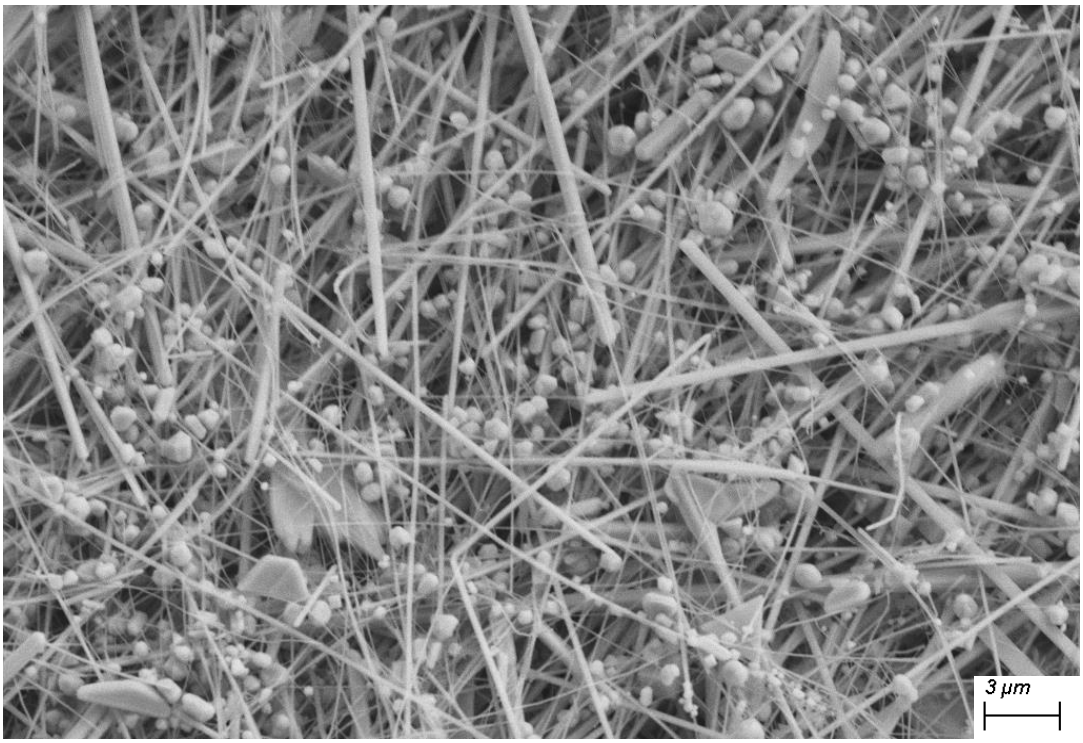

Figure 2-19. SEM image of silver particles with 0.02 M silver nitrate concentration.

As previously mentioned, glucose plays the role of soft reducer in the hydrothermal method for silver nanowires synthesis. The silver seeds concentration, which are needed for nanowires growth, is related to glucose concentration. To investigate the effects of glucose concentration on the silver nanowires yield and diameter, three other concentrations were tested and compared to the main concentration used previously. Mainly 0.12 g of glucose was dissolved into 5 ml of DI water. 0.06 g, 0.18 g, and 0.24 g of glucose, all dissolved in 5 ml of DI water, were used for silver nanowires synthesis and compared to the main point. Qualitatively, by decreasing the glucose concentration the yield of nanowires was decreased, as it is shown in Figure2-20. The reason could be explained in the way that by decreasing the glucose concentration, the rate of silver chloride particles reduction was decreased. It was similar to the increase of the PVP to silver seeds

ratio. Then, the PVP could block the (111) facets as well as (100) facets and prevent the silver seeds from anisotropic growth. Moreover, a lot of nanowires were observed in a different form compared to previous results. These nanowires were not straight as is shown in Figure 2-21. The reason could be related to the shortage of enough silver seeds for those nanowires during the formation to grow thick and straight. By increasing the glucose concentration as double as the main point (0.24 g glucose in 5 ml DI water), the silver nanowires yield was relatively lower than the main concentration point, but the diameter of some nanowires was considerably thicker, as is shown in Figure 2-22. The diameter of these nanowires was exceeded 200 nm. Additionally, these nanowires were in straight form. By increasing the glucose concentration, the silver chloride reduction rate was increased. Thus, the silver seeds concentration was increasing, resulting in a lower ratio of PVP to silver seeds. Excess silver seeds could not find enough PVP molecules to adsorb and grow anisotropically and then aggregated to each other and produced spherical particles at the end. However, some of those silver nanowires that found enough PVP molecules to grow in one dimension direction had enough silver seeds to grow in a straight form and thick diameter. Another silver nanowires sample, including 0.18 g glucose dissolved into 5 ml of DI water, was synthesized as a point between the highest glucose concentration and the main point. The result is shown in Figure 2-23. This sample had a similar nanowires yield compared to the main glucose concentration sample with approximately thicker nanowires. Thus, it was selected as the glucose concentration for the further experiments done in this study.

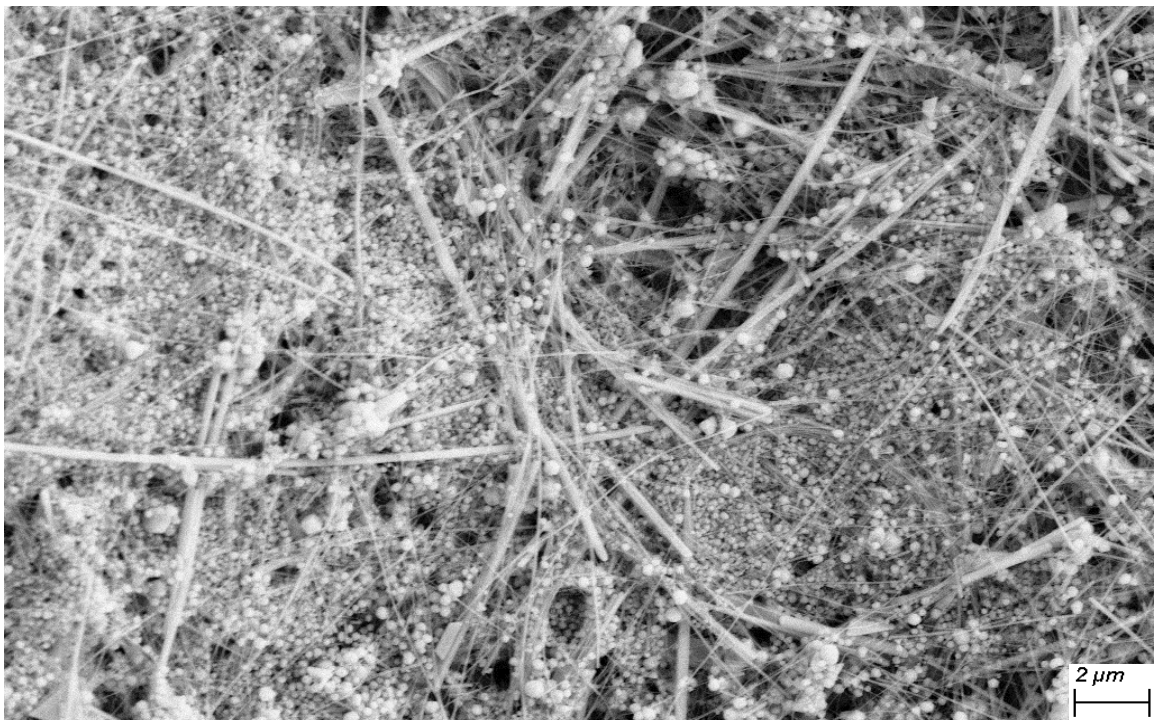

Figure 2-20. SEM image of silver particles with 0.06 g glucose dissolved into 5 ml of DI water.

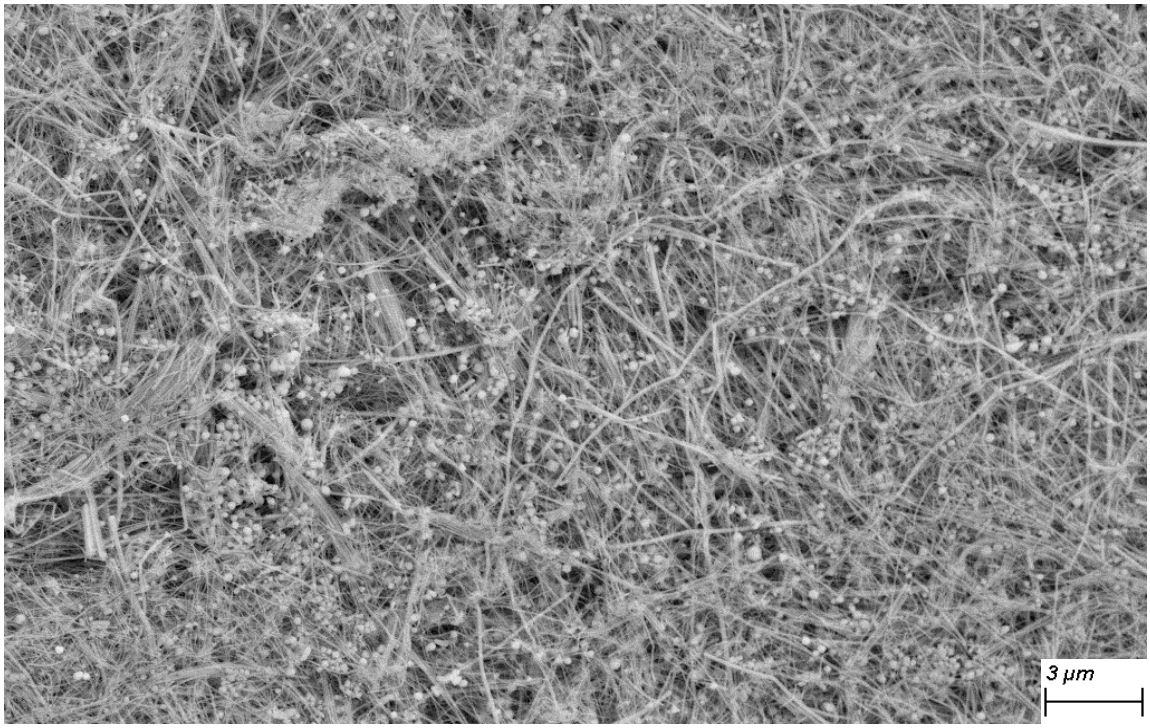

Figure 2-21. SEM image of silver particles with 0.06 g glucose dissolved into 5 ml of DI water.

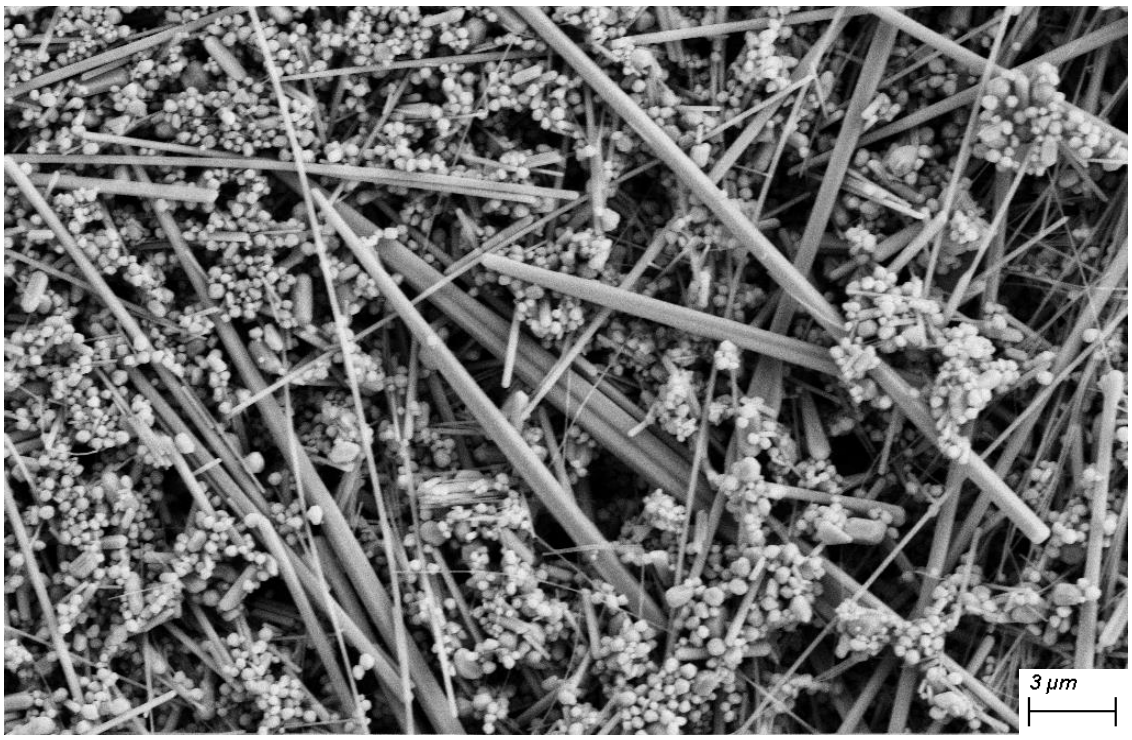

Figure 2-22. SEM image of silver particles with 0.24 g glucose dissolved into 5 ml DI water.

Figure 2-23. SEM image of silver particles with 0.18 g glucose dissolved into 5 ml of DI water.

Silver nanowires then needed to be impregnated on the support to be prepared for reaction conditions. Low surface alpha aluminum oxide is well-known as the common oxide support for ethylene epoxidation reaction catalysts. Incipient wetness/wet impregnation method was mostly used for impregnating silver particles onto aluminum oxide support[24,26,27]. As it was mentioned previously, after the centrifugation step, silver nanowires settled down at the bottom of centrifuge tube and formed a pellet. This pellet-shape of nanowires cannot be impregnated on the support in a uniform distribution. The aluminum oxide support was provided from Saint-Gobain company in form of 8 mm rings with a 0.7 m^2/g surface area and 0.49 m^3/g pore volume. About 3-5 mL of water added to the silver nanowires pellet, which was gently shook, and then mixed with enough powder support in 18-40 mesh size sieve particles to have roughly 10-15% silver on the surface of the support. Then the solution was stirred in less than one minute and put in the oven to be dried at 80℃. In the Figure 2-24, the distribution of nanowires on the low surface area α-Al_2O_3 without stirring is shown. The reason for not stirring the sample might be due to the potential for stirring to break apart the nanowires. The issue with a poor distribution of silver particles on the support is the existence of many spots without any silver particles, which can be attributed to the accumulation of silver particles in other spots, as it is shown in the Figure 2-24. This sample in the reactor might not be effective, since the spots without silver particles are completely inactive in the reaction. Then, stirring was tried to observe the silver particles distribution on the aluminum oxide support. Here, the sample was no longer dried in the oven, but the silver aggregate at the bottom of centrifuge tube were mixed with 3-5 mL of water and then transferred to a beaker, which was heated at same temperature as before on the stir plate under mild stirring condition.

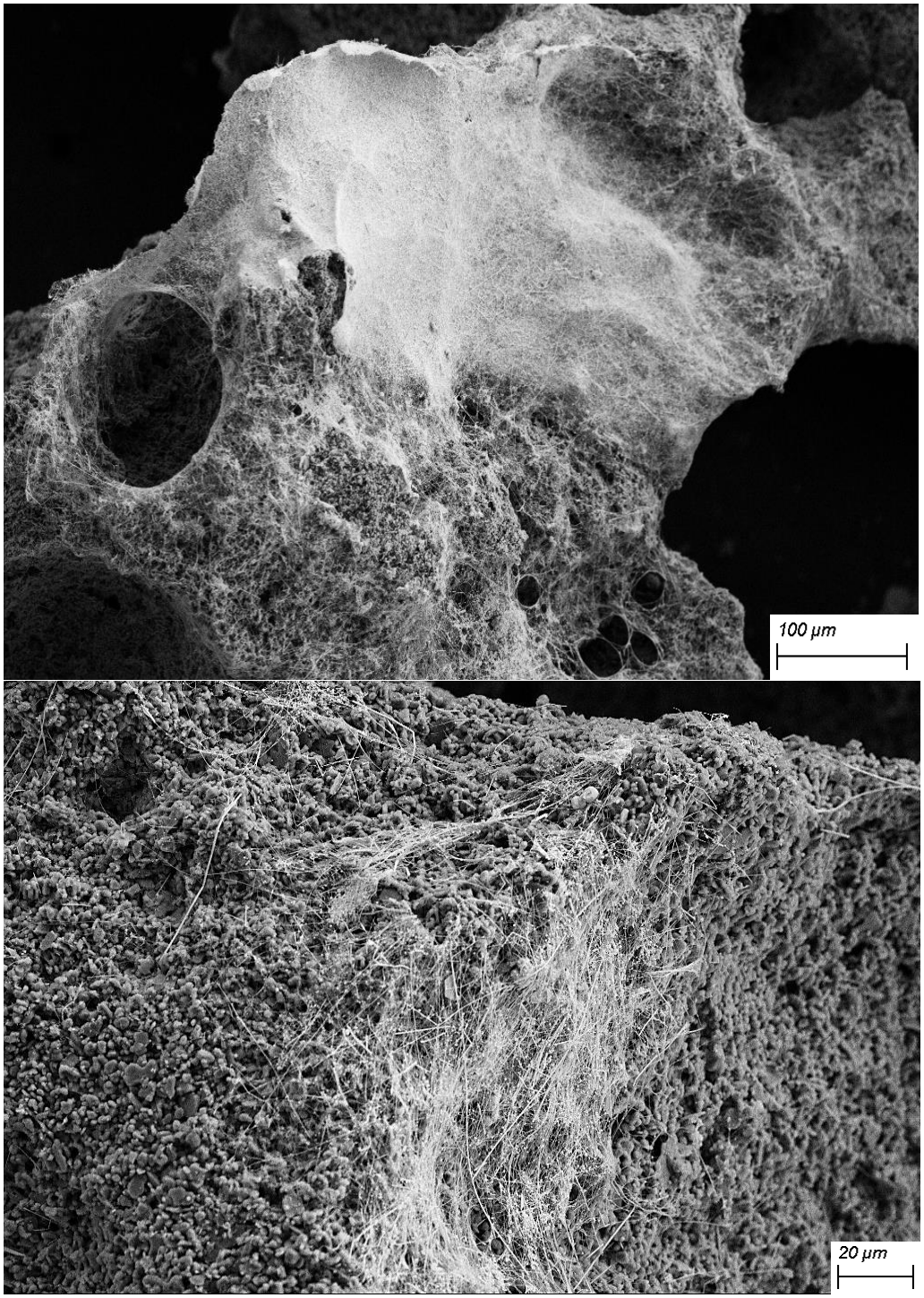

Figure 2-24. SEM images of silver nanowires distribution on low surface alumina support without stirring for impregnation.

Figure 2-25 shows the SEM image of the silver nanowires distribution on the low surface area aluminum oxide support. The surface composition for silver was about 10%, according to EDS. However, another issue was observed in this condition, as shown in Figure 2-26. A lot of silver semi-spherical particles were stuck to the silver nanowires and block by them. This could block the (100) facets of silver nanowires and make them inactive as a result.

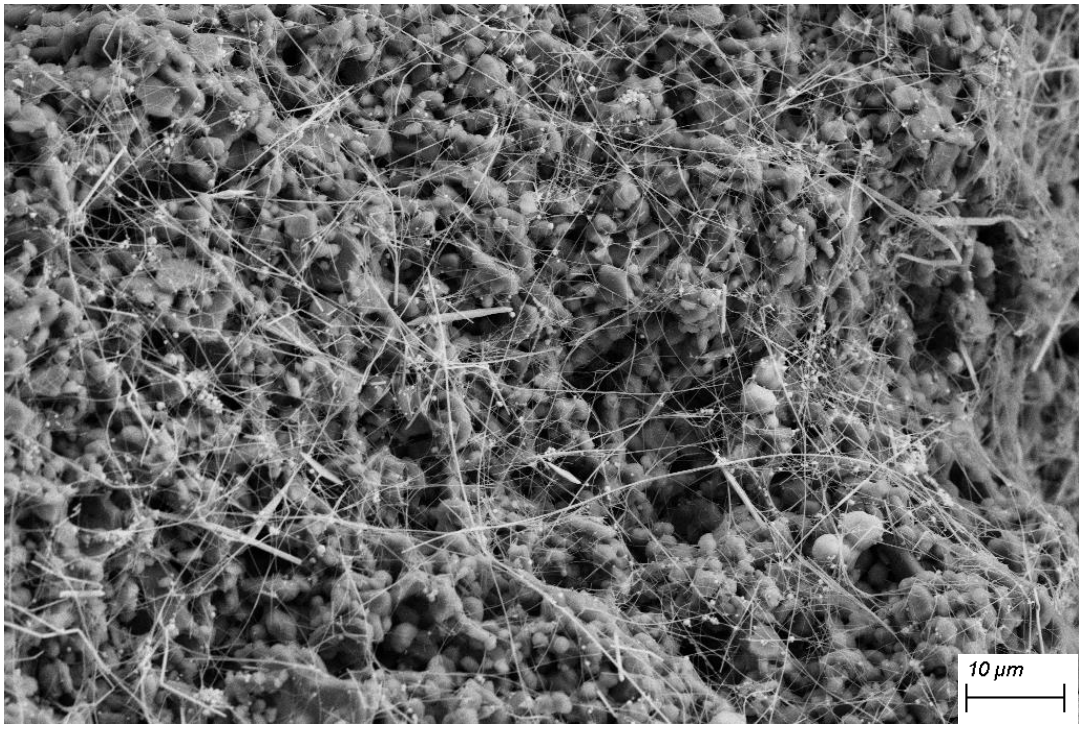

Figure 2-25. SEM image of silver nanowires on the aluminum oxide support with using mild stirring condition for impregnation.

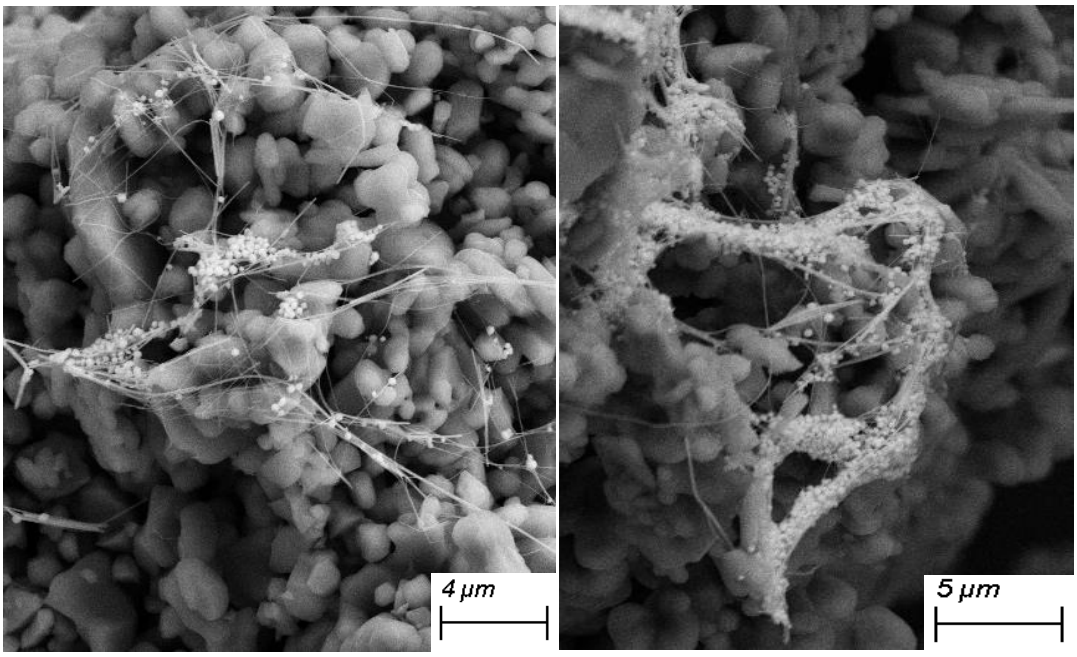

Figure 2-26. SEM images of sticking silver spherical particles to the silver nanowires.

The same phenomenon was also observed when another type of low surface area aluminum oxide support was used. 1-2 mm ball-shape low surface aluminum oxide was provided from Tipton Corp. company. The same procedure, as mentioned previously, was repeated to impregnate silver nanowires on the ball-shape support. Sticking of silver semi-spherical particles to the silver nanowires existed in this sample as well, as it is shown on Figure 2-27. Additionally, what was observed in large scale SEM imaging, shown in Figure 2-28, brought us to the conclusion that the silver particles were placed just physically on the support. The silver particles, including silver nanowires, were covered in a thick layer form on the 1-2 mm ball particles. They easily were separated and removed from the support by hard shaking.

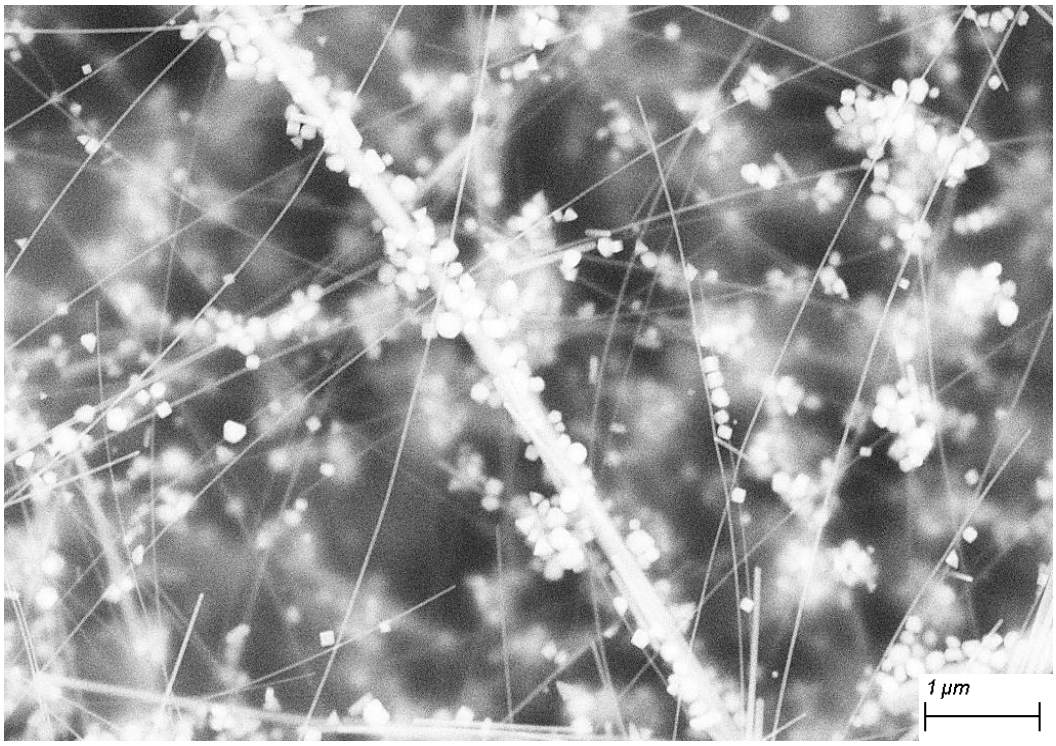

Figure 2-27. SEM image of sticking silver spherical particles to silver nanowires after impregnation on ball-shape alumina support.

One of the similar steps between impregnating the silver particles on both aluminum oxide supports, as mentioned previously, was the solvent that was used for said step. In the next step, ethanol was used as the solvent for impregnating the silver nanowires on the alpha alumina supports. Although other solvents other than DI water and ethanol were not tested, it was found that it is crucial to use ethanol as the solvent for this step. This fact is reported in the literature as well[27]. The distribution of silver nanowires was not perfect using water as solvent and stirring under mild condition during the drying of the solution of silver particles in the solvent. Thus, ethanol was chosen as solvent for impregnating silver nanowires on the alumina support in this study.

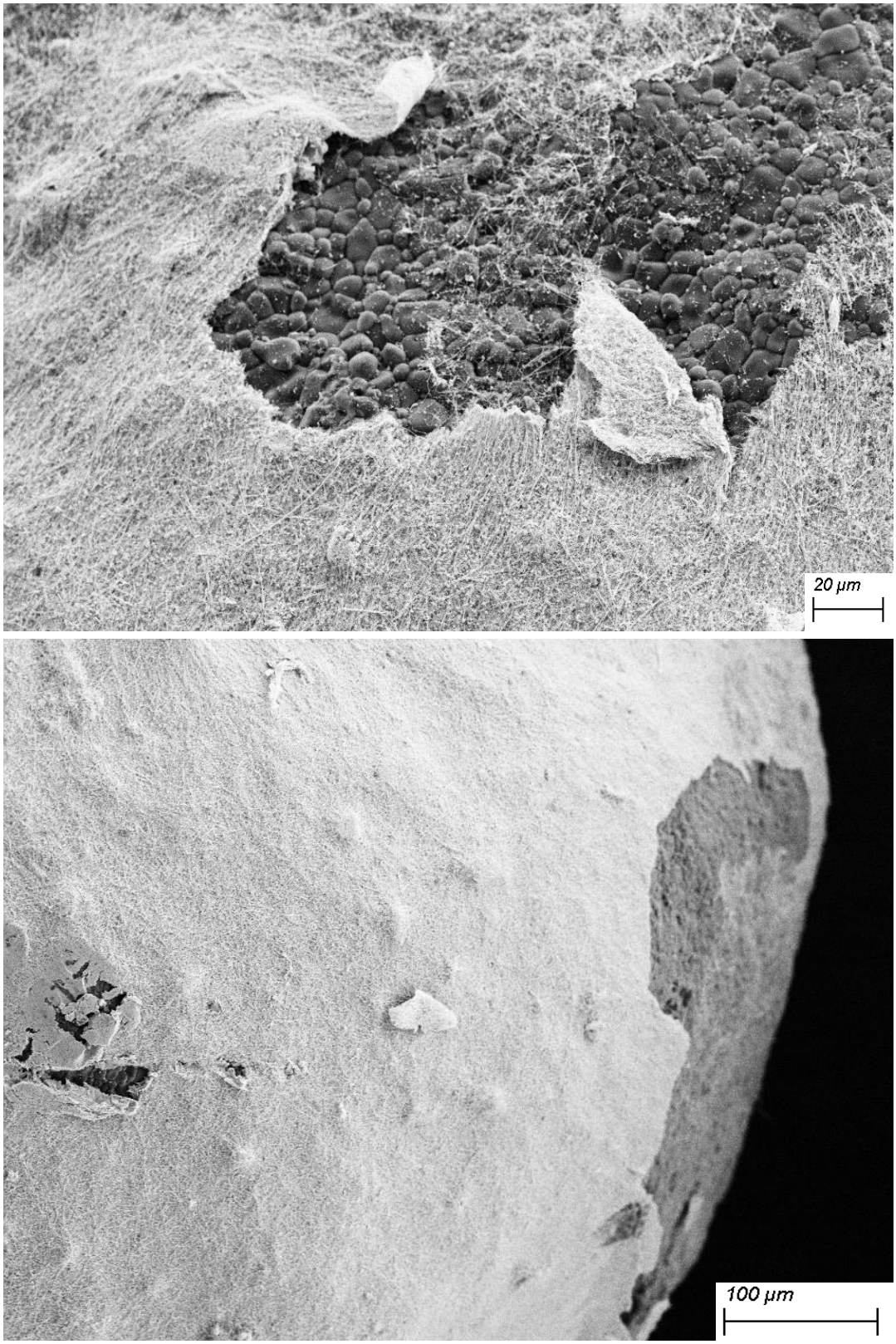

Figure 2-28. SEM images of silver particles on the ball-shape alumina support.

Depending on the centrifuge time and rpm and the number of centrifuge cycles, some big silver particles were occasionally observed during SEM imaging, which was probably because the silver particles formed a stronger pellet after centrifugation. In order to solve this issue, sonication was used to make a suspension of silver particles in ethanol. After centrifugation, the supernatant was removed completely, then the aggregate was weighed from the sample in order to calculate mass of support needed for making 10-15% of supported silver catalyst. Then, 3-5 ml of ethanol was added to the centrifuge tube and the solution was sonicated for 10-20 minutes. The color of the solution was gray and there should not be any large particle of silver in the solution. However, it needed to be checked whether the sonication can break the nanowires or not. After sonication, some droplets of suspension were dropped on the SEM stub pin and were left to dry for a couple of hours to be ready for conducting the SEM images in FESEM instrument. Figure 2-29 shows the sonicated silver nanowires without the support. The SEM image of this sample showed that the nanowires were not broken, and the sonication did not decrease the yield of nanowires. Thus, the sonication was concluded to be the crucial step needed to impregnate the silver nanowires on the support. Figure 2-30 shows the SEM image of silver nanowires using ethanol as the solvent for impregnation, sonication, and stirring; mild stirring conditions are also a crucial parameter needed for making a good silver supported catalyst. In this figure, ball-shape alpha alumina support was used. Figure 2-31 shows the SEM images of silver nanowires on the SA5562 low surface area alpha alumina support, which were synthesized using the same procedure previously discussed. These images were taken from different catalyst particles to be sure that silver nanowires were distributed perfectly in the various particles.

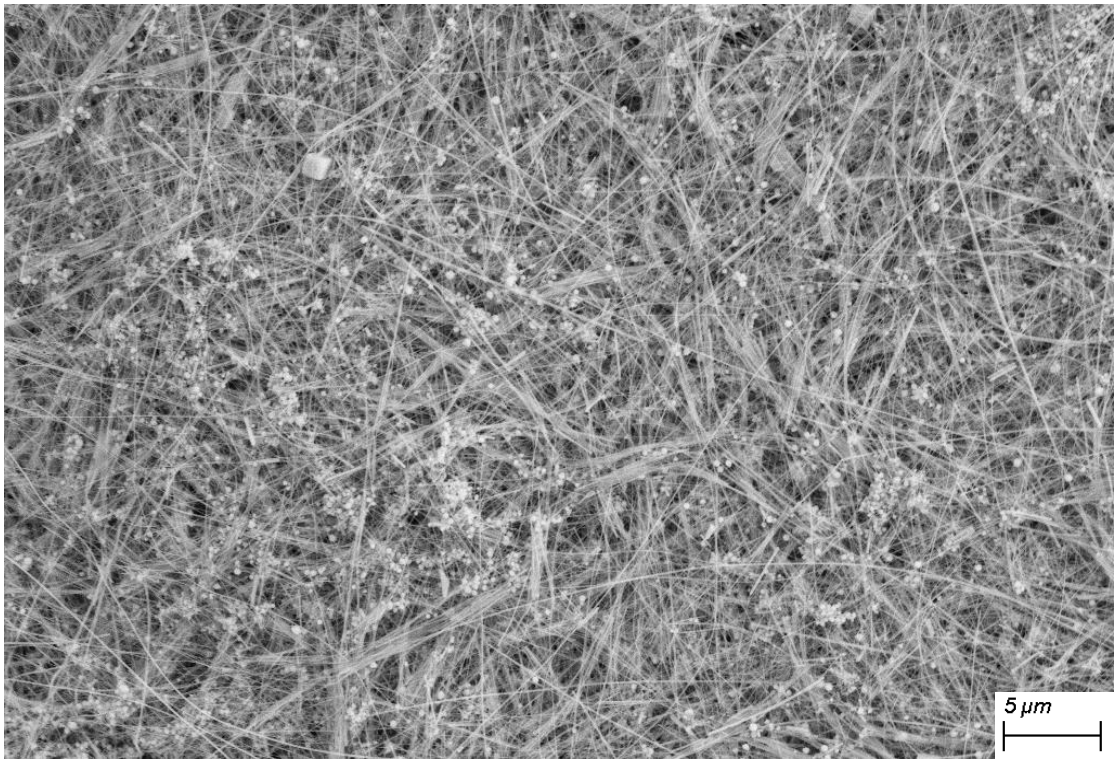

Figure 2-29. SEM image of unsupported silver nanowires after sonication.

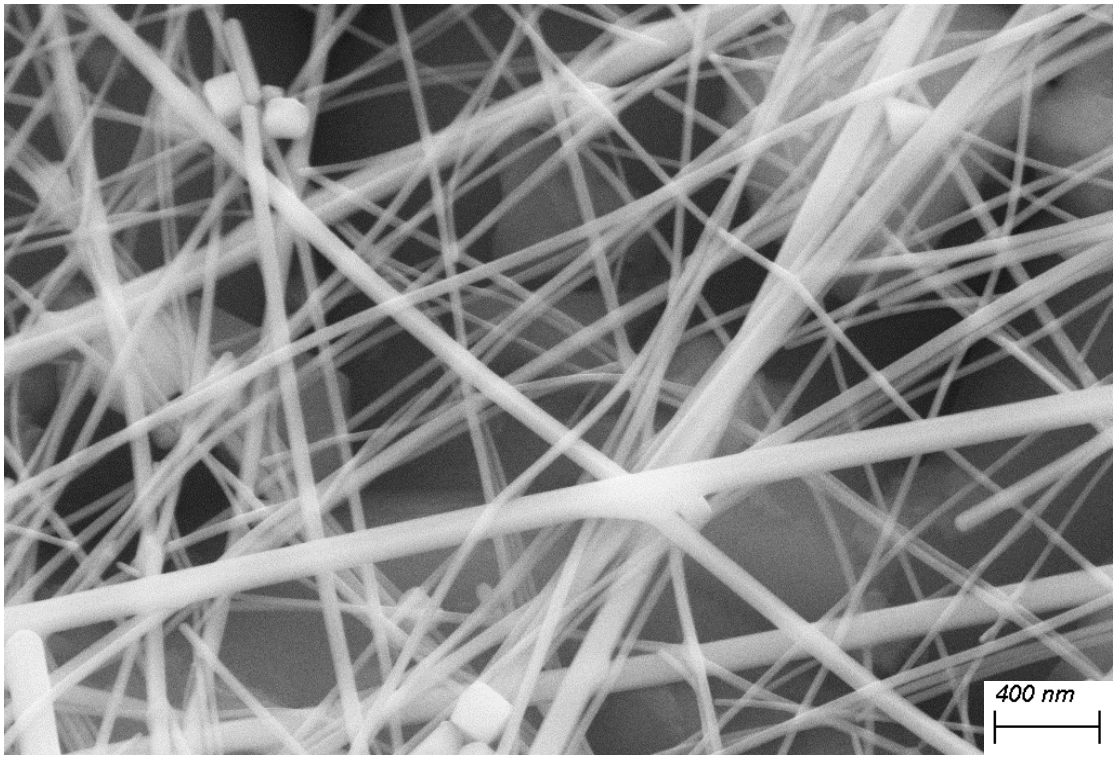

Figure 2-30. SEM image of silver nanowires on the ball-shape alumina support.

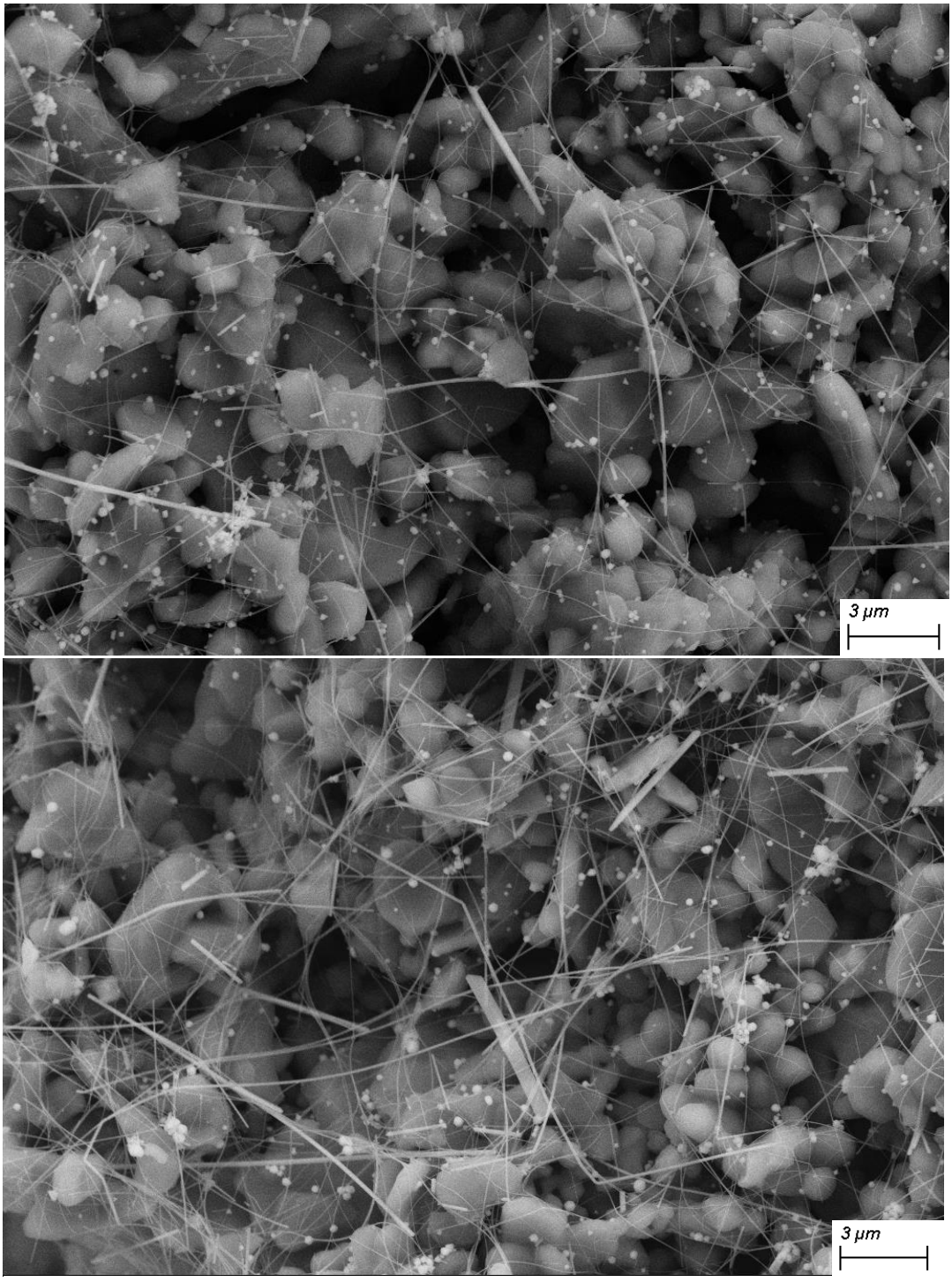

Figure 2-31. SEM images of well-distributed supported silver nanowires

Figure 2-32 shows the EDS element mapping and patterns for the related SEM image shown as well. In the EDS mapping, the green, red, and yellow colors belong to silver, oxygen, and aluminum, respectively. Silver surface composition is about 11% in this spot, which is the same as many other spots EDS mapping was conducted on; this shows that the silver nanowires were distributed uniformly with about 11 wt% in all the support's surface.

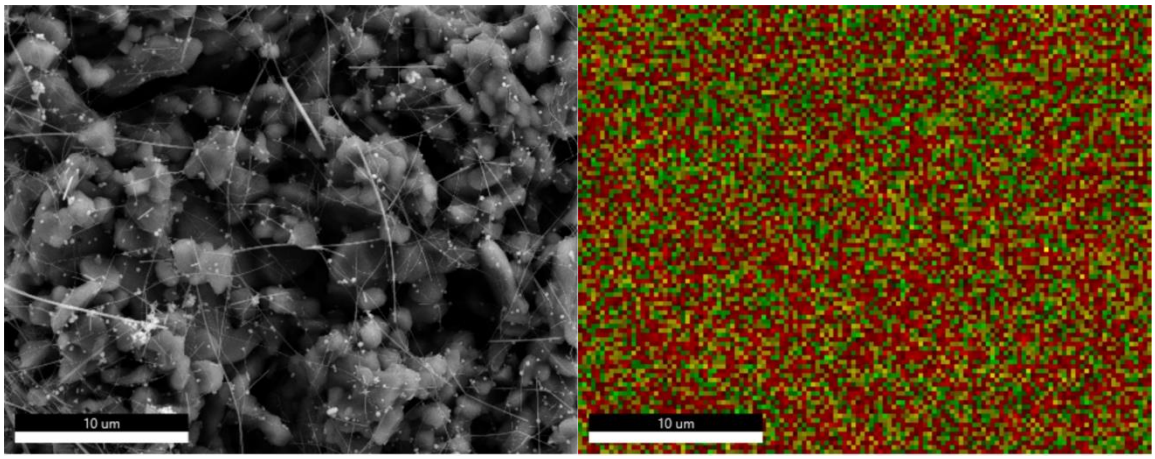

Element	Weight %
O K	43.76
AlK	45.52
AgL	10.72

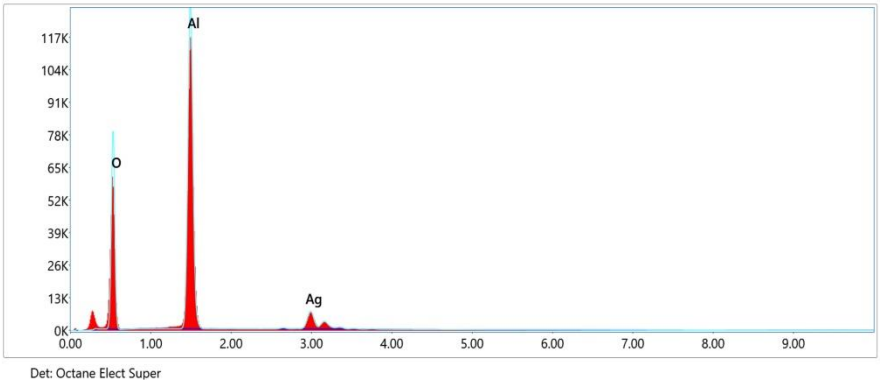

Figure 2-32. SEM-EDS image and mapping of silver nanowires on the alumina support.

2.2 Polyol Method

The polyol method is known as the most successful and popular method for synthesizing silver nanowires and silver nanocubes[45,46]. Although this method was introduced first by another group[47], Xia's group applied this method on metal nanoparticles synthesis such as silver and then developed it to the modified polyol process[25,48,49]. In the polyol process, ethylene glycol thermally decomposes to the acetaldehyde and water. Then silver cations, which bond to a lone pair electron of atomic oxygen, react with acetaldehyde easily, as their chemical potential was decreased, to produce the silver seeds and glycolaldehyde. In the next step the silver seeds were assembled, which leads to the production of the silver MTPs which are mostly in decahedral shape[45,50].

$$HOCH_2CH_2OH \xrightarrow{\Delta} CH_3CHO + H_2O$$

$$2Ag^+ + 2CH_3CHO \rightarrow 2CH_3COOH + 2Ag^0$$

The reason that silver seeds form the decahedra shape of MTPs is because they include(111) facets that are the most thermodynamically stable facets[35]. Due to the energy level of MTPs, more silver seeds are adsorbed on the MTPs surface, followed by the crystallization of silver seeds and the uniaxial elongation of MTPs, which result in the formation of silver nanorods[35]. Afterward, PVP molecules contribute to silver nanowires production where the nitrogen and oxygen atoms of the PVP react weakly to the (100) planes of silver nanorods to stabilize them and prevent further growth. Thus, silver nanorods start growing in [110] direction and produce silver nanowires. Figure 2-33 shows a schematic procedure of nanorod growth from the MTP particles with a pentagonal cross section[51]. Figure 2-34 shows a 3-D truncated decahedral of a nanorod with silver atoms arrangement and different faceting such as (100) and (111) and the FCC unit cell with a

lattice constant indicated with the letter "a"[52]. The same silver nanowire structure was observed in our samples. Figure 2-35(a) shows the SEM image of a single nanowire's end with the facets described in literature, as mentioned previously. The (111) and (100) facets, and [110] direction, which is the direction of nanowire growth, are specified with yellow. Moreover, an SEM image of two edges of a single nanowire is shown in the Figure 2-35(b). Two areas of different (100) facets were selected with red dashed boxes separated with a yellow dashed line. The SEM images in Figure 2-35 could be the proof of the same cross section and growth mechanism of silver nanowires that were synthesized in this study, as what have been done in the literature.

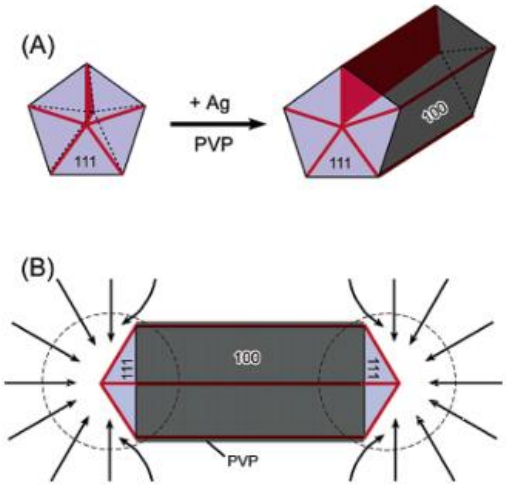

Figure 2-33. Schematic of silver nanorods formation from silver MTPs [51]

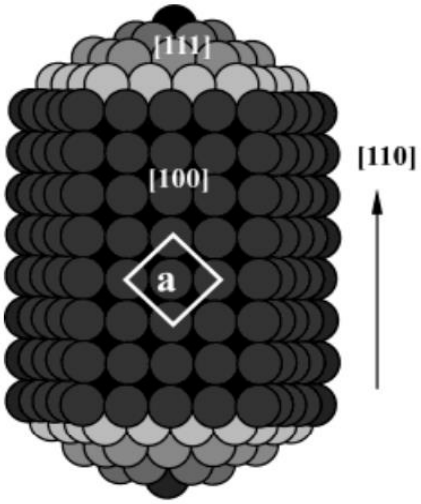

Figure 2-34. 3-D scheme of silver nanorod [52].

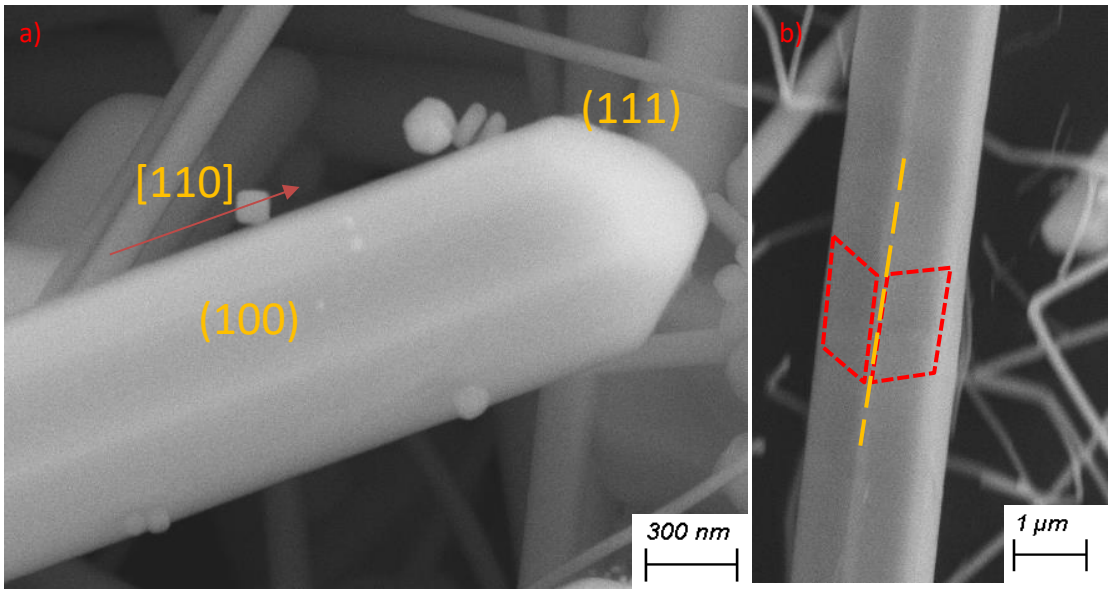

Figure 2-35. Structure of a single silver nanowire.

Experimental Procedure:

The focus in this study was on the hydrothermal method as one of the synthesis methods for making nanowires. However, the polyol method was first selected for making silver nanowires, much like previous studies operating supported silver nanowires for epoxidation reactions[24,26,27]. All the attempts before a change in one of the crucial steps, which is going to be explained in detail later, was unsuccessful. Changing in pivotal synthesis parameters such as PVP/$AgNO_3$ concentrations, injection rates, synthesis times, and temperatures did not change the outcome. It was found out that there is a crucial step during synthesis that was not mentioned by most papers. First, 5 mL of ethylene glycol is poured in a three-neck beaker, which is then connected to a reflux system (to avoid possible ethylene glycol evaporation) and heated up to 160 ℃ and left for an hour. During the meantime, following solutions were prepared: 0.1 M silver nitrate in 3 mL of ethylene

glycol and 0.6 M PVP in ethylene glycol. These two solutions were injected into the three-neck beaker containing ethylene glycol over the period of one hour, with a two-channel syringe pump at a rate of 0.375 mL/min. The schematic of the synthesis system we used is shown in Figure 2-36. The solution should be stirred at a vigorous stirring condition for an hour. The stirring rate is the crucial step was mentioned previously. 300 and 400 rpm were tried for the first attempts, but not a single nanowire was observed in the sample. Increasing the rpm to 550 rpm resulted in silver nanowire formation. The solution was then cooled at room temperature for a couple of hours and centrifuged at 2500 rpm for 20 minutes; this process was repeated a total of four times, two times with DI water and two times with ethanol. Then the supernatant was removed and the aggregate, including silver particles, was put on the SEM stub pin to be dried for a couple of hours.

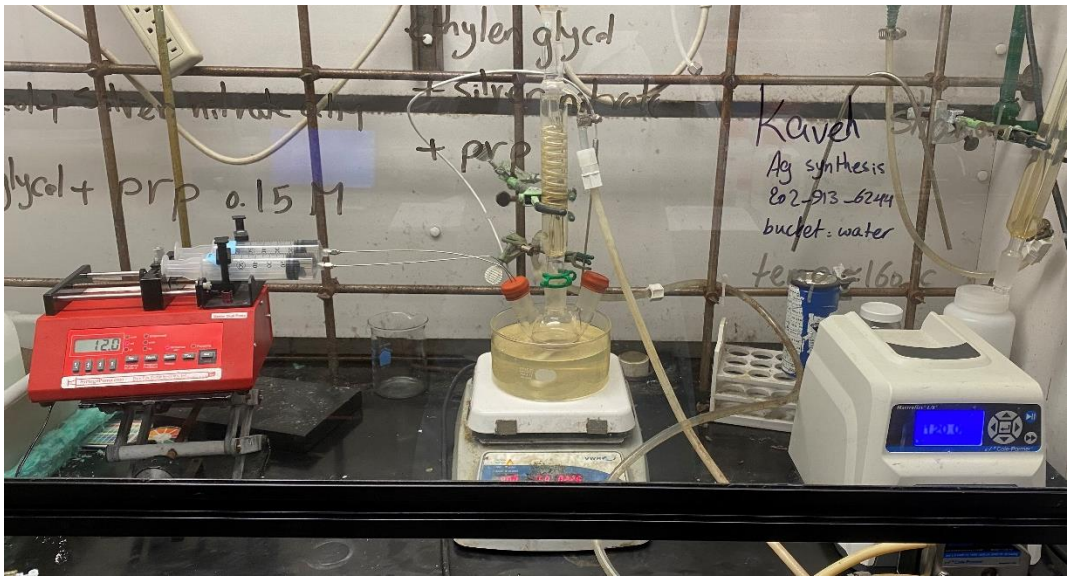

Figure 2-36. Experimental setup for synthesizing silver nanowires via the polyol process.

Figure 2-37 shows the SEM image of the silver nanowires in higher magnification. A larger scale SEM images is shown in Figure 2-38. Although the yield of silver nanowires made by polyol process here was qualitatively lower compared to silver nanowires synthesizes with hydrothermal method, the nanowires obtained by polyol process had uniform diameter. Silver nanowires, shown in Figure 2-37, have a diameter of about 170 nm. Then, based on what was obtained from Figure 2-38, it was concluded that the nanowires synthesized with polyol process at the conditions mentioned previously, had a uniform thicker diameter of about 170 nm, but lower yield compared to the hydrothermal method. This uniformity of silver nanowires is an important feature for gauging the performance of the catalyst in the reactor, since particles with different size (diameter in case of nanowires) showed different EO selectivity[24].

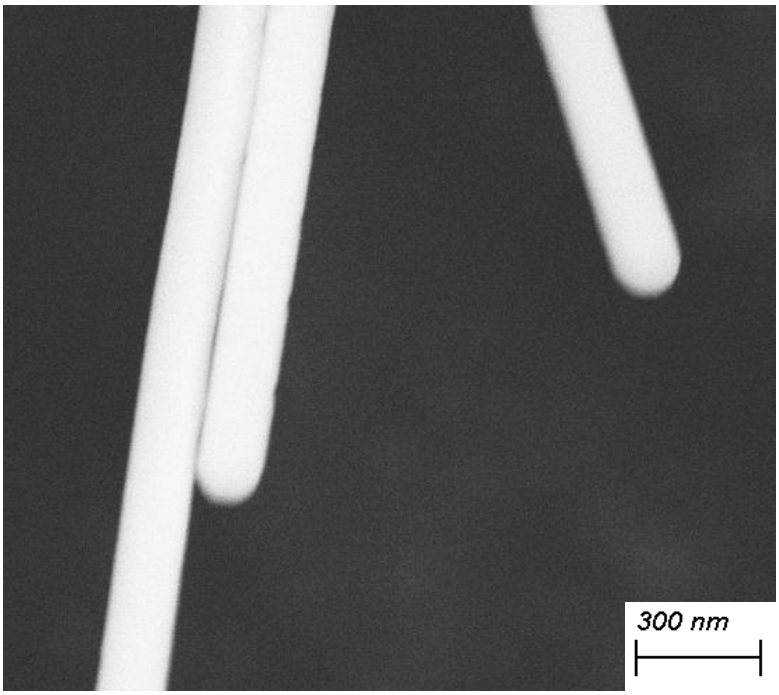

Figure 2-37. SEM image of silver nanowires with higher magnification.

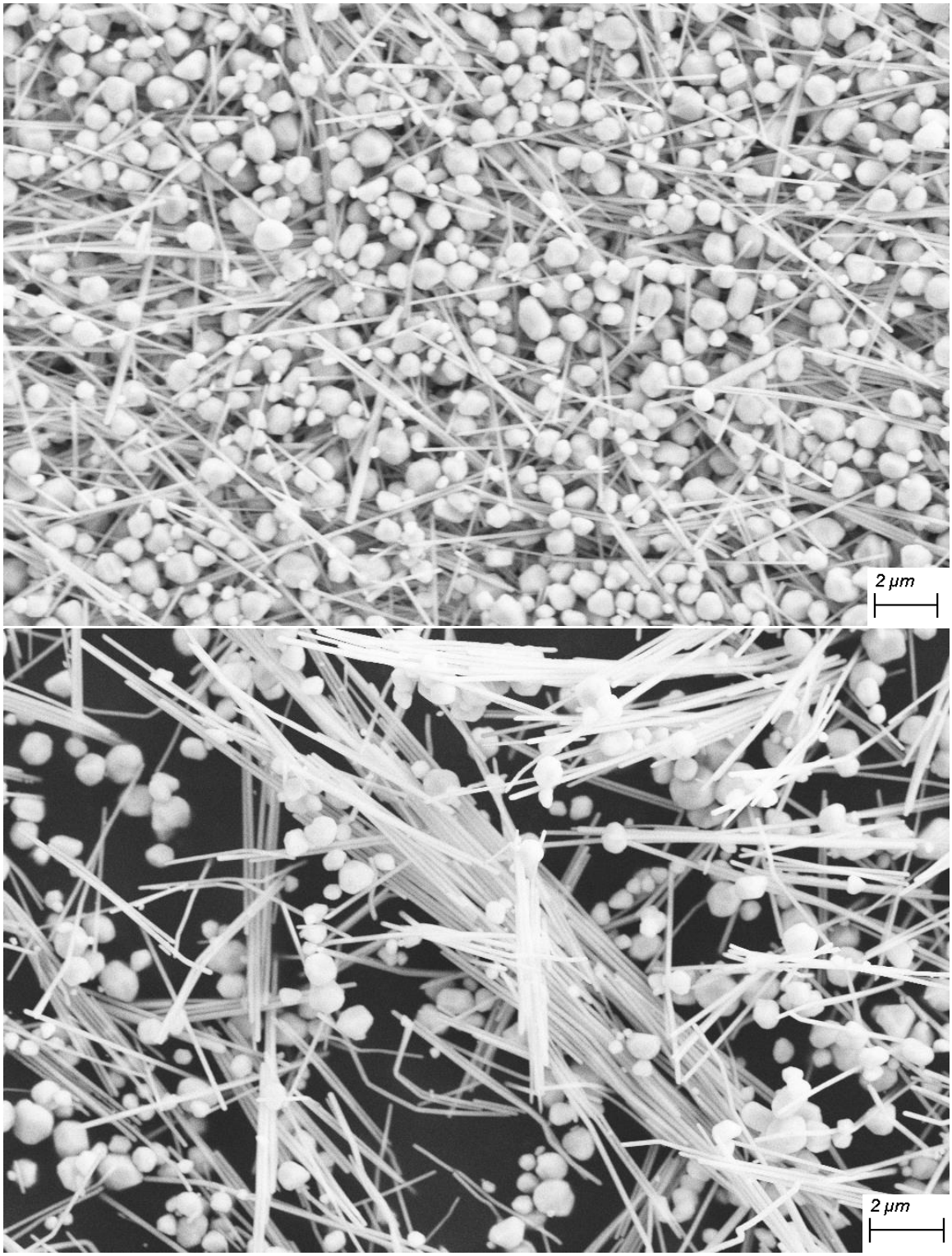

Figure 2-38. SEM images of silver nanowires synthesized via polyol process.

2.3 Wet Impregnation and Incipient Wetness

Silver spherical particles were synthesized using wet impregnation method as mentioned in the previous studies[7,31]. In order to make 2 g of 15 wt% supported silver catalyst with semi-spherical silver particles, 1.7 g of low surface area aluminum oxide support, that was provided from Saint-Gobain co. as mentioned previously, in a powder form (18-40 mesh size particles) was first pre-calcined and then was added to a solution of silver nitrate including 0.47 g $AgNO_3$ dissolved in slight excess of water. The amount of water needed for incipient wetness was calculated based on support pore volume and checked by titrating the support to reach the incipient wetness point. Then, the solution was dried at 80℃ under mild stirring condition for a couple of minutes. After water evaporation, the sample was put into the oven for calcination at 450℃ for 12 hours in atmospheric air for the full decomposition of the nitrate precursor. It has been noted that at a temperature below 400 ℃, the nitrate precursor does not decompose completely[31]. Figure 2-39 shows the SEM images of silver particles on the aluminum oxide support. Darker particles belong to aluminum oxide while the lighter, spherical particles belong to silver.

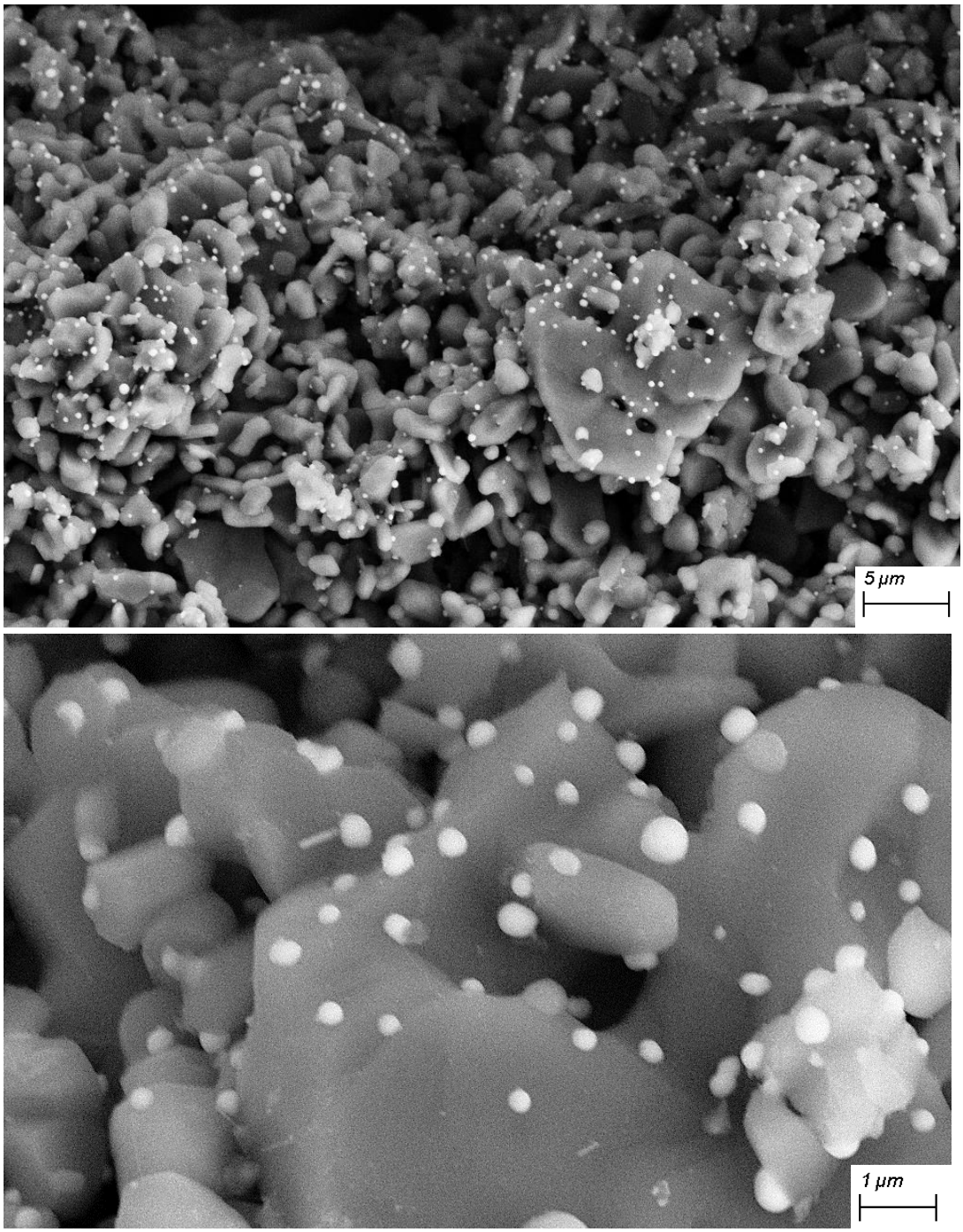

Figure 2-39. SEM images of silver particles on the aluminum oxide support synthesized via wet impregnation.

CHAPTER 3

REACTOR PREPRATION

The reactor system that was set up in this study included a single, vertical reactor for testing the silver catalysts supported on α-Al_2O_3 supports; the analysis portion of the reactor included a gas manifold and a gas chromatograph for analyzing the reactor effluent as shown in Figure 3-1. Ethylene and hydrogen gases pass through a backflow arrestor (indicated by bright pink in Figure 3-1) and are then connected to a 5850E Brooks mass flow controller (MFC). Oxygen and nitrogen gases also pass through two separate 5850E Brooks mass flow controllers, which all connected to a Brooks 0154 MFC controller box. All the gases are assumed to be well-mixed through a combination of ¼" stainless steel tees, port connectors, and tubing before the reactor. The MFC is connected to both ethylene and hydrogen lines, which has a Swagelok three-way valve before the backflow arrestor to switch between ethylene and hydrogen. ¼" stainless steel tubing was used for all the lines from the gas cylinders to the reactor. All the MFCs were calibrated for a wide range of flows between 4 sccm to 100 sccm. The flowrates used for running the reactor at different space velocities were double-checked with a Gilibrator in a range of 1 to 250 cc to be sure that there were not any errors of more than 3% for each flow passing through the MFCs, especially for low flowrates. For all the reaction runs, the pressure was atmospheric, and

the feed composition included 10% ethylene, 10% oxygen and 80% inert gas. Nitrogen was used mostly as an inert gas rather than argon because the ethylene epoxidation reaction is exothermic and to maintain the reactor in constant temperature, nitrogen was used rather than argon because nitrogen has a heat capacity which is double that of argon's heat capacity. Nitrogen was used as an inert gas in a lot of other epoxidation reaction studies[7,31,25]; however, methane, with a heat capacity of double that of nitrogen, could be used as well[30]. The reactor that was used in this study consisted of a ½" stainless steel tube sealed with two Viton o-rings at the beginning and end of the reactor tubing. The catalyst powder was put between two pieces of quartz wool and kept at the middle of the reactor tube. The K-type thermocouple was used to measure the bed temperature. A 10 to 20 ℃ temperature difference was observed between the bed temperature and furnace temperature. Thus, the temperature of furnace was set to have desirable bed temperature. All the temperature that are reported in this represent the bed temperature.

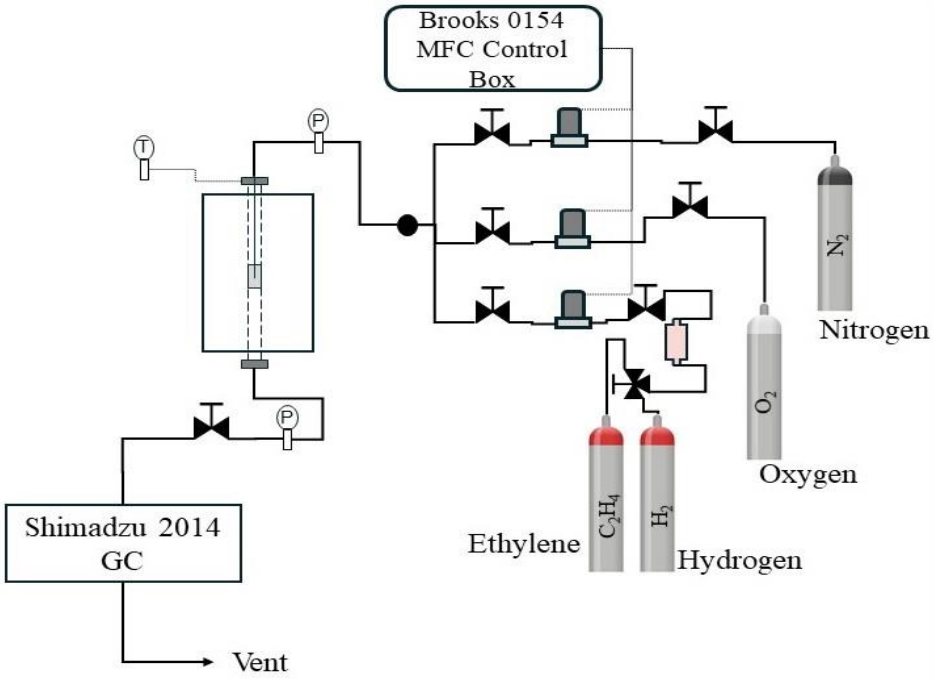

Figure 3-1. Schematic of reactor set up.

The lines of tubing that carried the effluent into the GC were wrapped with an electrical heat tape to avoid the liquid entrance into the GC. The effluent sent to a Shimadzu 2014 GC with two columns: a Q Plot fused silica capillary column provided from Supelco with 30 m*0.32 mm diameter connected to flame ionization detector (FID) for separating and detecting ethylene and ethylene oxide, and a packed column ShinCarbon 80/100 with 2 mm ID and 1/8" OD and 2 m length provided from RESTEK connected to thermal conductivity detector (TCD) for separating and detecting ethylene and carbon dioxide. Q PLOT columns are generally used for separation of small hydrocarbons giving it the possibility to separate ethylene and ethylene oxide. TCD is ideal choice for measuring the non-organic species because of the non-specificity of detectable components. TCD works based on different thermal conductivity of gases passing through the detector. There is a reference gas in a separate chamber (known as carrier gas, Helium in our case) and the gas is the effluent in other chamber where the change in thermal conductivity is measured there at isothermal conditions. The thermal conductivity of the stream was altered as various components passed through the column filament, causing the filament to heat up or cool down. Temperature changes resulted in resistance changes, which were measured and recorded as voltage changes over time[31]. The temperature of the GC oven was ramped as it is shown in Figure 3-2. Initial temperature was selected as 45 ℃ with the 10 minutes holding time and was increased to 240℃ and held for 2 minutes at the end. The carrier gas flowrate for the ShinCarbon column that, was connected to TCD, was set on 25 mL/min. Thus, the residence time of getting the carbon dioxide and ethylene peaks in TCD were about 14 and 17 minutes, respectively. FID is an ideal choice for detecting the organics

because they are generally the easiest to ionize and give the strongest signals. Then, the ionized molecules come into contact with a collector plate that is connected to an ammeter[31]. A hydrogen/Air (oxygen) flame was used to ionize the species in the gas stream. The ethylene and ethylene oxide peaks showed a residence time of about 1.5 and 4.5 minutes, respectively. An overlap between the ethylene and ethylene oxide peaks was observed when the carrier gas flowrate was set to 10 mL/min. For a better gas separation, column temperature and carrier gas flowrate through the capillary column was varied. The column temperature was decreased to 40 ℃, but a small change in the peaks' residence times were observed. Decreasing the column temperature to less than 40 ℃ is not recommended. Moreover, changing the carrier gas flowrate through the capillary column from 10 mL/min to 5 mL/min, as it is shown in Figure 3-3, was more effective. The area that is overlapped between the ethylene and ethylene oxide is negligible compared to total area, and therefore, the total ethylene and ethylene oxide concentrations can be calculated.

Calibration gases were provided from CAL GAS DIRECT company in the highest concentrations for each gas and balanced with nitrogen. Thus, 10% ethylene, 1% carbon dioxide and 1% ethylene oxide calibration gas cylinders all balanced with nitrogen were used. The GC was calibrated for carbon monoxide as well, but during the reaction, no carbon monoxide peaks were observed. Acetaldehyde also did not appear in the peak lists, since it reacts so fast and decompose to carbon dioxide and water. Then, the calibration gases were diluted with nitrogen for each gas to build the lower concentrations. 8%, 6%, and 4% were made for ethylene. 0.75%, 0.5%, and 0.25% were made for carbon dioxide. 0.75%, 0.5%, 0.25%, and 0.1% were made for ethylene oxide. For all the gases the calibration curved that are shown in Figure 3-4 to 3-7, forced to zero.

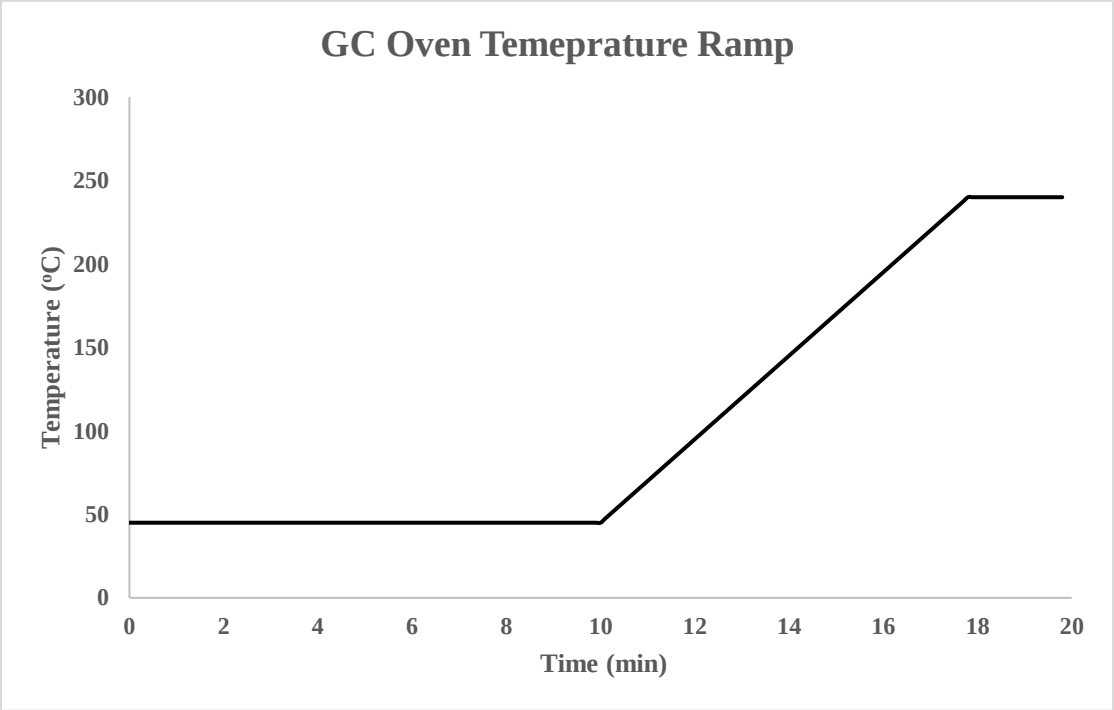

Figure 3-2. Temperature profile of the GC oven.

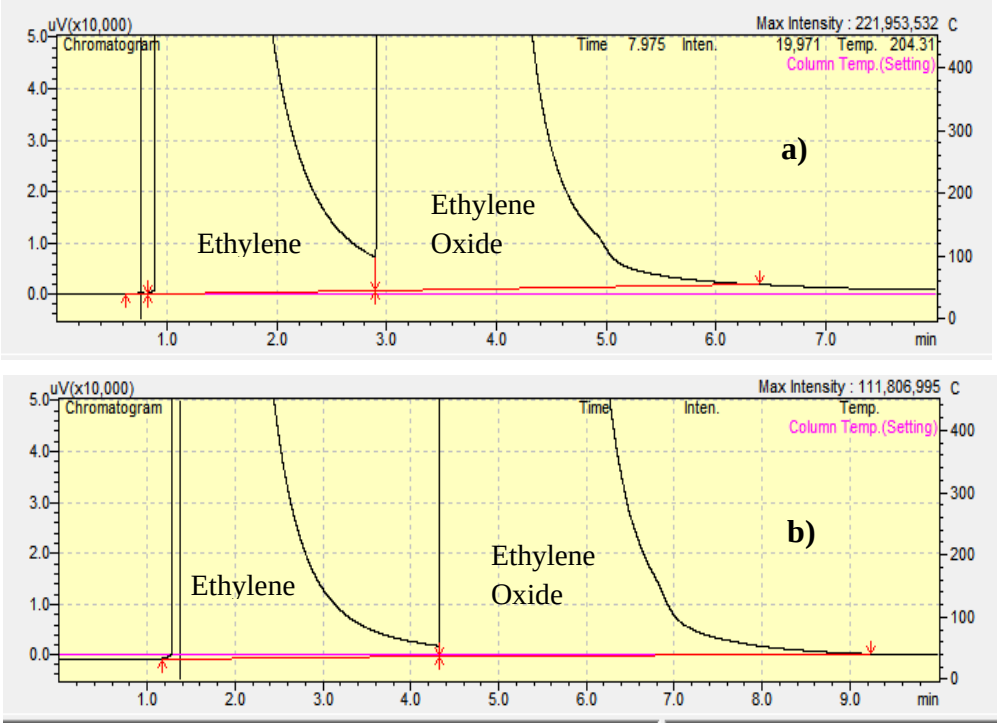

Figure 3-3. Ethylene and ethylene oxide peaks in FID with a GC carrier gas flowrate of a) 10 mL/min b) 5 mL/min.

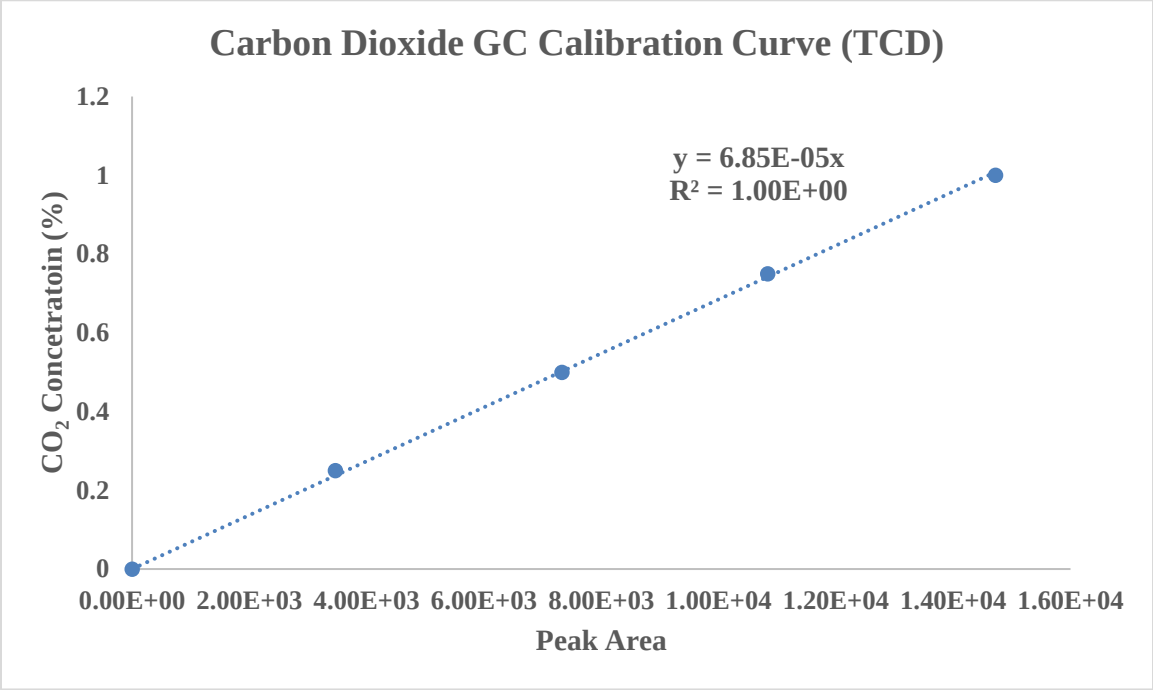

Figure 3-4. Carbon dioxide calibration curve in the TCD.

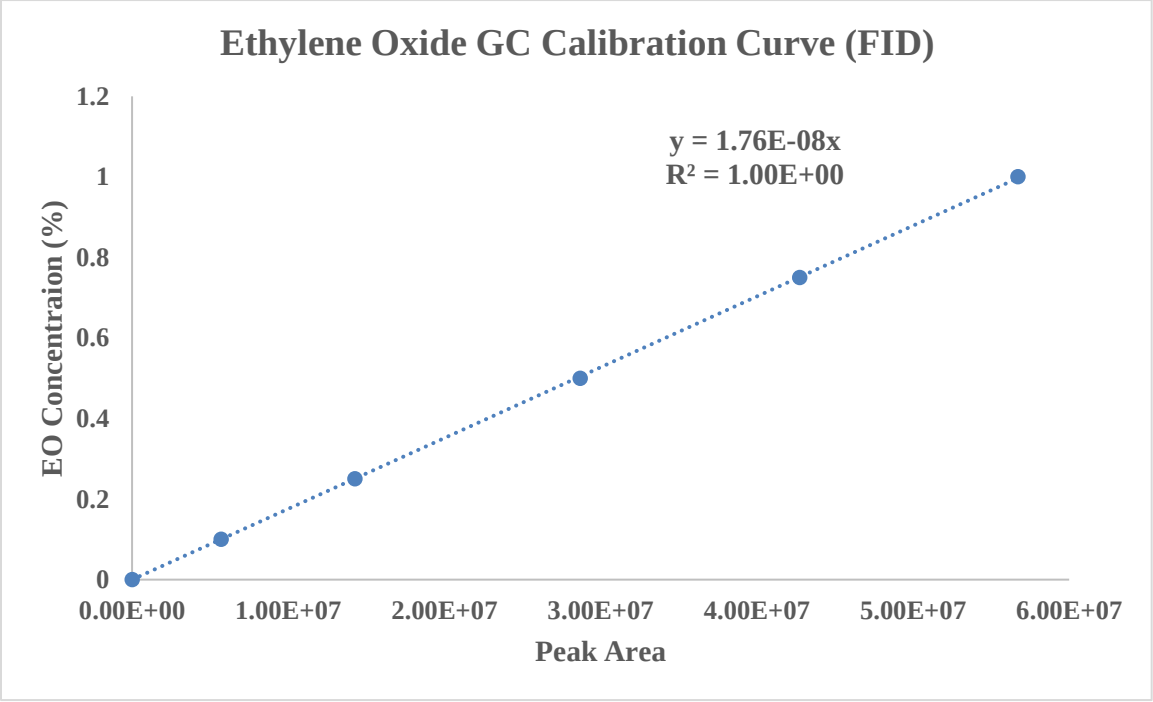

Figure 3-5. Ethylene oxide calibration curve in the FID.

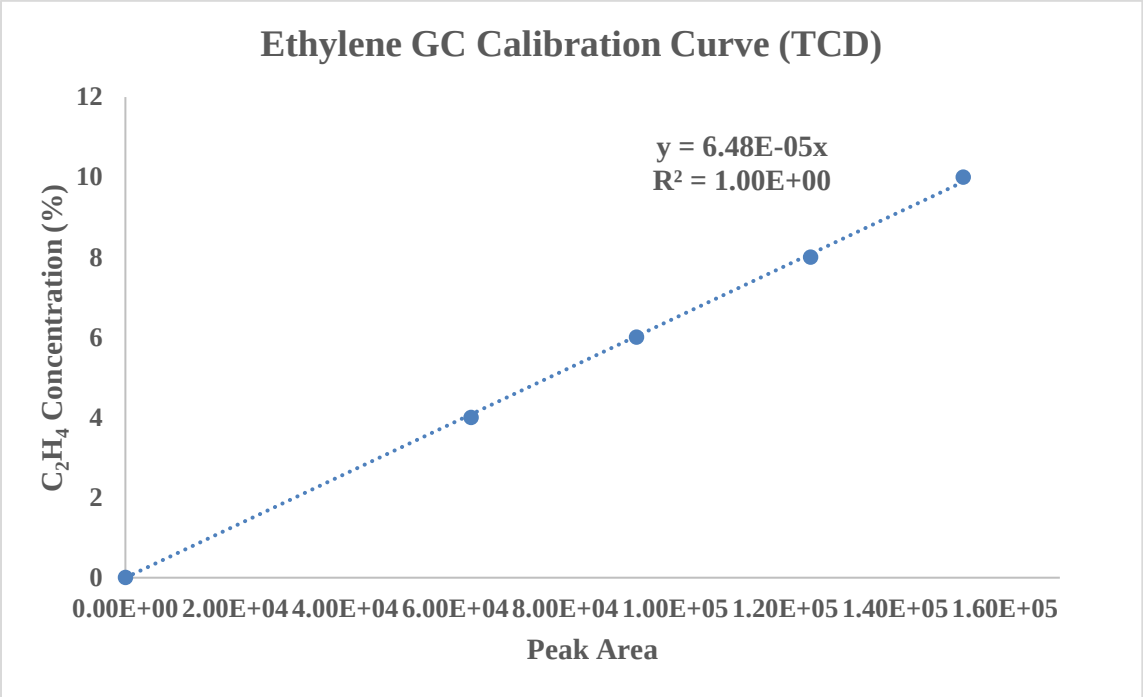

Figure 3-6. Ethylene calibration curve in the TCD.

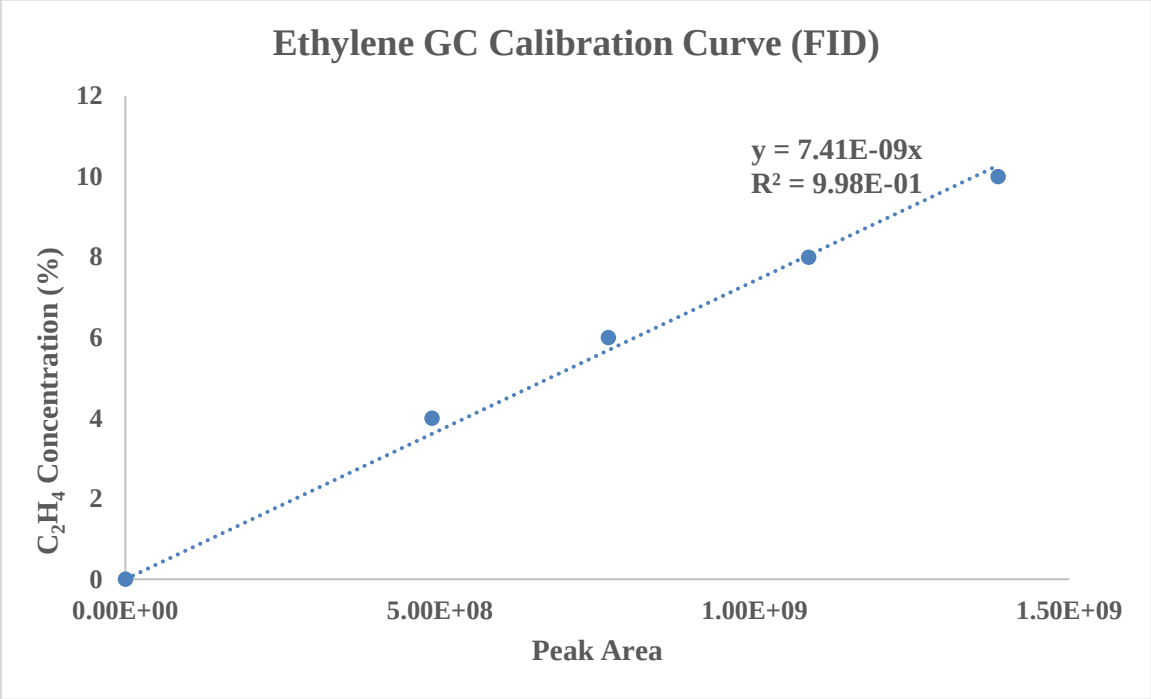

Figure 3-7. Ethylene calibration curve in the FID.

The first reactor runs, were unsuccessful; however, the conditions were adjusted accordingly. Upon initial testing, the synthesized catalysts showed low activity. It was unknown if the issues were related to either to the reactor or the catalysts. Thus, a benchmark catalyst sample was tested, which included silver nanoparticles in semi-spherical shapes with the particles size mostly between 100 to 200 nm. First, the catalyst was reduced at 300 ℃ and atmospheric pressure for 12 hours with a flow including 20% hydrogen balanced with argon. 1.1 g catalyst was loaded into the reactor, and it was operated at a total flowrate of 100 sccm including 10% ethylene, 10% oxygen, balanced with argon at 180 ℃ and atmospheric pressure. Although this condition was not a reasonable condition, because of high space velocity, it was chosen as a result of its ability to obtain data from a previous run. In epoxidation reactions, since the selectivity goes down with increasing conversion, the yield of reactions is also calculated to compare the results. The yield of reaction in this case, considering the obtained conversion and selectivity as 3% and 23.9%, respectively, was 0.0717. It should be mentioned that the obtained conversion and selectivity was an average of more than 10 GC sampling loops in order to be sure that the reactor reached steady state conditions. However, in higher temperature, this reaction needs more time to get to the steady state. The time needed for reaching to steady state condition in the literature has been reported with a lot of difference, which could be related to different condition or different catalysts structures. For example, for supported silver nanocubes catalyst, ethylene conversion and ethylene oxide selectivity showed no variation with time at a reaction condition of 230 ℃, and 10% O_2 and 40% ethylene[27]. While the time needed to get steady state for supported silver nanowires and nanocubes in another study was reported as 24 hours[25]. 36 and 48 hours are the other times

reported in the literature for reaching to steady state for supported silver spherical particles[30,3].

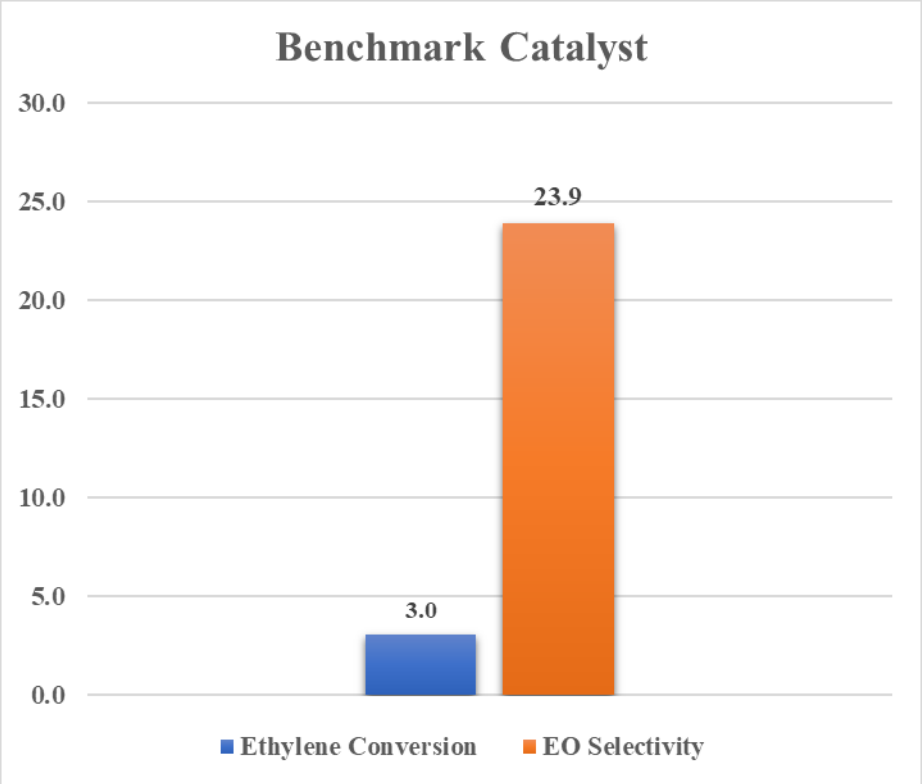

Figure 3-8. Ethylene conversion and EO selectivity for benchmark silver catalyst.

The next step was to try the catalysts made by our group with the corrected space velocity. In order to decrease the space velocity, the total flowrate needed to be decreased or/and the mass of the loaded catalyst could be increased. Since the flowrate composition was included with the 10% ethylene, 10% oxygen balanced with an inert gas, and the maximum MFCs flowrates were 100 sccm, it was preferred to not set the total flow rate lower than 60 sccm in this run to have accurate flowrate for ethylene and oxygen. About 2 g of 15% silver on low surface alumina (SA5562) synthesized with wet impregnation catalyst was loaded this time to have a space velocity about 7500 hr^{-1}. The catalyst was reduced at 300 ℃ for 12 hours at a stream that included 20% hydrogen balanced with

nitrogen, and then the reactor was operated at similar conditions discussed previously, except using nitrogen as inert gas rather than argon because of the higher heat capacity of nitrogen. Moreover, since the optimum temperature was reported differently in the literature, it was decided to change the temperature to observe the ethylene conversion and EO selectivity as a function of temperature. Thus, reactor runs for each temperature were operated for a couple of hours. The result is shown in Figure 3-9. It should be mentioned that the error bars for EO selectivity have been shown while the error bars related to ethylene conversion has not been shown because the error was too small to show. By increasing the temperature, as it was expected, the ethylene conversion was increased, because based on Arrhenius equation by increasing the temperature, the rate constant increased, which then resulted in the rate of reaction increased. This, in turn, resulted in more ethylene consumption and more ethylene conversion as a result. The EO selectivity was increased by about 10% with the temperature increase from 190 ℃ to 240 ℃. Selectivity temperature dependency was shown in a computational study with a reaction condition very similar to the conditions conducted in this study[6]. The computational results were very consistent with the experimental results[3,6,13]. To understand the enhancement in the EO selectivity with temperature increase, it is needed to reference the apparent activation energies for EO and acetaldehyde formation for the (111) silver facets that are the most common facets for semi-spherical silver catalysts. For the reaction conditions mentioned here previously, the EO apparent activation energy is higher than the acetaldehyde apparent activation energy. Thus, as it has been reported in Hus et al. study, the slope of 1/T vs. log (TOF) which is apparent activation energy is more in EO formation rather acetaldehyde formation, meaning that by increasing the temperature, the log(TOF)

is increased more for EO formation when compared to acetaldehyde formation. The ratio of EO mole formation to the acetaldehyde mole formation was defined as EO selectivity in this study. Generally, in epoxidation reactions, including the ethylene epoxidation reaction, the conversion and selectivity have different trends. It has been reported that by increasing the conversion, the selectivity goes down because of the initiation of ethylene oxide oxidation through the isomerization to acetaldehyde, which is decomposes fast to carbon dioxide. The result, shown in Figure 3-10, is obtained at the exact same conditions as were used for Figure 3-9. Based on these results, the EO selectivity went down by increasing the conversion. The only difference between what has been collected in these figures, is the time that catalyst was on the stream. It has been shown in literature that the catalysts for ethylene epoxidation reactions would take between 24 to 48 hours to reach the stable condition. Comparing the results with the same reaction condition that shown in the figures below, catalyst in the first reactor run was initiating. Moreover, the results shown in Figure 3-10, was similar to the results that were obtained previously in our group7. Although the space velocity in this study was higher than what was reported previously in literature, the yield was close to each other. In previous work, at about 230 ℃ the conversion was about 5% with a selectivity of 28% resulted in a yield of 1.4%. In this study, at the same temperature the yield of 1.9% was obtained that was similar to previous results. The reason of higher selectivity was calculated here could be addressed by the silver size effects. Larger silver particles size would result in higher EO selectivity. However, because of the sintering the lifetime activity of the catalysts would be lower.

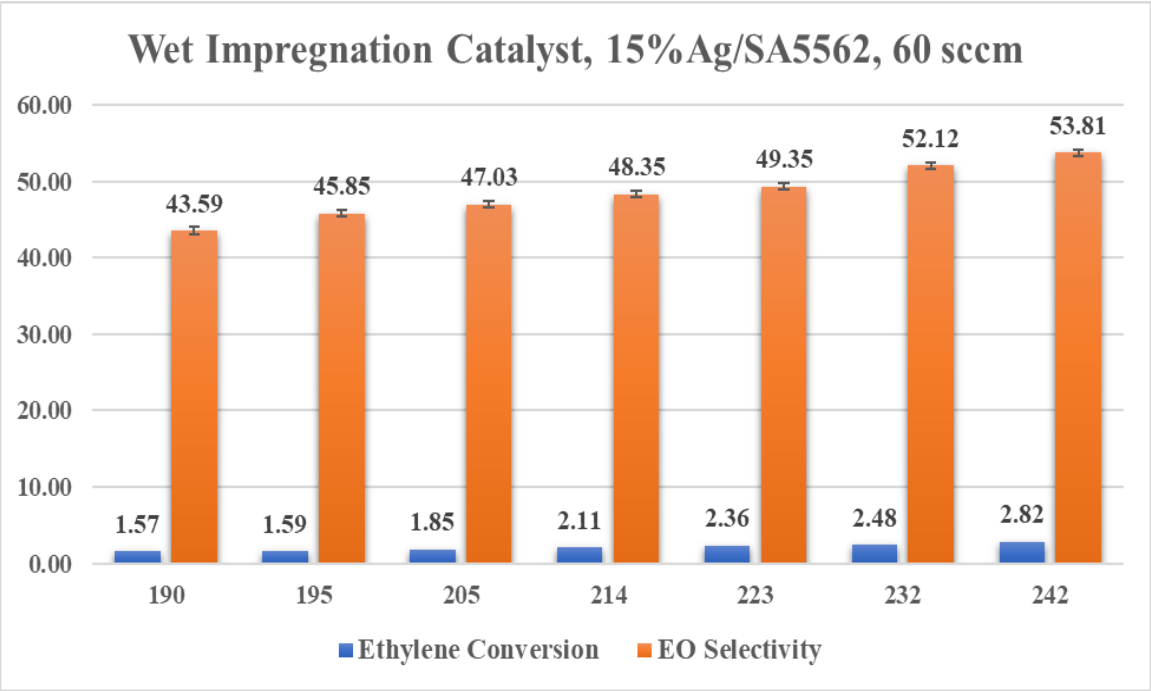

Figure 3-9. Ethylene conversion and EO selectivity for semi-spherical, fresh catalysts at different temperatures.

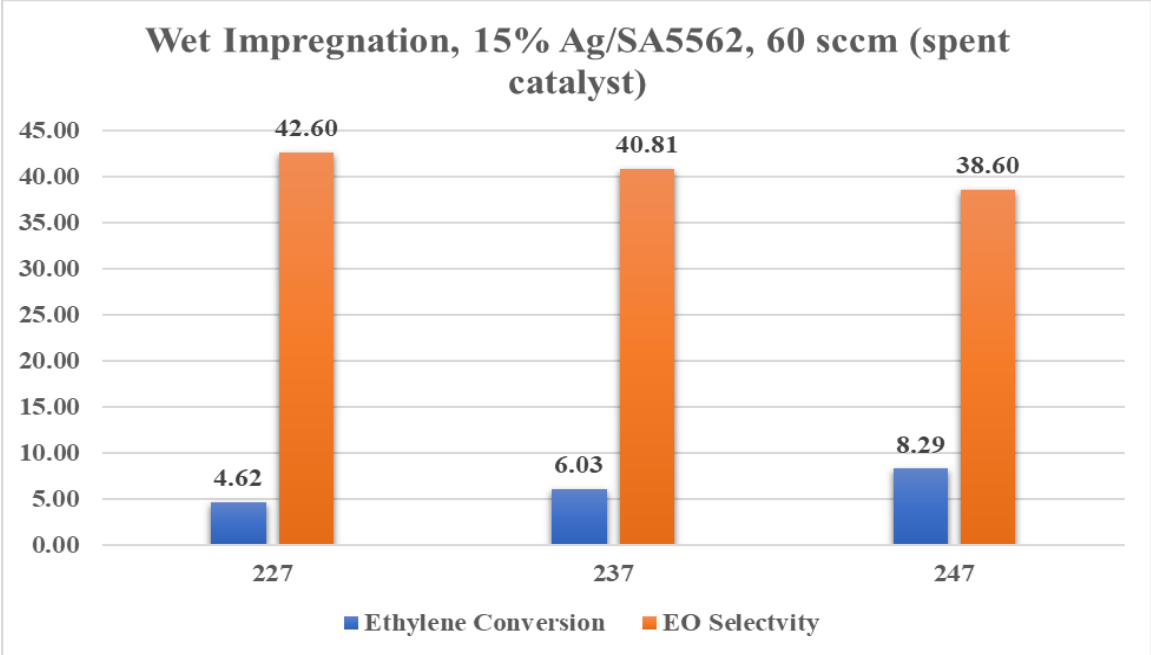

Figure 3-10. Ethylene conversion and EO selectivity for semi-spherical, silver catalysts during the second run.

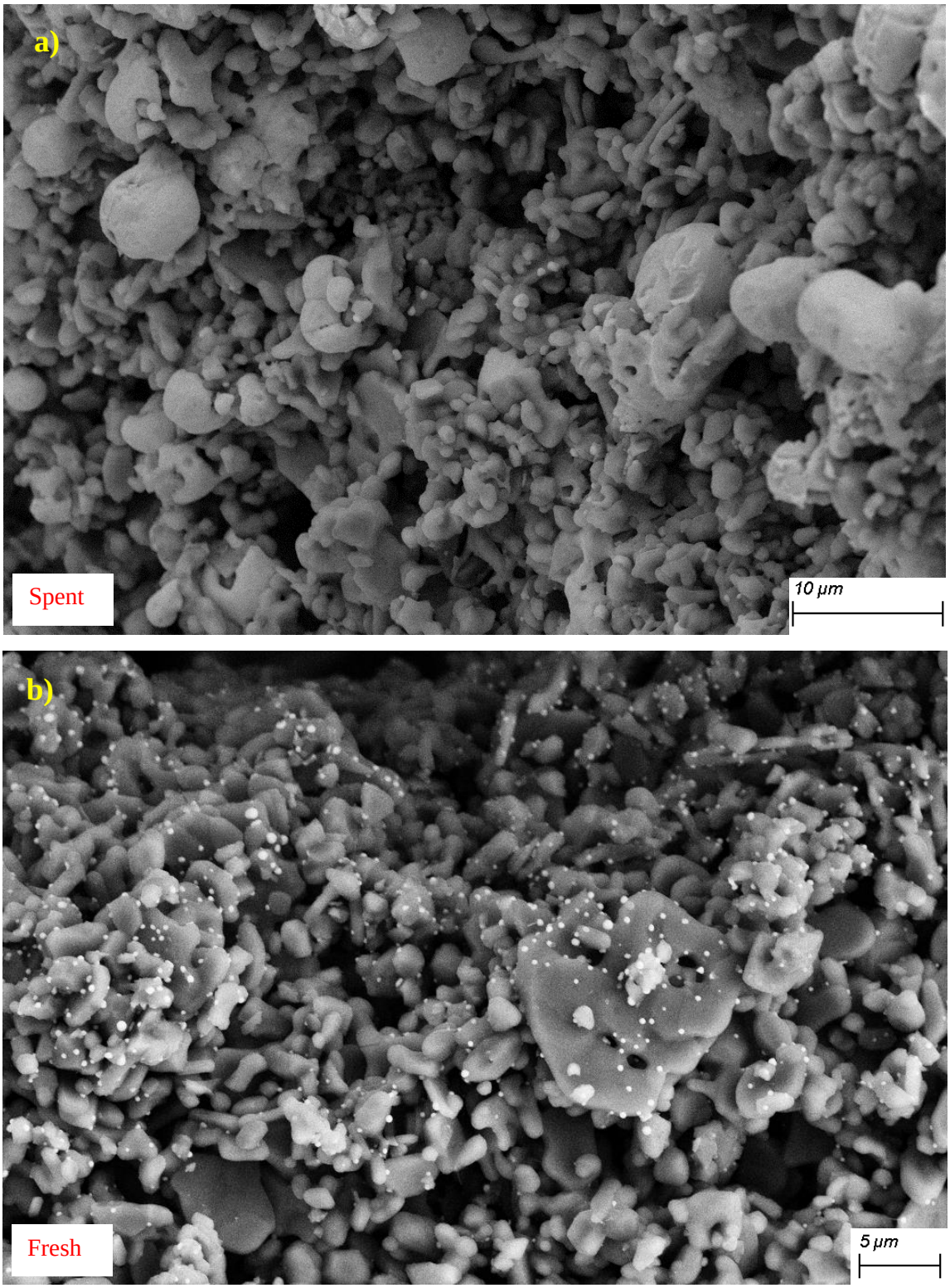

Figure 3-11. SEM images of silver particles on the low surface area aluminum oxide support a) spent catalyst b) fresh catalyst

For the silver nanowires sample, the reaction conditions were selected based on what had been reported in Linic et al. Thus, about 1.6 g of the supported silver nanowires sample, as shown before in chapter 2, was loaded into the reactor and pretreated at 230℃ for three hours in a stream of 25% O_2 balanced with nitrogen. Then, the reaction was started with a 50 sccm total flow which included 10% ethylene, 10% O2 and balanced with nitrogen, resulting in space velocity of 7400 h^{-1}. By using the hydrothermal synthesis method, about 0.6 g of supported silver nanowires were synthesized. To have enough catalyst mass for loading into the reactor, there were two ways: first to scale up the synthesis amount by a factor of three or to mix three batches of one typical synthesis cycle that was reported in chapter two. Both methods were tested, and it was preferred to mix three batches together to have enough amount for the reaction. The silver nanowires yield was of higher quality in the case of mixing the batches, which could be because of the fact that the reaction happening in the hydrothermal method is reversible; this, in turn, could potentially increase the probability that the backward reaction could occur, during longer synthesis times, which would result in lower silver nanowire yields. However, in order to mix three batches of supported silver nanowires, it must be ensured that all the three sample have similar silver nanowires yields and diameters, and that they also have similar distributions on the support. EDS mapping of silver particles on the support surface showed that the surface composition was between 8% to 11% by silver weight percent. Then, the three batches were mixed together and loaded into the reactor. The reaction operated at different temperatures from 190 ℃ to 280 ℃ for a while. Although the ethylene oxide peak was observed in the GC, the ethylene conversion was lower than 1%. Thus, the supported silver nanowires catalyst were not active at mentioned reaction conditions. One possible

reason could be due to impurities that covered the active sites of silver nanowires such as PVP molecules. As it has been mentioned in the literature and previously in chapter two, the PVP molecules adsorbed on the (100) and prevents growth and then the (111) starts to grow in [110] direction. It has been shown in the literature[6] that washing the silver nanowires with both water and an organic solvent, such as ethanol, removed most of the PVP molecules from the surface, and about 1.5%wt of PVP molecules can be removed by heating the sample in the TGA. However, it was decided to increase the reactor temperature to possibly remove some of the PVP molecules and to check the thermal stability of nanowires as well. 400℃ was selected as the temperature to continue the reactor run under the same pretreatment flowrate composition. At this temperature, almost all the nanowires decayed into segments and lost the (100) structures and deformed into silver semi spherical particles as it is shown in Figure 3-12.

There were some other potential changes to be had that could potentially make the catalyst active at said reaction conditions. In addition to a well distribution of silver nanowires on the α-Al_2O_3 that was mentioned in chapter two, the surface silver composition was the first place to investigate. As it was shown previously, with the amount that was selected to make 15 wt% silver on the support surface, EDS mapping showed about 10 wt% silver on the support surface. Thus, it was selected to make 20 wt% supported silver catalysts to reach the correct silver surface composition. Three batches of silver nanowires were synthesized and impregnated on the low surface area aluminum oxide support (SA5562) and the EDS mapping was conducted on all three samples. Silver distribution was between 15 wt% to 20 wt% on the support surface. An SEM image of one of the batches of supported silver nanowires is shown in Figure 3-13.

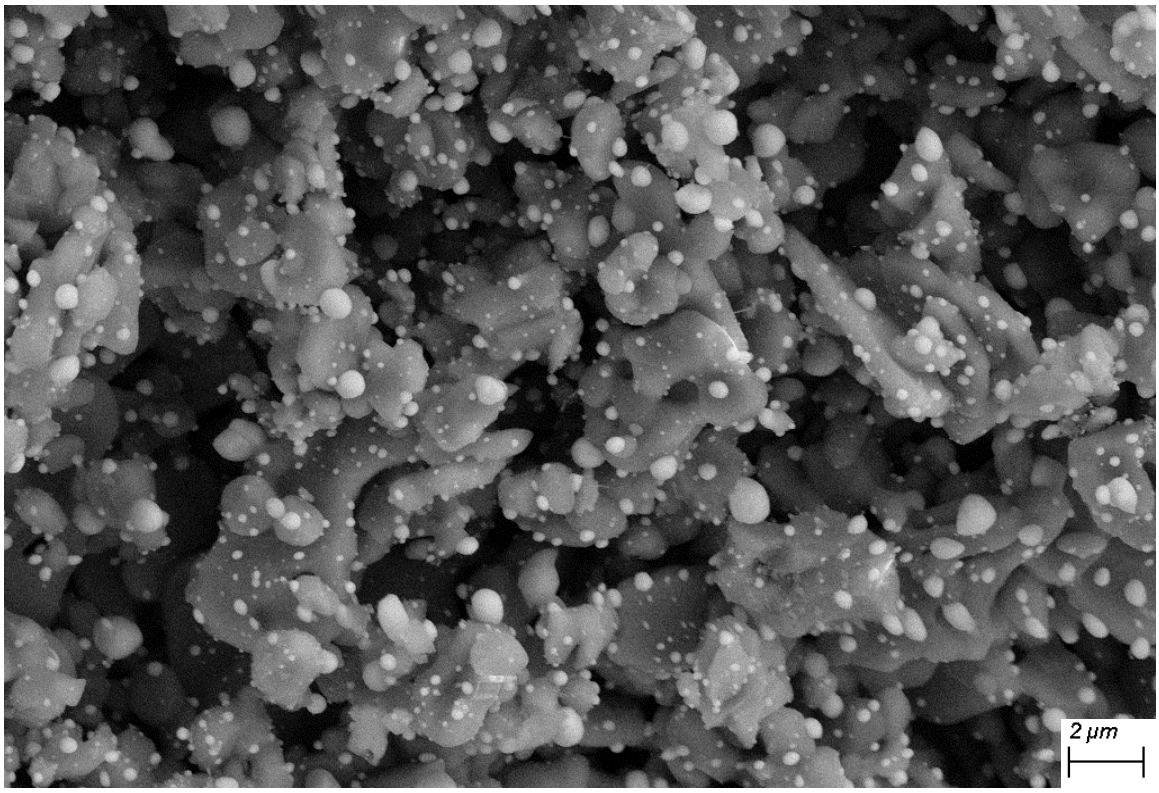

Figure 3-12. SEM image of deformed silver nanowires to silver semi spherical particles

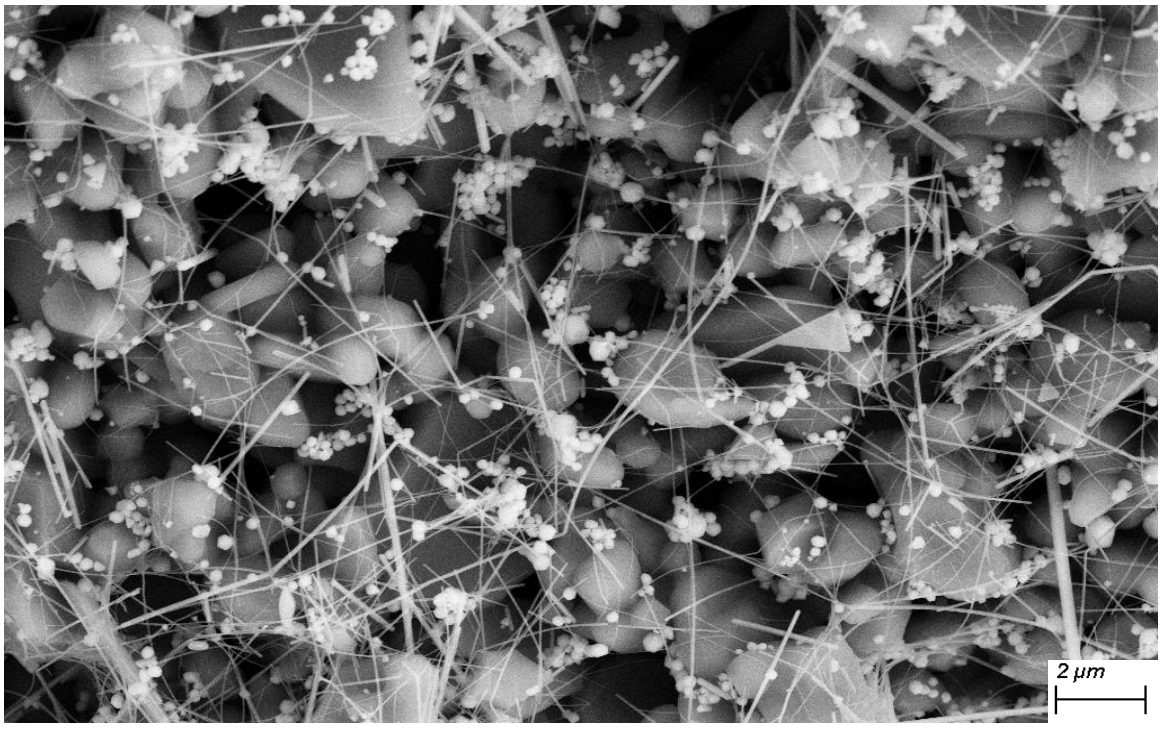

Figure 3-13. SEM image of fresh supported silver nanowires catalyst with 16 wt% silver surface composition.

The EDS pattern and surface composition of this SEM image is shown in Figure 3-14.

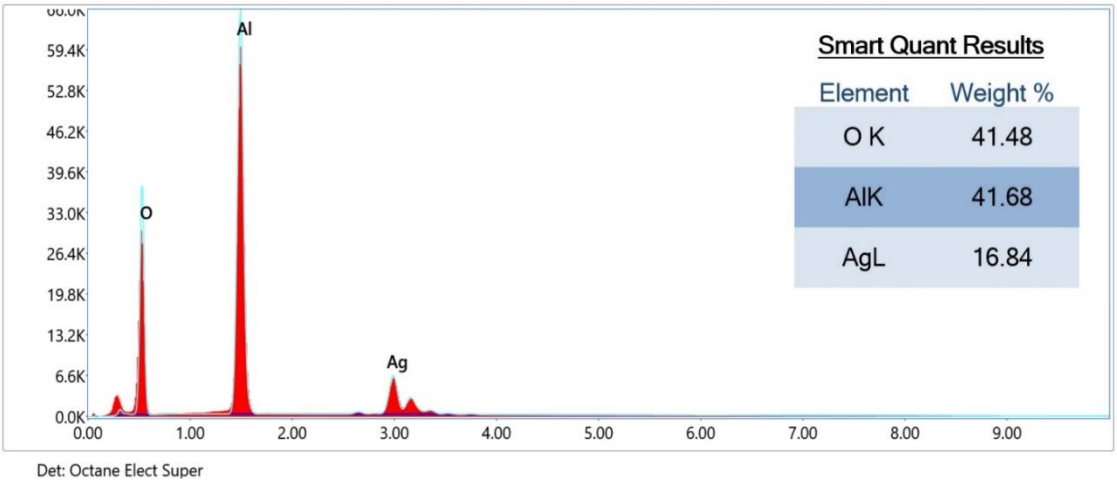

Figure 3-14. EDS pattern and surface composition of elements shown in Figure 3-14

This catalyst was loaded into the reactor and pretreated the same reaction conditions that were used before. Then the reactor was operated with the same reaction conditions: 50 sccm total flowrate including 10% ethylene, 10% oxygen, balanced with nitrogen at atmospheric pressure and different temperature starting from 190 ℃ to 270 ℃. The total EO mol formation was higher than what was observed in previous run; however, the conversion was still lower than 1%, which resulted in the inactivation of supported silver nanowires catalyst. Figure 3-15 shows the spent supported silver catalyst. In addition to semi-spherical silver particles that existed in the fresh catalysts, generally two types of silver nanowires could be observed in the spent catalyst. Nanowires with a thicker diameter existed almost intact while the thinner nanowires were decayed to smaller nanorods or nanoparticles. Comparing what has been reported in the literature about the gold and platinum nanowires, thermal stability to what has been observed in this study, could reach

us to a conclusion about the silver nanowires structure change. Platinum nanowire thermal stability was investigated in the literature by annealing the Pt nanowires in a vacuum furnace at temperatures between 600 ℃ to 1000 ℃ for 30 minutes. The same experiment was done for the gold nanowire in another study. Although these studies were conducted in different conditions compared to what has been done in this thesis, the same structure change procedure could also be conducted for silver nanowires at the reaction conditions.

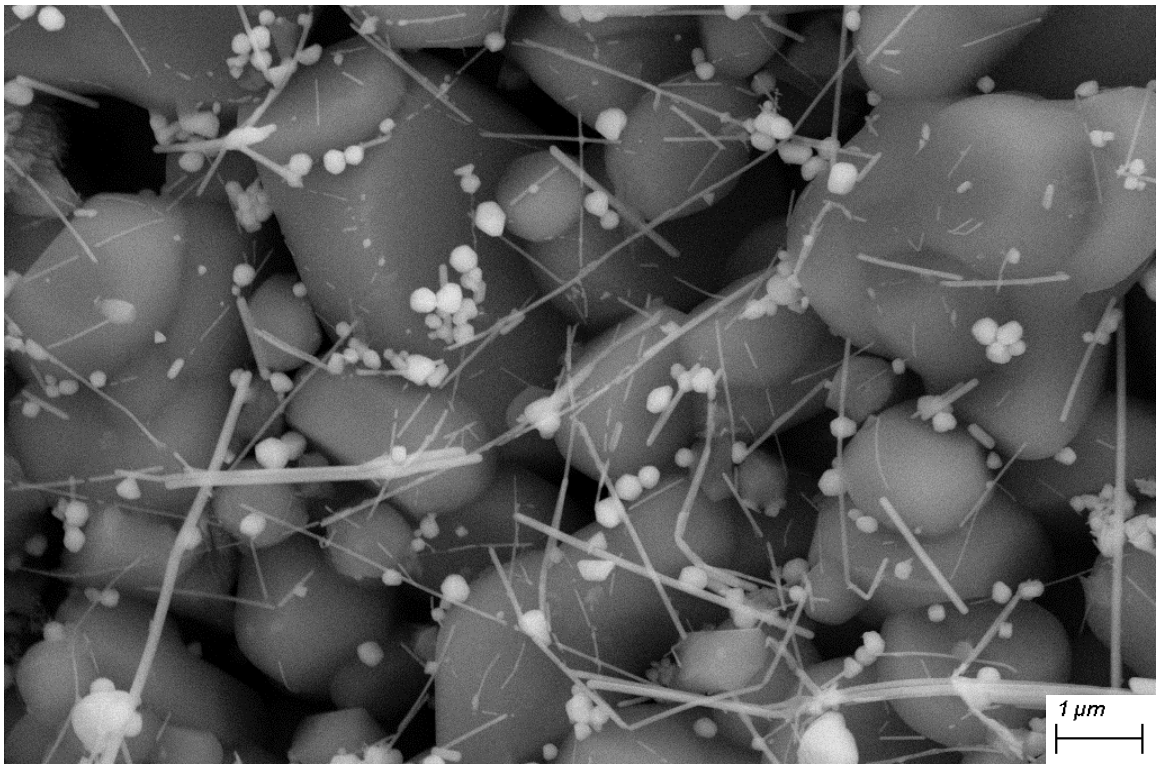

Figure 3-15. SEM image of spent supported silver nanowire catalyst.

A higher magnification SEM image of the spent catalyst is shown in Figure 3-16, which demonstrates that the thinner nanowires were broken under the reaction condition while thicker nanowires remained unchanged. Small nanorods were placed in continuation of each, other indicating that they might form a nanowire before the reaction, but then they were decayed to smaller parts by annealing under reaction condition. Generally, the

nanowires with a diameter of more than 100 nm remain intact under reaction condition (until about 270 ℃ for a couple of hours) while the thinner nanowires were broken and lost their initial structure.

Figure 3-16. Higher magnification SEM image of spent supported silver nanowire catalyst.

A quick review of some of the silver nanowires synthesis using hydrothermal method in the literature, resulted in the table shown below, Table 1. The average diameter of silver nanowires synthesizing with hydrothermal method is usually less than 100 nm. A result that was observed in this thesis as well. It could be the reason that the studies on the supported silver nanowires catalysts for ethylene epoxidation used the polyol method as a well-known method for making nanowires. The advantages of polyol method comparted to hydrothermal method in synthesizing silver nanowires can be summarized as follows: first, a better control on silver nanowires growth with favorable diameter of more than 100

nm and second, a better nanowire diameter distribution with more uniform diameter. What was mentioned previously are good results to learn by; however, they are not the reason for catalyst inactivity. As it was shown in this thesis, the silver spherical particles with (111) facets were active and had a reasonable EO selectivity as an unpromoted supported silver catalyst. Thus, one of the most possible reasons, which will be investigated in future experiments, is the adsorption of gases on the supported silver nanowire catalyst.

Table 3-1. Diameter and length scale of silver nanowires synthesized by hydrothermal method in the literature.

Study	**Diameter**	**Length**
Xu et al.[53]	Ave ~ 30 nm	Micrometer scale
Yang et al.[43]	Ave ~ 53 nm	Up to 6 μm
Tetsumoto et al.[39]	70 to 300 nm	Up to 100 μm
Tang et al.[54]	60 to 140 nm	Micrometer scale
Zhang et al.[55]	Ave ~ 50 nm	Ave ~250 μm
Bari et al.[36]	Ave ~ 45-65 nm	200 to 500 μm
Wang et al.[38]	Ave ~ 100 nm	Ave ~ 500 μm
Cwik et al.[56]	Ave ~100 nm	Ave ~ 160 μm
Liu et al.[57]	Ave ~ 50nm	Micrometer scale

CHAPTER 4

CONCLSION AND FUTURE WORK

The goal of this thesis was to synthesize different silver, nanostructured catalysts and evaluate their activity for an ethylene epoxidation reaction. Among the different silver catalysts structures, semi-spherical silver catalysts, which include (111) facets in abundance, have been investigated vastly in the literature[31,7,3,13,58]. Ag (111) is the most stable the least active facet for silver, as the metal with FCC structures[6]. Industrially, some promoters, such as cesium and rhenium, in addition to feed additives, such as chlorine, are being added to silver catalysts in order to increase EO selectivity[13,58]. It has been reported, both experimentally and computationally, that the unpromoted silver catalysts with Ag (100) facets are more selective toward the ethylene oxide formation in an ethylene epoxidation reaction[6,25,24]. Silver nanowires and silver nanocubes are well-known silver structures, which consist primarily of (100) facets[25,26]. Although silver nanocubes catalysts have higher EO selectivity than silver nanowires[24], in this study silver nanowire structure were chosen as the starting point, since there are considerably more literature studies in silver nanowires synthesis compared to silver nanocubes. Based on what was mentioned in previous chapters, synthesizing these structures were challenging. Thus, in this study it was

imperative to report every step, regardless of how small, required to prepare a better silver nanowires sample.

Both the polyol and hydrothermal methods were utilized in this study for synthesizing silver nanowires. The hydrothermal method was found to be more straightforward for making silver nanowires but resulted in thin nanowires compared to the polyol method. Various adjustments were made to the synthesis parameters to try and improve the nanowire yields and investigate their effects on the diameters of the nanowires. The centrifuge method was selected as a better separation method compared to vacuum filtration. For both methods, a cycle including two times washing with DI water and two times washing with ethanol (or other organic solvents such as acetone and isopropanol) was chosen. For the centrifuge method, the samples were centrifuged for 20 minutes at 2500 rpm for each cycle and then were put on the glass slide or SEM stub pins to be dried. For the method using vacuum filtration, samples were poured on a filter paper and washed with the same solvents; the sample was then transferred onto the SEM stub pins to be dried. By comparing SEM images of these two samples, as shown in chapter two, it was concluded that the yield of nanowires was higher in the sample that silver spherical particles were removed with the centrifuge method compared to filter paper separation method. This result could happen because the spherical particles would stick between the net of nanowires and could not be removed perfectly. Additionally, some trace amounts of filter paper were observed in the SEM images.

Moreover, among other synthesis parameters, time was found as one of the crucial variables affecting the yield and the diameter of nanowires. Silver nitrate and sodium chloride first were reduced in an aqueous solution to produce silver chloride particles. The

solubility of silver chloride in water is weak, so the glucose helps in the reduction of silver chloride particles to release the silver nuclei needed for nanowires formation. In the short synthesis time (12hours), silver chloride particles were reduced partially, and a lot of silver chloride particles, with high XRD peak intensity, were seen in the SEM images and XRD patterns, respectively. By increasing synthesis time, more silver chloride particles were reduced, which resulted in more silver nuclei being released. A lower concentration of silver chloride particles was observed in the SEM images for 15 hours compared to 12 hours with less intense XRD peaks. These peaks were not collected in XRD pattern for the 18 hour synthesis time, but the sample was consistent with the related SEM images that showed the silver chloride particles were in a lower concentration compared to the two others. Thus, it can be seen that the 18 hour synthesis time, with the concentrations and temperatures, was selected for this thesis as the transition synthesis time that majority of silver chloride particles were reduced to form the silver particles. Two more synthesis times were tested: 21 hours and 24 hours. A few silver chloride particles were observed for the 21 hour sample while there were not any for the 24 hours sample. The primary reason for choosing a higher synthesis time than the time that major silver chloride particles were reduced to silver nuclei, was that the silver seeds should have enough time to adsorb PVP for blocking the (100) facets and facilitate the anisotropic growth of nanowires. Considering the peaks that were obtained for silver particles in XRD, 24 hours was selected as a better choice for the synthesis time because of the ratio of Ag(111) to Ag(220), which was higher in the 24 hours sample, showing a decrease in high index of Miller planes. Comparing the diameter of silver nanowires from the sample synthesized by 12 hours and 24 hours, it brought us to the conclusion that higher synthesis times resulted in a thicker

diameter, in this case, as well as the silver precursor concentration. However, longer synthesis time is not necessarily good for silver nanowires yield and diameter. Too lengthy of a synthesis time resulted in a very low yield of silver nanowires, which is because of the reversibility of silver chloride particles and reduction by glucose.

Silver nitrate, sodium chloride, PVP, and glucose concentrations were changed in small ranges to increase the yield and diameter of nanowires. The silver nitrate concentration was decreased to increase the yield of silver nanowires, because excess amounts of silver nitrate would result in the excess silver seeds concentration, which is required to agglomerate to each other and produce large semi-spherical silver particles. 0.01 M silver nitrate aqueous solution was tested at lower concentrations, which resulted in a lower yield of the silver nanowire sample compared to the 0.02 M silver nitrate concentration, which acted as the basis concentration that was used in this study. The ratio of silver to PVP molecules together played a pivotal role, since when there were a lot of PVP molecules in the sample compared to silver nitrate molecules, then during the silver seeds formation and anisotropic growth, the PVP molecules would get adsorbed on the (111) planes as well as the (100) planes and stop them from growing in the [110] direction to form nanowires. Thus, the silver spherical particles would be dominant. This could be the reason of low silver nanowire yield when the silver nitrate concentration was chosen as 0.01 M. Silver nanowires yield was increased by increasing the silver nitrate concentration to 0.015 M with the same yield as 0.02 M but with thinner nanowires. Changing other chemical concentrations in a small range did not change the story, and the yield of nanowires was not increased more than what has been shown in this study. However, with a larger change in chemical concentrations, considerable changes were observed.

Increasing the glucose concentration in DI water, resulted in thicker nanowires with a lower yield, which was because of an increase in silver chloride particles, the reduction rate and abundance of silver seeds, which aggregate to each other, provided the silver spherical particles in addition to thicker nanowires.

In the next step, the procedure of impregnating silver nanowires in the low surface α-aluminum oxide was explained in detailed. The silver nanowire sample, after centrifugation, was diluted with 3 to 5 mL of ethanol and then was sonicated for about 10 to 20 minutes to be sure that all the aggregates at the bottom of the centrifuge tube were changed to a suspension of silver nanowires and ethanol. The suspension was contacted with enough aluminum oxide support powder to have 15% silver nanowires surface composition. The solution was stirred in the beaker on the stir plate at 80 ℃until it was dried. Calcination was not needed here, because almost all the impurities were removed during the washing with DI water and ethanol in the centrifuge. It was found that the solvent for wet impregnation should be ethanol while the usage of DI water, a weak bond between silver particles and supports weas formed, which resulted in the removal of the silver particles on the support easily by shaking. Additionally, stirring, during the drying, is necessary to have a well distributed silver nanowires on the support surface. Sonication would ease the separation of the aggregate of silver particles and help to achieve a better silver particle distribution. EDS mapping shows that with the amount to make 15% silver surface composition, we finally reached 10% silver composition while making a 20% silver to support ratio gave us a 15% silver distribution on the surface.

Supported silver spherical catalysts with 15% silver surface composition that were synthesized with wet impregnation, were tested in the reactor as well as the supported silver

nanowires with the same composition. The pretreatment and reaction conditions were selected based on what was done previously in the literature[7]. The semi-spherical catalysts with diameter of more than 500 nms were reduced at 300 ℃ for 12 hours in a 20% hydrogen stream balanced with nitrogen. The reactor was then operated at different temperatures and atmospheric pressure at a stream consisting of 10% ethylene, 10% oxygen and balanced with nitrogen at a space velocity of about 7500 hr^{-1}. By increasing the temperature, the ethylene conversion was increased due to the increase in the reaction rate defined by the Arrhenius equation. For the first run, the increase in temperature also resulted in an increase in EO selectivity, which was consistent with DFT papers explained by the fact that the apparent energy barrier for EO production is higher than the apparent energy barrier for acetaldehyde production. Thus, by increasing the temperature, the rate of increase in TOF would be higher in EO formation than AA formation. However, for the next reactor run, it was observed that by increasing the temperature, the EO selectivity went down as previously mentioned in the experimental papers. In the same stream, the EO selectivity goes down since the isomerization reaction rate increases and more EO converts to AA as time goes on. However, in the case was mentioned previously, it could be related to the size of the particles effect on the EO selectivity and ethylene conversion. The more catalysts that were spent in the stream, the more sintering that occurred, which resulted in much bigger silver particles, up to 5 μm diameter size. Then the EO selectivity decreased while ethylene conversion increased.

The supported silver nanowire catalysts were not active. The ethylene conversion was less than 1%. To find out the reason many experiments and suggested and tested. In addition to the good silver nanowires distribution that was mentioned before, the surface

composition was increased from 10% to 15%. However, the activity of the catalysts was not greatly changed. The spent catalysts showed that some of the silver nanowires lost their structure and they decayed into smaller nanorods and nanospherical particles. Based on what was observed in the SEM images, nanowires thinner than 100 nm were mostly decayed into nanoparticles while thicker nanowires remained intact. Fresh silver nanowires catalysts, in addition to the literature review, showed that the silver nanowires synthesized with hydrothermal method with different conditions and chemicals have a diameter less than 100nm. This result proved why all the studies working on different silver structure catalysts used the polyol method rather than the hydrothermal method. The Advantages of the polyol process compared to the hydrothermal could be summarized in two points: 1. Thicker nanowires could be synthesized 2. The diameter distribution in the polyol method is more uniform. However, synthesizing the nanowires in the hydrothermal method is much easier than the polyol process method. It was found that the stirring rate in polyol synthesis method is crucial. Even a single nanowire was not obtained when a stirring rate of 300 and 400 rpm was used; however, increasing the stirring synthesis rate to 520 rpm resulted in a low yield of silver nanowires with a great uniform diameter. However, the reason of inactivity of these catalysts may not be structural changes, since they were decayed into spherical particles that have been shown to be active before. Another hypothesis, that is going to be tested in future, is that impurities covered the active sites of the silver particles. It has been reported that the glucose starts to be carbonized or polymerized in the temperature between 140 ℃ to 160 ℃. A layer of graphite and amorphous carbon resulted from the glucose was reported with Raman spectroscopy in the literature[39]. Sample of silver nanowires synthesized in this study will be tested using Raman spectroscopy to investigate

the graphite and carbon existence, same as previously mentioned. Additionally, based on what was said in the literature, more than 98% of PVP molecules adsorbed on the silver nanowires were removed by washing the sample during centrifugation. Moreover, the EDS pattern obtained in this study showed that almost all the chemicals were removed in a considerable percentage. However, in order to understand the layer of the impurities that could block the silver particles site, the IR spectrum of a probe molecule gas on the silver surface at the reaction temperature and pressure will be investigated. Comparison between the collected spectrum of the probe molecule gas on the silver surface in literature and the sample synthesized in this study would help to illuminate the adsorption of reactants on the silver nanowires catalysts.

As it was mentioned in chapter one, silver nanocubes showed a higher EO selectivity rather than silver nanowires in experimental studies. Although both silver nanowires and nanocubes have (100) facets, resulting in higher EO selectivity compared to (111) facets, silver nanocubes have the highest EO selectivity. This is due to the greater number of active sites on a concentration per volume basis and a lower concentration of defect sites that accompany them. Synthesizing silver nanocubes in different sizes is the next step of this study in future experiments to compare their activity and size effects to the activity of silver nanowires and semi-spherical silver catalysts of different sizes. The experimental procedure for making silver nanocubes with both the hydrothermal and polyol methods is same as synthesizing silver nanowires, but at different concentrations or synthesis conditions, such as time and temperature.

In epoxidation reactions, promoting the catalysts and using feed additives is very common and well-known. Cesium and rhenium are two well-known silver catalyst promoters which increase the EO selectivity considerably[13]. Promoting silver nanowires and silver nanocubes catalysts with cesium and other promoters could greatly improve the ethylene epoxidation catalysts and overall reaction yields[26].

REFERENCES

(1) Théodore Ernie Lefort. Fr 729 952. **1931**, No. 12.

(2) Chongterdtoonskul, A.; Schwank, J. W.; Chavadej, S. Effects of Oxide Supports on Ethylene Epoxidation Activity over Ag-Based Catalysts. *J. Mol. Catal. A Chem.* **2012**, *358*, 58–66. https://doi.org/10.1016/j.molcata.2012.02.011.

(3) Jankowiak, J. T.; Barteau, M. A. Ethylene Epoxidation over Silver and Copper-Silver Bimetallic Catalysts: I. Kinetics and Selectivity. *J. Catal.* **2005**, *236* (2), 366–378. https://doi.org/10.1016/j.jcat.2005.10.018.

(4) https://www.statista.com/statistics/1065885/global-ethylene-oxide-production-capacity.

(5) https://www.statista.com/statistics/1244434/global-market-value-ethylene-oxide/.

(6) Huš, M.; Hellman, A. Ethylene Epoxidation on Ag(100), Ag(110), and Ag(111): A Joint Ab Initio and Kinetic Monte Carlo Study and Comparison with Experiments. *ACS Catal.* **2019**, *9* (2), 1183–1196. https://doi.org/10.1021/acscatal.8b04512.

(7) Mingle, K. B. Combinatorial Study of Oxidation Catalysts : Uncovering Synthesis-Structure-Activity Relationships. **2018**.

(8) https://www.mordorintelligence.com/industry-reports/ethylene-oxide-market https://www.mordorintelligence.com/industry-reports/ethylene-oxide-market.

(9) Rebsdat, S. Ethylene Oxide. *Encycl. Toxicol. Third Ed.* **2014**, 535–538. https://doi.org/10.1016/B978-0-12-386454-3.00021-X.

(10) Kirk-Othmer Encyclopedia of Chemical Technology. *Kirk-Othmer Encyclopedia of Chemical Technology*. 2000. https://doi.org/10.1002/0471238961.

(11) Chorkendorff, I.; Niemantsverdriet, J. W. *Concepts of Modern Catalysis and Kinetics*; 2005; Vol. 2005. https://doi.org/10.1055/s-2005-866709.

(12) Rocha, T. C. R.; Hävecker, M.; Knop-Gericke, A.; Schlögl, R. Promoters in Heterogeneous Catalysis: The Role of Cl on Ethylene Epoxidation over Ag. *J. Catal.* **2014**, *312*, 12–16. https://doi.org/10.1016/j.jcat.2014.01.002.

(13) Jankowiak, J. T.; Barteau, M. A. Ethylene Epoxidation over Silver and Copper-Silver Bimetallic Catalysts: II. Cs and Cl Promotion. *J. Catal.* **2005**, *236* (2), 379–386. https://doi.org/10.1016/j.jcat.2005.10.017.

(14) Mavrikakis, M.; Doren, D. J.; Barteau, M. A. Density Functional Theory Calculations for Simple Oxametallacycles : Trends across the Periodic Table. **1998**, *5647* (97), 394–399.

(15) Özbek, M. O.; Van Santen, R. A. The Mechanism of Ethylene Epoxidation Catalysis. *Catal. Letters* **2013**, *143* (2), 131–141. https://doi.org/10.1007/s10562-012-0957-3.

(16) Linic, S.; Barteau, M. A. Construction of a Reaction Coordinate and a Microkinetic Model for Ethylene Epoxidation on Silver from DFT Calculations and Surface Science Experiments. *J. Catal.* **2003**, *214* (2), 200–212. https://doi.org/10.1016/S0021-9517(02)00156-2.

(17) Stegelmann, C.; Schiødt, N. C.; Campbell, C. T.; Stoltze, P. Microkinetic Modeling of Ethylene Oxidation over Silver. *J. Catal.* **2004**, *221* (2), 630–649. https://doi.org/10.1016/j.jcat.2003.10.004.

(18) Kilty, P. A.; Sachtler, W. M. H. Catalysis Reviews : Science and Engineering THE MECHANISM OF THE SELECTIVE OXIDATION OF ETHYLENE TO ETHYLENE. No. September 2012, 37–41.

(19) Boreskov, A G.K.; Khasin, A. V. Reaction of Ethylene with Oxygen Adsorbed on Silver: Reactivity of Adsorbed Oxygen Atoms and Modifying Effect of the Reaction Products. *Dokl. Phys. Chem. (Engl. Transl.); (United States)* **1984**, *274:1-3*.

(20) Santen, V. A. N.; Groot, D. E. The Mechanism of Ethylene Epoxidation. **1986**, *539*, 530–539.

(21) Linic, S.; Jankowiak, J.; Barteau, M. A. Selectivity Driven Design of Bimetallic Ethylene Epoxidation Catalysts from First Principles. *J. Catal.* **2004**, *224* (2), 489–493. https://doi.org/10.1016/j.jcat.2004.03.007.

(22) Linic, S.; Barteau, M. A. Formation of a Stable Surface Oxametallacycle That Produces Ethylene Oxide. *J. Am. Chem. Soc.* **2002**, *124* (2), 310–317. https://doi.org/10.1021/ja0118136.

(23) Christopher, P.; Linic, S. Engineering Selectivity in Heterogeneous Catalysis: Ag Nanowires as Selective Ethylene Epoxidation Catalysts. *J. Am. Chem. Soc.* **2008**, *130* (34), 11264–11265. https://doi.org/10.1021/ja803818k.

(24) Christopher, P.; Linic, S. Shape- and Size-Specific Chemistry of Ag Nanostructures in Catalytic Ethylene Epoxidation. *ChemCatChem* **2010**, *2* (1), 78–83. https://doi.org/10.1002/cctc.200900231.

(25) Christopher, P. Design of Nanostructured Ag Catalysts for Selective Heterogeneous Catalytic and Photocatalytic Oxidation Reactions. **2011**.

(26) Chimentão, R. J.; Medina, F.; Fierro, J. L. G.; Sueiras, J. E.; Cesteros, Y.; Salagre, P. Styrene Epoxidation over Cesium Promoted Silver Nanowires Catalysts. *J. Mol.*

Catal. A Chem. **2006**, *258* (1–2), 346–354. https://doi.org/10.1016/j.molcata.2006.07.028.

(27) Sangaru, S. S.; Zhu, H.; Rosenfeld, D. C.; Samal, A. K.; Anjum, D.; Basset, J. M. Surface Composition of Silver Nanocubes and Their Influence on Morphological Stabilization and Catalytic Performance in Ethylene Epoxidation. *ACS Appl. Mater. Interfaces* **2015**, *7* (51), 28568–28576. https://doi.org/10.1021/acsami.5b09927.

(28) Chimentão, R. J.; Kirm, I.; Medina, F.; Rodríguez, X.; Cesteros, Y.; Salagre, P.; Sueiras, J. E. Different Morphologies of Silver Nanoparticles as Catalysts for the Selective Oxidation of Styrene in the Gas Phase. *Chem. Commun.* **2004**, *4* (7), 846–847. https://doi.org/10.1039/b400762j.

(29) Chimentao, R. J.; Medina, F.; Sueiras, J. E.; Fierro, J. L. G.; Cesteros, Y.; Salagre, P. Effects of Morphology and Cesium Promotion over Silver Nanoparticles Catalysts in the Styrene Epoxidation. *J. Mater. Sci.* **2007**, *42* (10), 3307–3314. https://doi.org/10.1007/s10853-006-0570-1.

(30) Diao, W. Preparation and Characterization Of Pt-Ru Bimetallic Catalysts Using Electroless Deposition Methods And Mechanistic Study Of Re And Cs Promoters For Ag-Based, High Selectivity Ethylene Oxide Catalysts. **2015**, 111.

(31) Dellamorte, J.; Barteau, M. A.; Lauterbach, J. Investigation of Ag Based Catalysts for Ethylene Epoxidation: High Throughput Studies and Characterization, 2009.

(32) Zhang, P.; Wyman, I.; Hu, J.; Lin, S.; Zhong, Z.; Tu, Y.; Huang, Z.; Wei, Y. Silver Nanowires: Synthesis Technologies, Growth Mechanism and Multifunctional Applications. *Mater. Sci. Eng. B Solid-State Mater. Adv. Technol.* **2017**, *223*, 1–23. https://doi.org/10.1016/j.mseb.2017.05.002.

(33) Yugagn Sun and Younan Xia. Large-Scale Synthesis of Uniform Silver Through a Soft, Self-Seeding, Polyol Process. *Adv. Mater.* **2002**, No. 11, 833–837. https://doi.org/10.1002/1521-4095(20020605)14:11<833::AID-ADMA833>3.0.CO;2-K.

(34) Fahad, S.; Yu, H.; Wang, L.; Zain-ul-Abdin; Haroon, M.; Ullah, R. S.; Nazir, A.; Naveed, K. ur R.; Elshaarani, T.; Khan, A. Recent Progress in the Synthesis of Silver Nanowires and Their Role as Conducting Materials. *J. Mater. Sci.* **2019**, *54* (2), 997–1035. https://doi.org/10.1007/s10853-018-2994-9.

(35) Wiley, B.; Sun, Y.; Mayers, B.; Xia, Y. Shape-Controlled Synthesis of Metal Nanostructures: The Case of Silver. *Chem. - A Eur. J.* **2005**, *11* (2), 454–463. https://doi.org/10.1002/chem.200400927.

(36) Bari, B.; Lee, J.; Jang, T.; Won, P.; Ko, S. H.; Alamgir, K.; Arshad, M.; Guo, L. J. Simple Hydrothermal Synthesis of Very-Long and Thin Silver Nanowires and Their Application in High Quality Transparent Electrodes. *J. Mater. Chem. A* **2016**, *4* (29), 11365–11371. https://doi.org/10.1039/c6ta03308c.

(37) Coskun, S.; Aksoy, B.; Unalan, H. E. Polyol Synthesis of Silver Nanowires: An Extensive Parametric Study. *Cryst. Growth Des.* **2011**, *11* (11), 4963–4969. https://doi.org/10.1021/cg200874g.

(38) Wang, Z.; Liu, J.; Chen, X.; Wan, J.; Qian, Y. A Simple Hydrothermal Route to Large-Scale Synthesis of Uniform Silver Nanowires. *Chem. - A Eur. J.* **2005**, *11* (1), 160–163. https://doi.org/10.1002/chem.200400705.

(39) Tetsumoto, T.; Gotoh, Y.; Ishiwatari, T. Mechanistic Studies on the Formation of Silver Nanowires by a Hydrothermal Method. *J. Colloid Interface Sci.* **2011**, *362* (2), 267–273. https://doi.org/10.1016/j.jcis.2011.05.079.

(40) Zannotti, M.; Rossi, A.; Giovannetti, R. SERS Activity of Silver Nanosphere, Triangular Nanoplates, Hexagonal Nanoplates and Quasi-Spherical Nanoparticles: E Ect of Shape and Morphology. **2020**.

(41) An, J.; Tang, B.; Ning, X.; Zhou, J.; Xu, S.; Zhao, B.; Xu, W.; Corredor, C.; Lombardi, J. R. Photoinduced Shape Evolution: From Triangular to Hexagonal Silver Nanoplates. *J. Phys. Chem. C* **2007**. https://doi.org/10.1021/jp0745081.

(42) Callegari, A.; Tonti, D.; Chergui, M. Photochemically Grown Silver Nanoparticles with Wavelength-Controlled Size and Shape. *Nano Lett.* **2003**, *3* (11), 1565–1568. https://doi.org/10.1021/nl034757a.

(43) Yang, Z.; Qian, H.; Chen, H.; Anker, J. N. One-Pot Hydrothermal Synthesis of Silver Nanowires via Citrate Reduction. *J. Colloid Interface Sci.* **2010**, *352* (2), 285–291. https://doi.org/10.1016/j.jcis.2010.08.072.

(44) Hemmati, S.; Barkey, D. P. Parametric Study, Sensitivity Analysis, and Optimization of Polyol Synthesis of Silver Nanowires. *ECS J. Solid State Sci. Technol.* **2017**, *6* (4), P132–P137. https://doi.org/10.1149/2.0141704jss.

(45) Skrabalak, S. E.; Wiley, B. J.; Kim, M.; Formo, E. V.; Xia, Y. On the Polyol Synthesis of Silver Nanostructures: Glycolaldehyde as a Reducing Agent. *Nano Lett.* **2008**, *8* (7), 2077–2081. https://doi.org/10.1021/nl800910d.

(46) Sun, Y.; Gates, B.; Mayers, B.; Xia, Y. Crystalline Silver Nanowires by Soft Solution Processing. *Nano Lett.* **2002**, *2* (2), 165–168. https://doi.org/10.1021/nl010093y.

(47) Fievet, F.; Lagier, J. P.; Figlarz, M. Preparing Monodisperse Metal Powders in Micrometer and Submicrometer Sizes by the Polyol Process. *MRS Bull.* **1989**, *14* (12), 29–34. https://doi.org/10.1557/S0883769400060930.

(48) Sun, Y.; Xia, Y. Shape-Controlled Synthesis of Gold and Silver Nanoparticles. *ChemInform* **2003**, *34* (10), 2176–2180. https://doi.org/10.1002/chin.200310226.

(49) Xia, B. Y.; Yang, P.; Sun, Y.; Wu, Y.; Mayers, B.; Gates, B.; Yin, Y.; Kim, F.; Yan, H. One-Dimensional Nanostructures : Synthesis , Characterization , and Applications **. **2003**, No. 5, 353–389.

(50) Chen, T.; Wang, H.; Yang, H.; Guo, X. Synthesis and Characterizing of High Aspect Ratio Silver Nanowires by Polyol Process. *Key Eng. Mater.* **2018**, *768 KEM*, 75–84. https://doi.org/10.4028/www.scientific.net/KEM.768.75.

(51) Sun, Y.; Mayers, B.; Herricks, T.; Xia, Y. Polyol Synthesis of Uniform Silver Nanowires: A Plausible Growth Mechanism and the Supporting Evidence. *Nano Lett.* **2003**, *3* (7), 955–960. https://doi.org/10.1021/nl034312m.

(52) Gao, Y.; Jiang, P.; Liu, D. F.; Yuan, H. J.; Yan, X. Q.; Zhou, Z. P.; Wang, J. X.; Song, L.; Liu, L. F.; Zhou, W. Y.; Wang, G.; Wang, C. Y.; Xie, S. S.; Zhang, J. M.; Shen, D. Y. Evidence for the Monolayer Assembly of Poly(Vinylpyrrolidone) on the Surfaces of Silver Nanowires. *J. Phys. Chem. B* **2004**, *108* (34), 12877–12881. https://doi.org/10.1021/jp037116c.

(53) Xu, J.; Hu, J.; Peng, C.; Liu, H.; Hu, Y. A Simple Approach to the Synthesis of Silver Nanowires by Hydrothermal Process in the Presence of Gemini Surfactant. *J. Colloid Interface Sci.* **2006**, *298* (2), 689–693. https://doi.org/10.1016/j.jcis.2005.12.047.

(54) Tang, C.; Sun, W.; Lu, J.; Yan, W. Role of the Anions in the Hydrothermally Formed Silver Nanowires and Their Antibacterial Property. *J. Colloid Interface Sci.* **2014**, *416*, 86–94. https://doi.org/10.1016/j.jcis.2013.10.036.

(55) Zhang, Y.; Guo, J.; Xu, D.; Sun, Y.; Yan, F. One-Pot Synthesis and Purification of Ultralong Silver Nanowires for Flexible Transparent Conductive Electrodes. *ACS Appl. Mater. Interfaces* **2017**, *9* (30), 25465–25473. https://doi.org/10.1021/acsami.7b07146.

(56) Ćwik, M.; Buczyńska, D.; Sulowska, K.; Roźniecka, E.; Mackowski, S.; Niedziółka-Jönsson, J. Optical Properties of Submillimeter Silver Nanowires Synthesized Using the Hydrothermal Method. *Materials (Basel).* **2019**, *12* (5), 1–12. https://doi.org/10.3390/ma12050721.

(57) Liu, W. J.; Liu, M. L.; Lin, S.; Liu, J. C.; Lei, M.; Wu, H.; Dai, C. Q.; Wei, Z. Y. Synthesis of High Quality Silver Nanowires and Their Applications in Ultrafast Photonics. *Opt. Express* **2019**, *27* (12), 16440. https://doi.org/10.1364/oe.27.016440.

(58) Diao, W.; Digiulio, C. D.; Schaal, M. T.; Ma, S.; Monnier, J. R. An Investigation on the Role of Re as a Promoter in Ag-Cs-Re/α-Al2O3 High-Selectivity, Ethylene Epoxidation Catalysts. *J. Catal.* **2015**, *322*, 14–23. https://doi.org/10.1016/j.jcat.2014.11.007.